THESIS

EARLY MORNING EVOLUTION OF THE CONVECTIVE BOUNDARY LAYER AT THE BOULDER ATMOSPHERIC OBSERVATORY

Submitted by

Daniel Edward Wolfe

Department of Atmospheric Science

In partial fulfillment of the requirements

for the Degree of Master of Science

Colorado State University

Ft. Collins, Colorado

Spring 1985

COLORADO STATE UNIVERSITY

22 March 1985

WE HEREBY RECOMMEND THAT THE THESIS PREPARED UNDER OUR SUPERVISION BY Daniel Edward Wolfe

ENTITLED Early Morning Evolution of the Convective Boundary Layer at the Boulder Atmospehric Observatory

BE ACCEPTED AS FULFILLING IN PART REQUIREMENTS FOR THE DEGREE OF Master of Science

Committee on Graduate Work

Adviser

Department Head

ABSTRACT OF THESIS

Early Morning Evolution of the Convective

Boundary Layer at the Boulder Atmospheric Observatory

The growth of the earth's planetary boundary layer is an extremely interesting and complex phenomenon. Awareness of its significance has risen over the years due in part to the increase in atmospheric pollution that becomes trapped within this layer. Its importance does not stop there as local weather conditions such as summer thunderstorms and surface circulation patterns are also directly related to daily changes in the planetary boundary layer. Missing from many of today's studies are details of its evolution over complex terrain. Observations of the early morning evolution of the CBL at the Boulder Atmospheric Observatory even under similar synoptic and local conditions show marked differences in growth patterns. Potential temperature, wind and moisture profiles along with sodar and synoptic data are analyzed in an attempt to explain the growth behavior of the mixed layer from just prior to sunrise until several hours after sunrise. Entrainment, horizontal advection, vertical motion and upper level stability are investigated as they pertain to the observed growth patterns. It is intended that these results may be used in conjunction with other analyses to better

understand and describe the growth of the atmospheric layer in which man lives.

Daniel Edward Wolfe
Atmopheric Science Department
Colorado State University
Fort Collins, Colorado
Spring 1985

ACKNOWLEDGMENTS

I wish to thank Dr. Richard H. Johnson for his professional guidance and my committee members for their review of and suggestions to the manuscript. I also wish to thank my fellow workers and all those I have talked with; especially John Gaynor, Dr. Chandran Kaimal and Norbert Szczepczynski who gave me support and encouragement throughout my work. Not to be forgotten are my wife Carolyn and my daughter Stephanie, for without their patience and smiles I would not have succeeded. Typing by Mildred Birchfield and drafting by Alison Aragon were invaluable and greatly appreciated.

TABLE OF CONTENTS

		Page
I.	INTRODUCTION	1
	1.1 The PBL	1
	1.2 Inversions and the CBL	5
	1.3 Need for more Studies	6
	1.4 Thesis Outline	8
II.	LITERATURE REVIEW	9
	2.1 General Review	9
	2.2 Studies of the CBL	13
	2.3 Models vs. Observations	16
	2.4 Variables in Boundary Layer Growth	18
	2.5 Estimation of CBL Heights	24
	2.6 Work related to the BAO	26
III.	DATA SOURCES AND REDUCTION TECHNIQUES	28
	3.1 Overview of the BAO Facility	28
	3.2 Terrain Features	32
	3.3 Instrument Design and Tower Structure Effects	35
	3.4 Tower Data Set	39
	3.5 Sodar Data	41
	3.6 Other Supporting Data	44
	3.7 Data Reduction	45

IV. SELECTION OF DAYS..... 47

4.1 Sky Cover..... 47

4.2 Data Continuity..... 50

4.3 Solar Radiation..... 51

4.4 Nocturnal Inversion..... 54

4.5 Undisturbed Synoptic Conditions..... 61

V. OBSERVATIONAL RESULTS..... 65

5.1 Potential Temperature..... 65

5.1.1 Pre-Growth (Inversion)..... 65

5.1.2 Growth Processes in the Early Morning..... 66

5.1.3 Sunrise Transition (0400-0620 MST)..... 69

5.1.4 Mixed Layer Development (0640-0900 MST)... 79

5.1.5 Maturing Mixed Layer (0920-1140 MST)..... 97

5.2 Winds..... 105

5.3 Moisture..... 110

VI. SUMMARY AND CONCLUSION..... 116

6.1 Summary..... 116

6.2 Conclusion..... 117

6.3 Future Studies..... 122

REFERENCES..... 124

APPENDIX A..... 131

APPENDIX B..... 132

APPENDIX C..... 141

APPENDIX D..... 155

APPENDIX E..... 161

LIST OF FIGURES

Page

Fig. 1. Planetary Boundary Layer growth cycle (adapted from Carson, 1973) Inversion rise vs. sensible heat flux..... 3

Fig. 2. Zero order jump model (adapted from Deardorff, 1979)..... 12

Fig. 3. Diurnal trend of the surface heat flux ($\overline{w'\theta'}$) and corresponding inversion rise (z_i) (Kaimal, 1976)..... 15

Fig. 4a. View of three-axis sonic anemometer, fast-response platinum wire temperature probe, and slow-response aspirated quartz thermometer in a radiation shield..... 31

Fig. 4b. View of propeller-vane anemometer and cooled mirror dew point hygrometer..... 31

Fig. 5. Contour map of local BAO terrain (circle = 5 km radius)..... 33

Fig. 6. 3-D view of BAO (w/exaggerated vertical scale)..... 34

Fig. 7. BAO location relative to the Rocky Mountain Front Range, Denver and major river drainage systems..... 36

Fig. 8. Horizontal cross-section extending out from BAO at the four major points of the compass..... 37

Fig. 9. BAO site showing sensor positions..... 42

Fig. 10. BAO solar radiation time series of 20 min means (direct and diffuse) 0400-2000 MST; 11 days..... 52

Fig. 11. BAO 0400 MST $\Delta\theta$ profiles of 20 min means ($\Delta\theta = \theta_z - \theta_{10\ m}$); 13 days..... 55

Fig. 12. DEN 0500 MST rawinsonde $\Delta\theta$ profiles ($\Delta\theta = \theta_z - \theta_{sfc}$); 8 days..... 56

Fig. 13. BAO (0400 MST) vs. DEN (0500 MST) $\Delta\theta$ profiles; BAO $\Delta\theta = \theta_z = \theta_{10\ m}$ and DEN $\Delta\theta = \theta_z = \theta_{sfc}$; 10 days..... 58

Fig. 14. BAO θ time series profiles of 20 min means (0400-0620 MST); 13 days..... 70

Fig. 15. BAO θ time series profiles of 20 min means (0640-0900 MST); 13 days..... 80

Fig. 16. Temperature fluctuations (horizontal lines) and vertical heat flux (shaded regions) during a 10 min period (Kaimal, 1976)..... 89

Fig. 17. BAO z_i (20 min mean) vs. sodar record z_i (single point) (0400-0900 MST); 8 days..... 91

Fig. 18. Calculated mixed layer depths $(z_i)_c$ versus observed BAO tower depths $(z_i)_o$; 13 days..... 95

Fig. 19. BAO θ time series profiles of 20 min means (0920-1140 MST); 12 days..... 98

Fig. 20. Wind direction time series composite of BAO 20 min means (0400-1140 MST) and Johnson and Toth (July 1981) hourly averages (0400-1200 MST)..... 106

Fig. 21. Wind speed time series composite of BAO 20 min means (0400-1140 MST)..... 107

Fig. 22. BAO Δq profiles of 20 min means (0400, 0840, 1140 MST) ($\Delta q = q_z - q_{10\ m}$); 13 days..... 111

Fig. 23. BAO θ and wind profiles of 20 min means, a) sunrise transition b) mixed layer development c) maturing mixed layer..... 118

LIST OF SYMBOLS

a	constant (specific humidity equation; 17.269).
b	constant (specific humidity equation; 35.86).
e	natural logarithm (ln).
k	entrainment ratio.
g	gravity.
q	specific humidity.
t	time.
w	vertical velocity.
z	height.
B	Bowen ratio.
H	initial surface heat flux.
N	Brunt Viäsälä frequency.
P	1000 mb.
Q	diabatic heating.
e_p	vapor pressure.
w_i	large scale vertical velocity at z_i.
z_i	base height of the temperature inversion.
z_l	height of tower level.
C_p	specific heat at constant pressure.
M_w	molecular weight of water.
M_d	molecular weight of dry air.

P_o surface pressure.

P_1 pressure at z_1.

R_d gas constant for dry air.

Ri Richardson number.

T' temperature fluctuations.

T_d dew point temperature.

T_m mean temperature in mixed region.

T_v virtual temperature.

$\vec{V}$ horizontal velocity.

β vertical stability $\frac{\partial \theta}{\theta \partial z}$.

ρ density.

θ potential temperature.

θ_v virtual potential temeprature.

γ local lapse rate.

Γ dry adiabatic lapse rate.

$\vec{\nabla}_h$ horizontal gradient.

$(\overline{w'\theta_v'})_i$ buoyancy flux at z_i.

$(\overline{w'\theta_v'})_s$ buoyancy flux at surface.

$-\overline{u'w'}$ shear stress.

$(\Delta\theta_v)_i$ gradient of θ_v at z_i.

$(\frac{\partial \bar{T}}{\partial z})_o$ initial lapse rate.

I. INTRODUCTION

1.1 The Planetary Boundary Layer

The Planetary Boundary Layer (PBL) is one of the most important height regions in the atmosphere. It is within this layer that pollution is generated and trapped and where many important controls affecting our everday weather begin. Wyngaard (1982) uses the following simple definition when describing the PBL:

> "the layer through which the earth's surface influences the vertical profiles of the mean quanities (wind, temperature, moisture)".

This layer has a diurnal cycle with the daytime portion often referred to as the convective boundary layer (CBL) and the nighttime portion as the nocturnal boundary layer (NBL). The convective boundary layer, the subject of this study, is often subdivided into three distinct layers. The lowest of these layers is known as the surface or constant flux layer and typically several tens of meters deep, where wind shear is important. Above the surface layer and making up the largest portion of the CBL is the mixed, adiabatic or neutral layer, where convective mixing creates a nearly adiabatic layer. The depth of this layer is variable and normally increases in proportion to the heating of the earth's surface during undisturbed synoptic conditions. Above the mixed layer is the stable or capping layer that works against upward growth and mixing.

Over land the depth of the CBL and its evolution are controlled in an important way by short wave solar radiation intercepted by the earth. During the daytime, heating at the earth's surface creates warm buoyant plumes (thermals) which effectively mix heat, moisture and momentum vertically. The intensity and depth of mixing is a function of season, latitude, local surface properties and all scales of weather conditions. It is the purpose of this thesis to study the evolution of the CBL and report findings of an observational study of the early morning boundary layer growth. The mixed layer is analyzed on clear summer days using data from the Boulder Atmospheric Observatory (BAO) 300 m tower (Kaimal and Gaynor, 1983).

In Fig. 1 (adapted from Carson 1973) is a schematic of the diurnal cycle of mixed layer growth over land on clear days. Carson divides boundary layer evolution into five phases controlled by four factors (subsidence, interfacial mixing, lapse rate of the capping layer and sensible heat flux). These phases (illustrated in Fig. 1) are:

Phase I. The surface sensible heat flux reverses sign, negative to positive, as solar flux density increases. Most early morning thermals and their overshoot are quickly supressed by the nocturnal inversion, leading to little significant interfacial mixing (entrainment).

Phase II. The nocturnal inversion is essentially gone. The capping layer at this height is now less stable, thermal strength is growing and mixing at the upper boundary intensifies.

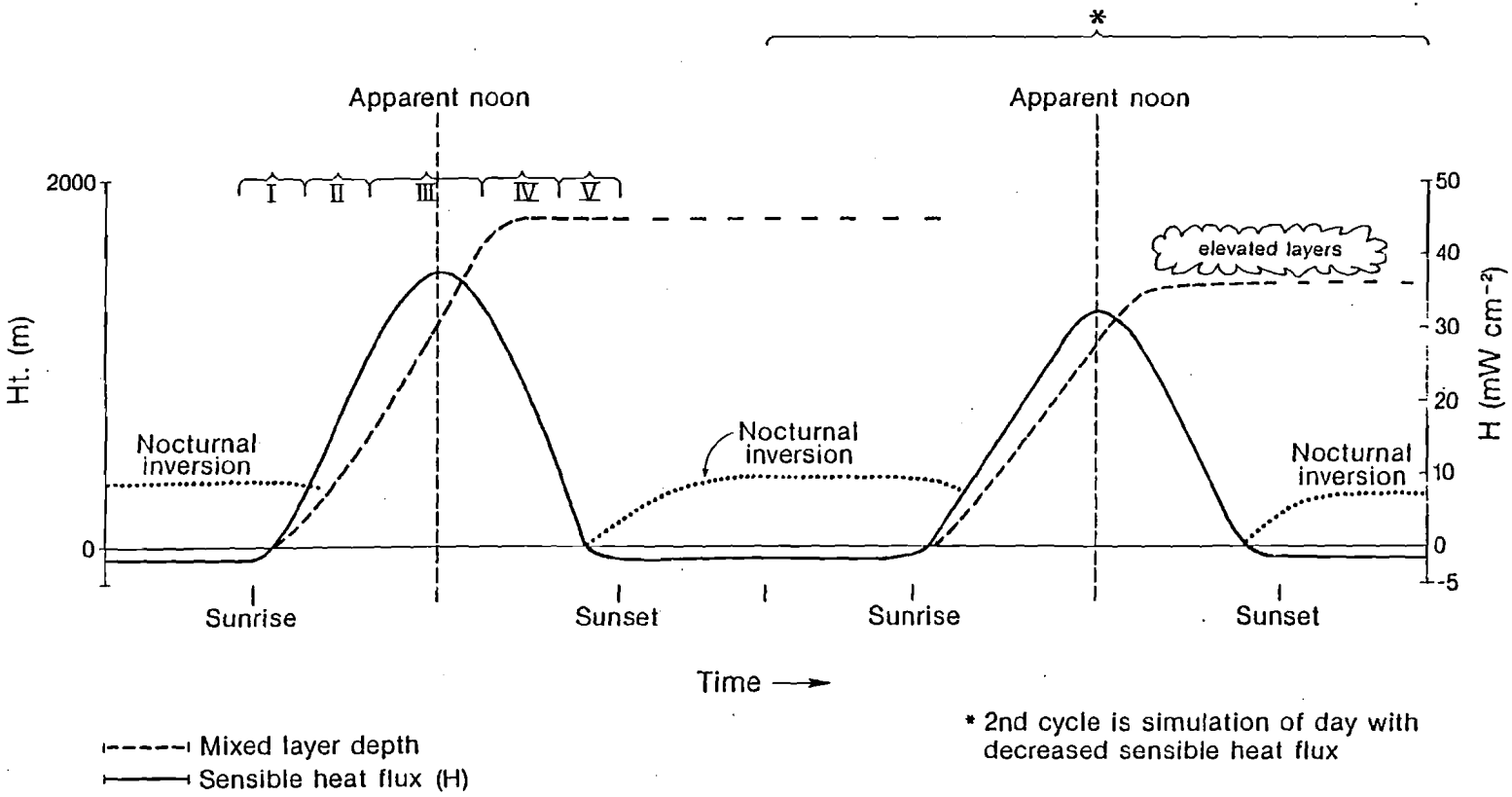

Fig. 1. Planetary Boundary Layer growth cycle (adapted from Carson, 1973) Inversion rise vs. sensible heat flux.

Phase III. Sensible heat flux reaches a maximum with siginificant thermal penetration present. This penetration displaces cool air aloft and also brings warmer air down into the mixed layer.

Phase IV. Here we find sensible heat flux though still positive beginning to drop off. Thermals are weaker and unable to mix throughout the complete convective layer and entrainment is nearly gone. Mechanical mixing and subsidence become dominant.

Phase V. During the last phase, just prior to sunset when surface sensible heat flux once again reverses sign, the nocturnal inversion begins to form. The inversion remains shallow often growing slowly throughout the night until just after sunrise.

This thesis will examine the first three phases described by Carson.

The daytime and nocturnal cycles are repeated over many days especially in the late spring and summer. Rebirth of the nocturnal inversion interacting with daily differences in surface moisture, heating and pollutants can produce changes in the evolution process. Even though these differences may be slight, moisture, temperature and pollutants are occasionally trapped between the previous day's mixed layer and above the newly developing boundary layer. Kaimal et al. (1982b) examine similar situations while tracking the mixed layer depth with a variety of remote sensors. Reible et al. (1983) discuss these layers and their importance with respect to pollution problems. Another way

pollution influences the boundary layer is its interaction with solar radiation. Peterson and Flowers (1976) analyze and describe how pollution affects the atmospheric turbidity and also the photochemical processes taking place.

1.2 Inversions and the CBL

When observing a growing CBL, one must also deal with the temperature inversion aloft. Inversions serve as a lid restricting growth and vertical mixing in the CBL. There are generally four types of inversions whose names either directly or indirectly describe where they are located or by what process they formed in the atmosphere.

First and most common to the boundary layer is the radiation inversion, also referred to as a ground, surface or nocturnal inversion. Frontal, turbulence induced and subsidence inversions also play a part in the evolution and growth of the CBL, but are not focused on in this thesis. Frontal inversions are associated with air mass separation and occur primarily during disturbed conditions. Turbulence induced inversions produce small scale variations in the detail of the vertical temperature structure and CBL growth. Subsidence inversions are found predominantly above 500 m and restrict growth later in the evolution of the boundary layer.

None of these inversions is mutually exclusive and all can conceivably exist at the same time. Hosler (1961) finds from analyzing radiosonde data (taken four times daily) within the United States that

25% of the time during a year inversions or low-level isothermal layers exist limiting vertical mixing. Hosler's specific figures for Denver at 0500 MST show even higher values of 65% in spring and 84% in summer.

1.3 Need for more Studies

Until recently, the study of the evolution of the boundary layer was limited to radiosonde flights widely spaced in time (Holzworth 1964) or well planned field experiments such as O'Neill, 1953 (Lettau and Davidson, 1957), Wangara, 1967 (Clarke et al. 1971), and Kansas, 1968 (Haugen et al. 1971). With the development of many CBL models, Coulman (1978) points out how some of these models fail to adequately trace the evolution of the boundary layer. Two aspects that can affect the accuracy or applicability of model results are their simplification or the data put into them. Simplification can generalize or completely eliminate parameters that control boundary layer growth. Data used to initialize and run many models are often lacking the details to describe the atmosphere, especially the vertical stability. As the time scale of the model increases, so do the necessary scale sizes and complexity of the input data.

The BAO is a facility that can provide data sets of sufficient time and vertical resolution to adequately look at the evolution of the boundary layer. Kaimal and Gaynor (1983) state that the BAO tower data represent at least 25% of the daytime convective layer until almost noon on a majority of days. Goff and Hudson (1972) show some analyses

from a 450 m tower over homogeneous terrain in Oklahoma. Their analysis consists of mean temperature and lapse rate characteristics as well as the effects of different air masses and sky conditions on the thermal structure. Only one individual study is undertaken on the dissipation of a mid-winter nocturnal inversion after sunrise.

The BAO, with its compliment of sensors, proximity to the Rocky Mountains and continuous data logging, presents a unique opportunity to study the evolution of the CBL over non-homogeneous terrain. Kaimal et al. (1982a) report similarities of BAO spectral data to that of other uniform terrain studies. Differences, caused mainly by mountain wave effects in the low frequency range, also exist in the spectral analysis. Investigations by Schotz and Panofsky (1980) and Johnson and Toth (1982a) point out the importance of uneven terrain and the Rocky Mountain front range topography to mesoscale circulation and therefore to the BAO. All three studies examined what effects non-homogeneous terrain can have on measured parameters in the boundary layer.

Generalizing or compositing boundary layer data must be done carefully. Johnson and Heywood (1938), after examining composites of temperature profiles from a short tower in England, discuss the need for analyzing individual days because, the temperature of the air depends on many meteorological factors. The purpose of Johnson and Heywood's study was to observe winds and temperature up to 100 m and to determine the characteristics and errors of the instruments used to measure them.

From their five years of data mean variations in the wind and temperature fields are calculated. Inversion statistics as well as some early turbulence measurements are also examined.

1.4 Thesis Outline

This thesis presents analyses of observations from the BAO showing the early morning growth of the CBL. Thirteen meteorologically undisturbed days are selected during the summers of 1981 and 1982. Using time series from the BAO along with synoptic and nearby Denver (DEN) radiosonde data, some insight into the role mesoscale, upper interface and surface physical processes play in the evolution of the daytime boundary layer rise is offered.

First a review of literature is undertaken to find out how knowledge of the boundary layer and its growth have progressed over the years. Recent related work, including models and observations, are covered along with studies tied to the BAO. Prior to analysis of the thirteen days, the BAO data, other supporting data sources and how particular days were chosen are described.

To achieve the goals of this thesis, observations are analyzed and compared to previous work showing consistencies and dissimilarities to what already is known. In the summary, future needs and studies of the entire PBL are discussed, especially as they pertain to the BAO.

II. LITERATURE REVIEW

2.1 General Review

Mahrt (1983) reviews a large number of studies on the atmospheric boundary layer from 1979 through 1982. Such a wide selection of studies specifically on the boundary layer was not previously available. Literature on climate and inversions were often an excellent source of knowledge on the CBL. The work of Geiger (1965) and Yoshino (1975) on climatology often relates to the boundary layer. They examine both local climatic conditions such as vegetation and terrain, and larger scale climatic factors like positioning of pressure systems, relating their effects to boundary layer growth and depths. One of the earliest reviews on temperature inversions is that of Quiroz (1956). In his review he provides a reference list of both studies and experiments which are closely tied to boundary layer growth. It was not until the last 20 to 25 years, with improved technology, instrumentation and the forming of a few basic theories, that work concerning the CBL increased dramatically.

The O'Neill experiment in Nebraska was a major step taken to analyze a homogeneous boundary layer. Publishing this data in 1957, Lettau and Davidson provide the scientific community with a comprehensive boundary layer data set. After Lettau and Davidson's book, Ball

(1960) developed a thermodynamic model describing inversion break-up due to convection. Two key observational studies of the boundary layer using past rawinsonde data soon follow. Hosler (1961) looks at low-level inversion frequency and Holzworth (1964) defines mixed layer depths across the United States. Two important points shown by Holzworth are the strong mixing depth gradient along the Rockies (E/W) and that lifting condensation levels (LCL's) on the average are less than the mean mixing depths in July for the BAO region. These conditions make determining mixing depths difficult and aid in the formation of convective clouds. Hosler classifies inversions by climate and geography. For the Rocky Mountain region inversions are directly related to the diurnal cycle and the seasons are important to the strength and duration of the inversion. Hosler acknowledges deficiencies in his data such as time resolution, but still feels his results are representative of actual conditions.

Lilly (1968) heads a long list of authors concerned with modeling the CBL. This work includes Deardoff et al. (1969), Carson (1973), Tennekes (1973), Stull (1973), Deardorff (1974), Mahrt (1976), Stull (1976 a,b,c), Zeman and Tennekes (1977) and Benkley (1977). Most of these models deal with clear skies and real atmospheric data. Lilly (1968) examines the mixed layer under a strong inversion and cloud layer while Deardorff et al. (1969) use laboratory experiments in an attempt to model the atmospheric boundary layer.

As was discovered in the models above, entrainment processes are very important to the growth of the mixed layer. Surface heating is

fairly well understood, but in what manner and how much entrainment takes place at the top of the boundary layer interface is not fully understood. Ball (1960) defines an entrainment ratio (k) of one in relating surface heat flux to downward heat flux at the top of the mixed layer during convection. This process of heat transfer is also associated with mass transfer. Carson (1973) and others point out that entrainment depends not only on the surface heating, but also on the strength and stability of the capping layer. Stull (1976b) uses a diagnostic entrainment equation in place of the downward to upward heat flux ratio. Stull's entrainment value includes the effects of infrared radiation, gravity waves and clouds which reduce his ratio to 0.1 as compared to a range 0.2-0.3 for Lilly (1968). Consideration of these additional mechanisms places a greater demand on the initial data in more complete models than exists for the simplest models.

How extensive the convection is within a region is also important to entrainment. Isolated thermals produce less mixing than widespread convection (Deardorff et al., 1969). Stull (1976b) and Deardorff (1979) make use of a zero order "jump" model to describe entrainment, idealizing the boundary layer interface zone as a finite jump in potential temperature over a zero height change (Fig 2). The entrainment analyses and models by Tennekes and Driedonks (1981), Driedonks (1982 a,b) and Wilczak and Bussinger (1982) consider the dynamics and microstructure of this interface region. Driedonks (1982a) looks at the sensitivity of the entrainment ratio and also the effects of initial

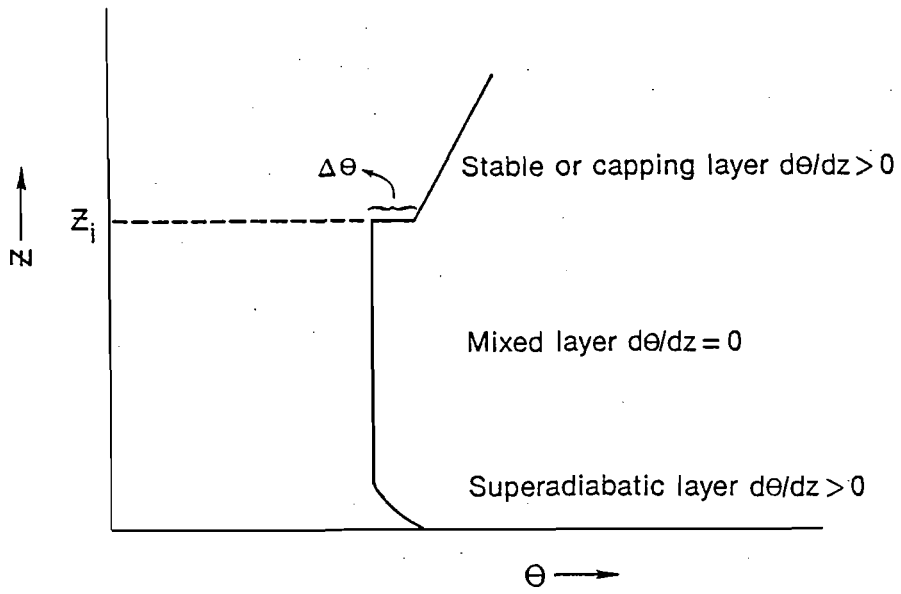

Fig. 2. Zero order jump model (adapted from Deardorff, 1979).

boundary layer conditions in models. Initial conditions quickly lose their influence on the boundary layer height and the mean temperature of the mixed layer. Because of the inaccuracies in measuring the boundary layer height, the true effect of entrainment is often obscured. What Driedonks did find is that a change from 0.2 to 0.5 in the entrainment ratio only causes a variation in the boundary layer depth of 20%.

2.2 Studies of the CBL

Beginning with the O'Neill experiment in 1953, there have been at least seven major CBL experiments (Table 1). Each experiment was conducted during predominantely convective periods. Of these seven, six fit the basic criteria for horizontal homogeneity while only one takes place over non-homogeneous terrain, Project Phoenix (Hooke et al., 1979) at the BAO. Data from both the O'Neill and Wangara experiments have been used extensively in comparisons with models and other experiments over the years. A majority of these experiments had as their goal the continuous measurement of boundary layer properties throughout its depth.

The Kansas and Minnesota experiments collected data on short towers instrumented with sonic anemometers and fast response temperature probes for measurement of heat and momentum flux. Kaimal et al. (1976) present results from the Minnesota data of heat flux versus mixed layer depths (Fig. 3). These data show very similar trends of

Table 1. Major CBL Experiments

Experiment	Site	Date	Initial Publication
Project Great Plains	O'Neill, Neb. USA	Aug-Sep., 1953	Lettau and Davidson (1957)
Wangara	Hay, N.S.W. Australia	Jul-Aug., 1967	Clarke et al. (1971)
Kansas	SW Kansas USA	Summer 1968	Haugen et al. (1971)
Minnesota	NW Minnesota USA	Sep., 1973	Kaimal et al. (1976)
Koorin	Daly Water Australia	Jul-Aug. 1974	Clarke and Brooks eds. (1979)
Sangamon	Auburn, Ill. USA	Jul-Aug. 1975 (convective)	Hicks et al. (1981)
		Jul-Aug. 1976 (nocturnal)	Sisterson et al. (1976)
Project Phoenix	Erie, Co. USA	Sep., 1978	Hooke ed. (1978)

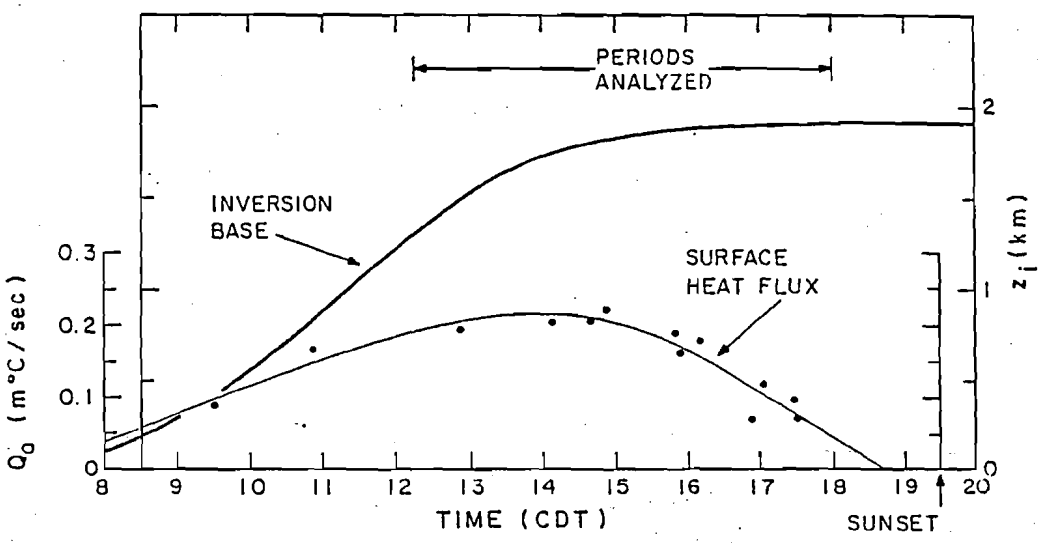

Fig. 3. Diurnal trend of the surface heat flux ($\overline{w'\theta'}$) and corresponding inversion rise (z_i) (Kaimal, 1976).

sensible heat flux and boundary layer growth to that of the O'Neill data used by Carson (1973) in Fig. 1.

The Sangamon experiments were two in a series examining the physics of the boundary layer. The 1975 experiment concentrated on early to mid-morning evolution of the mixed layer and the 1976 experiment on late afternoon to early evening periods. Data consisted of tower and balloon profiling with sodar for upper level information.

Project Phoenix at the BAO was the first experiment to incorporate detailed measurement of the lower boundary layer using in situ and remote sensors. Use of different types of remote and in situ sensors allowed the intercomparison of measurement techniques.

2.3 Models versus Observations

Comparison of model results with observational studies is instrumental in developing new and reliable models. There are still questions concerning how well models describe the boundary layer and its growth. Mahrt (1983) and others feel models fail to simulate mesoscale influences or take into account horizontal advection. Mahrt also suggests that errors in observations are sometimes too large to verify these models. Kaimal's (1982b) work with remote sensors described earlier helps to confirm this point. Signatures used by sensors to locate and measure the height of the boundary layer interface often become weak and undefined as growth progresses into the less stable upper regions.

Models can reproduce actual atmospheric conditions under certain circumstances. Kuo and Sun (1976) looking at the effects of dry convection in the lower atmosphere, compare their model results with three case studies. For one particular case they are able to simulate the slow growth and weak thermal activity observed under a strong nocturnal inversion. Using a 300 m tower near Hamburg, Germany with an attached profiling sensor package, Klöppel et al. (1978) examine the formation and dissipation of ground based inversions. Resulting entrainment rates are compared to a few models depicting both free and forced convection. Klöppel cites how a slight change in the surface roughness under similar meteorological conditions can result in substantially different shear induced turbulence. These types of differences must be accounted for if the models are going to trace the boundary layer evolution process. They also point out how Kuo and Sun (1976) use commonly measured surface data in contrast to Tennekes (1973) who requires surface heat flux and stress and the approximate value of the entrainment ratio as input to his model. Both types of models are capable of predicting boundary layer growth, but with different accuracies and amount of time necessary to run the model. Garrett (1981) is able to modify Tennekes' (1973) equations, eliminating the need for an entrainment coefficient and surface heat flux, making his model more attractive as an operational tool.

Coulman (1978) stresses the importance of subsidence caused by large scale anticyclonic circulation and again the varying complexity

of models. Coulman also believes models can predict final mixing heights and times fairly well, but fail to accurately track their evolution. Yamada and Berman (1979) obtained 93% correlation between Wangara mixing heights and results of their simple model which includes variable inversion strengths and an entrainment ratio of 0.2. They believe that this may be good enough for regional scale models but, admit many improvements are necessary for more precise local pollution dispersion requirements.

Driedonks (1982b) lists two ways for comparing models to observations and also the problems associated with them. Each differential term can be compared to the observations but, like Mahrt (1983), he suggests that errors in the measurements may be too large. A second method is to integrate the model in time and compare. A major problem with this is the reliability of the initial conditions and any unknown changes. Driedonks also points out that it is unclear how sensitive the solutions of coupled equations are to variations in constants of one of them.

2.4 Variables in Boundary Layer Growth

Deardorff et al. (1969) begin with a simple equation when defining the growth of a mixed region in their laboratory experiments,

$$\frac{\partial z_i}{\partial t} = \frac{\partial T_m}{\partial t} \left(\frac{\overline{\partial T}}{\partial z}\right)_o^{-1} , \qquad (1)$$

where T_m is the mean temperature of the mixed region, $\left(\frac{\overline{\partial T}}{\partial z_o}\right)$ is the initial lapse rate and with z_i defined to be the height of the lowest

point or base of the inversion. Using the fact that heat flux decreases linearly with height (neglecting the small negative flux region near z_i) they replace $\partial T_m/\partial t$ with $H/\rho C_p$, where H is the initial surface heat flux. If the surface heat flux is defined by a constant, this expression integrates to give

$$z_i = 2^{1/2} \left[\frac{(H/\rho C_p)}{(\partial \bar{T}/\partial z)_o}\right]^{1/2} t^{1/2} \quad . \tag{2}$$

It is along these same lines that Tennekes (1973), Deardorff (1974), Kuo and Sun (1976), Benkley (1977) and Driedonks (1982a a,b) have continued to work on atmospheric mixed layer growth models.

In his 3-D model of the heated PBL, Deardorff (1974) writes another expression,

$$\frac{dz_i}{dt} = - \frac{(\overline{w'\theta_v'})_i}{(\Delta\theta_v)_i} + w_i \quad , \tag{3}$$

where w_i is the large scale vertical velocity, $(\overline{w'\theta_v'})_i$ the buoyancy flux at z_i and $(\Delta\theta_v)_i$ the jump or gradient of virtual potential temperature at z_i. In situations where large amounts of water vapor are present, it is important to use the virtual potential temperature, $\theta_v = \theta(1+0.61q)$, where q is the specific humidity. The total derivative of z_i, (dz_i/dt), includes not only the local but advective changes in the depth of the boundary layer. An expression for determining $(\Delta\theta_v)_i$ is given as

$$\frac{d(\Delta\theta_v)_i}{dt} = \left(\frac{dz_i}{dt} - w_i\right) \frac{\partial\overline{\theta}_v}{\partial z} - \frac{(\overline{w'\theta_v'})_s - (\overline{w'\theta_v'})_i}{z_i} \qquad (4)$$

by Deardorff (1974), with $\partial\overline{\theta}_v/\partial z$ the stability above the interface jump and $(\overline{w'\theta_v'})_s$ the near surface sensible heat flux. The second term on the right hand side of (4) can also be written as $(d\overline{\theta}_v/dt)$. This total derivative incorporates advective changes as well as the entrainment process.

Driedonks (1982a) uses an expression similar to Deardorff (1974)

$$\frac{dz_i}{dt} = \left[\frac{(\overline{w'\theta_v'})_s}{z_i}(1+k) + \frac{d(\Delta\theta_v)_i}{dt}\right]\left(\frac{\partial\overline{\theta}_v}{\partial z}\right)^{-1} \qquad (5)$$

and examines the sensitivity of this equation for a convective mixed layer. Driedonks (1982b) carries the analysis further examining the entrainment portion of (5), $(\overline{w'\theta_v'})_s k$. The importance of buoyancy due to moisture and mechanical entrainment, both near surface and at z_i caused by wind shear, are discussed with additional correction terms given for each.

From the simple equations above, we find five terms important to the growth of the convective boundary layer:

1. Advection of z_i
2. Stability
3. Vertical motion
4. Surface buoyancy flux
5. Entrainment

1. Advection of z_i may seem unclear or unimportant at first, but as mentioned earlier there is a strong west to east mixing depth gradient along the front range of the Rockies (Holzworth, 1964). Reasons for this gradient are not discussed by Holzworth, but a possible explanation involves mesoscale circulation in the region. Dirks (1969) examines convective patterns of the Colorado Front Range and develops a model of the circulation perpendicular to the Rocky Mountains. In his model a two-cell circulation pattern is evident. Uneven surface heating sets up a pattern of rising air (deeper mixed layer) to the west and subsiding air (shallower mixed layer) to the east. Another area to be considered here is what effect the Rocky Mountains may have. Advection of z_i from the west includes mountain influenced air. North/south gradients of z_i are also highly variable, with differences as large as three to one expected along the front range (personal communication with Dr. J. Wilczak). Actual studies to substantiate these gradients have not been conducted.

2. Because the strength of the stable layer is not constant in time, it is necessary to examine what causes it to change. The United States Air Force Manual AWSM 105-124 (1969) on analysis of Skew-T, Log P diagrams and Whiteman (1980) both present equations describing $d\gamma/dt$ (Appendix A), where γ is the lapse rate. (Whiteman neglects three of his terms after a scale analysis.) The five terms common to each equation are:

A. Vertical gradient of diabatic heating

B. Non-shearing advection of the lapse rate

C. Differential shearing advection of the temperature gradient

D. Vertical advection of the lapse rate

E. Shrinking and sretching of an air column

Diabatic controls include radiation, conduction, evaporation and condensation which are most important near the ground in the early stages of mixed layer growth. Diabatic heating is responsible for diurnal changes in the lapse rate. Radiational heating is dominant in the formation of superadiabatic layers found at the surface.

The only difference in the two horizontal advection terms (B and C) is the vertical gradient of the wind. Non-shearing advection ($d\vec{V}/dz=0$) is not capable of changing the existing stability, but can displace it with the stability from another location. Shearing advection ($d\vec{V}/dz \neq 0$) can change the stability. Remembering there are two components of the wind, geostrophic and ageostrophic, helps one to understand this process a little more. Differential shearing advection due to the vertical wind shear is very important to mixed layer growth, because any differences in the cooling or warming rates with height influence the stability. Rapid cooling above decreases the stability and can enhance growth of the boundary layer.

Vertical motion is possible on all scales. Subsidence is a good example of vertical motion on a large scale. Turbulence, vertical as well as horizontal, usually occurs over a broad range of scales. Vertical motion caused by subsidence, orographic lifting or other comparable means can change the existing stability.

The presence of a lower boundary at the earth's surface influences the vertical motion in the air above. This fixed boundary forces descending air to diverge, converging air to ascend and mechanical turbulence through frictional forces. Vertical motions in the boundary layer are difficult to measure accurately.

Shrinking and stretching pertain to the relative motion of air parcels within a column of air. Shrinking occurs when the air at the top of a column rises slower than at the bottom, so that the upper region cools at a slower rate and increases the stability. Stretching destabilizes in a manner opposite to shrinking. Both processes are ones that affect the stability above the growing boundary layer and can occur before or during the evolution process.

3. Equation (3) of Deardorff (1974) includes w_i. This term and its importance are partially explained when examining vertical motion and its effects on the local change in the lapse rate ($\partial\gamma/\partial t$). A Chinook is a common form of vertical motion found on the lee side of the mountains producing warming downslope winds. Most large scale downward motions (sudsidence) work in a similar manner, warming the air at the dry adiabatic lapse rate (1°C/100m) and increasing the stability of the atmosphere. For a more complete picture of the large scale vertical motion there is the omega equation. The two main terms in this equation are the differential vorticity advection and thickness advection. Because these terms require knowledge of the synoptic pattern over time, its use in simple models is somewhat limited.

4. Surface buoyancy flux is fundamental in the growth of the CBL. Without it, conditions are similar to what takes place after sunset when the NBL forms and vertical mixing is controlled by the extent of the mechanical turbulence and buoyancy. As was recognized by Ball (1960), buoyancy flux is closely related to entrainment. Although it is not a 1:1 ratio as first suggested, entrainment as it pertains to penetrative convection is almost non-existent without surface buoyancy flux. As seen and used in many studies (Carson, 1973, Stull, 1973 and Kaimal, 1976), a sinusoidal function is a good first order approximation of the changing buoyancy term on clear days. This assumption has its limitations during the initial growth of the CBL, where many other processes (e.g., surface warming, evaporation) are occurring.

5. Entrainment, though most often represented as a constant, is much more complex (Stull, 1976a and Driedonks, 1982b). Laboratory simulations and modeling are excellent ways to study the physics behind entrainment. The fact that the entrainment region varies in depth and follows a constantly changing z_i makes studying it in the real atmosphere difficult. Entrainment and more of the concepts behind it will be discussed later in Chapter V.

2.5 Estimation of CBL Heights

As with most models, basic assumptions are made either to simplify or to concentrate on specific areas of interest. Models in simplified

form are estimations or educated guesses based on a few measured parameters and equations. Whenever the basic assumptions are wrong the estimates fail. Kaimal et al. (1982b) suggest a method for estimating z_i from the peak of the spectrum of vertical velocity (w). As stated earlier z_i is often difficult to identify when the inversion is rising. However, changes in the wavelength of maximum energy in the w spectrum can be related to changes in the depth of the boundary layer and used for verification of its position. This technique is useful when mixing heights are not well defined or when weak layering occurs below the true capping inversion. These conditions are normally found later in the evolution process when the mixed layer is deep.

Another method of estimating z_i is possible from calculations using the vertical velocities measured on the BAO tower and the horizontal convergence obtained from an optical triangle (Tsay et al., 1980) measuring path-averaged winds along each side of the triangle. Cross correlation between horizontal convergence and vertical velocities, related through the equation of continuity

$$w(z) = - \int_0^z \vec{\nabla}_h \cdot \vec{V}(z)\, dz \ .$$

can help to identify z_i. This method is limited to values of z_i between 50 m and 300 m because of constraints imposed by the optical triangle and the height of the tower. It is conceivable that measurements of vertical velocity from remote sensors in conjunction with an optical triangle could produce z_i estimates to greater heights.

A cruder but simpler boundary height estimation scheme (CBL and NBL) is proposed by Benkley and Schulman (1979). The three factors Benkley and Schulman key on are the NBL's dependence on surface winds and roughness, the difficulty in distinguishing mechanical from convective mixing regimes during the daytime and the effects of horizontal temperature advection. The only inputs they require are soundings from the nearest rawinsonde station and local surface winds, temperature and roughness lengths. Mixing depths are determined by a line drawn up the dry adiabat from the current surface temperature to its intersection with the morning sounding. The height of the intersection is taken as z_i. This method assumes no advection and should have a tendency to underestimate z_i because entrainment is not directly considered. Benkley and Schulman (1979) do offer suggestions on what effect a superadiabatic layer may have and an approach to horizontal advection using 700 mb (500 mb in mountainous regions) temperatures. Other assumptions and adjustments are needed based on the particular situation. Garrett's (1981) intercomparison of Benkley and Schulman's estimation scheme and his model to observed data shows both have potential for future use in predicting boundary layer growth.

2.6 Work Related to the BAO

In addition to Kaimal and Gaynor (1983) many other papers and reports have been written using BAO data or data with conditions close to those at the BAO.

A large number of these deal with boundary layer wind profiles, characteristics, diurnal patterns and correlation with drainage flow (Korrell et al., 1982; Schotz and Panofsky, 1980; Panofsky, 1984; Hahn, 1981; Johnson and Toth, 1982b; Hootman and Blumen, 1983). Mahrt (1976) analyzes rawinsonde flights taken during the National Hail Research Experiment (NHRE) between 1972 and 1974 for the vertical moisture structure of the mixed layer. Lenschow et al. (1979) concentrate on a shallow layer near the surface during early morning hours. Using data from both NHRE (1976) and Haswell, Colorado (1975) they analyze rapid changes in a non-homogeneous morning boundary layer. Discussion of how their results might affect observations reported in this thesis are presented in Chapter IV and V.

III. DATA SOURCES AND REDUCTION TECHNIQUES

In this chapter data sources and analysis schemes are discussed. The BAO is described, avoiding some details previously written, while still covering aspects important to this thesis. Table 2 summarizes the entire data set used.

3.1 Overview of the BAO Facility

The BAO is a 300 m research tower completed in early 1978 capable of collecting data year round from eight fixed levels (10, 22, 50, 100, 150, 200, 250, 300 m) and a moveable instrument carriage (Kaimal and Gaynor, 1983). Each level is equipped with a sonic anemometer, fast response temperature, slow response temperature, cooled mirror dew point hygrometer, and a propeller-vane anemometer. In conjunction with the tower instruments, there are several other ground based sensors considered part of the BAO facility. Those sensors used or discussed in this thesis are an Eppley pyranometer, absolute pressure sensor, and an optical system for measuring winds and convergence at the tower. Configuations and characteristics of this instrumentation can be found in Table 3 and Figs. 4a,b.

Signals from all instruments are recorded by an on-site PDP 11/34 computer. Data are sampled at 10 or 1 Hz and averaged into 10 s and 20 min points for storage on tape, except for special experiments when 10

Table 2. Data Summary

	P	SR	T_d	T	Prop S/D	Sonic S/D	DEN 12Z Rawin	DEN 00Z Rawin	Daily WX Map	Sodar Record	Date Code
	BAO	BAO	BAO	BAO	BAO	BAO				BAO	
810622	M	M	P	P	P	P	M	M		M	1
810625	M	M						M		M	2
810711								M		M	3
810728										M	4
820604										M	5
820616				300 m out			M				6
820620				300 m out							7
820621				300 m out						P	8
820708	P	P	P	P	P	P					9
820720											10
820721											11
820724											12
827031							M				13

M - missing
P - partial

Table 3. BAO Sensor Characteristics and Sampling Rates

Standard sensors	Location	Parameters measured	Rate sampled (Hz)	Response characteristics	Basic accuracy
Sonic anemometer	Eight levels on tower, on either boom	$\vec{V}_H$, A_z, u, v, w	10	20-point low-pass filter (~5 Hz cut-off)	>1% or >1 cm s^{-1}
Propeller-vane anemometer	All levels on opposite side from sonic anemometer	S, D	1	1 m distance constant	~3%
Platinum wire thermometer	All levels attached to sonic probe	T'	10	5-10 Hz cut-off	~1%
Quartz thermometer	All levels on SSE boom	T	1	~1 min time constant	0.05°C
Cooled-mirror hygrometer	All levels on NNW boom	T_d	1	~1 s cycle time	0.5°C
Absolute pressure	Surface near tower base	P	1	3 min time constant	1 mb
Solar radiation	Surface, 100 m W of tower	SR	1	~5 min	~5%
Optical triangle sensors	Surface, outer anchor points	S,D,convergence, C_N^2	1	Spatial average over 450 m equilateral triangle	~5%

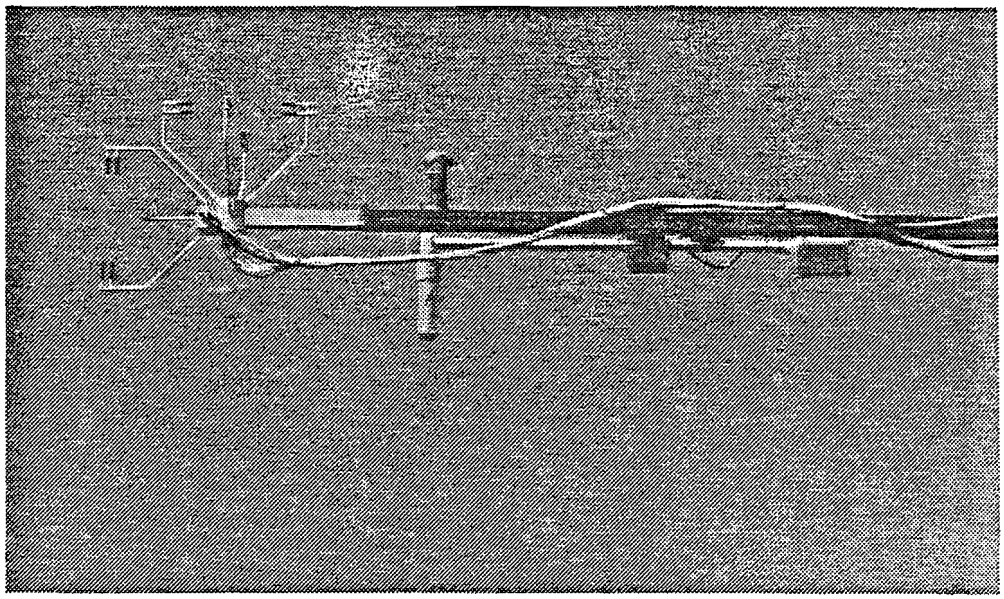

a

Fig. 4a. View of three-axis sonic anemometer, fast-response platinum wire temperature probe, and slow-response aspirated quartz thermometer in a radiation shield.

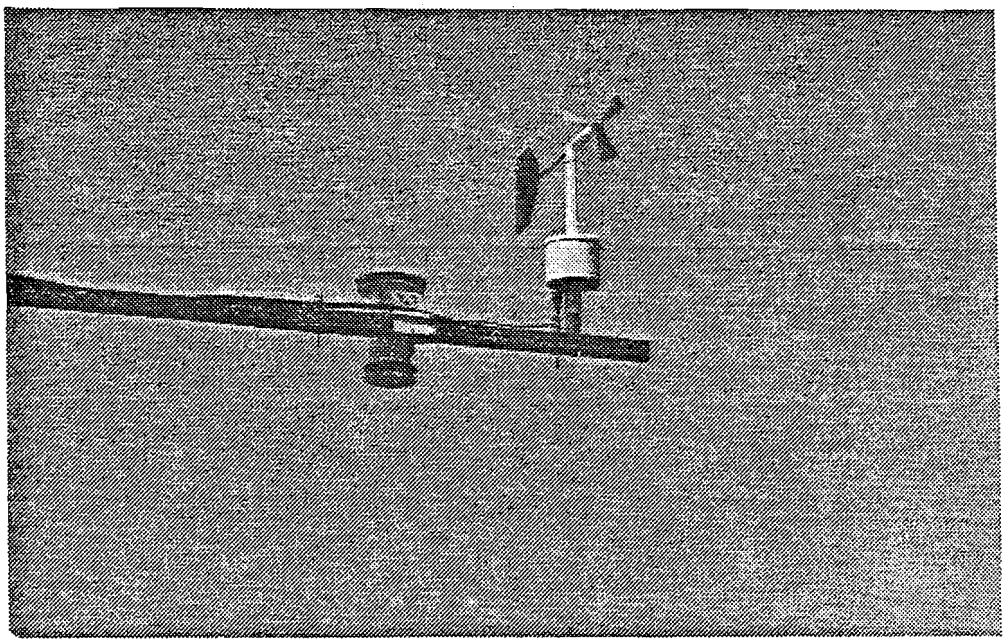

b

Fig. 4b. View of propeller-vane anemometer and cooled mirror dew point hygrometer.

and 1 Hz data are recorded directly. The 20 min mean data are printed out continuously at the tower providing a real-time picture. Near real-time data analysis capabilities are also available on a PDP 11/70 computer receiving the data via a dedicated phone line in Boulder. This second system has numerous programs written to facilitate analyzing these data in either a time series or vertical profile form. All these capabilities have encouraged the study of the early morning CBL at the BAO. Many of the figures in this thesis are products of the BAO data analysis programs.

3.2 Terrain Features

The BAO is situated 45 km east of the Continental Divide and 31 km north-northwest of the city of Denver. Fig. 5 is a two dimensional and Fig. 6 a localized three dimensional topographical map showing the complex terrain surrounding the BAO. The tower lies in a rural setting composed of farms, feed lots, widely spaced private homes, a dairy and the small town of Erie all within a radius of 5 km. The Rocky Mountains are the major terrain feature, with numerous smaller scale topographic features of importance to the BAO. Approximately 90 km to the north and 102 km to the south are the Cheyenne Ridge and Palmer Lake Divide respectively, both extending eastward onto the plains and adding to the already uneven surface heating and flow pattern. Coupled with this high ground are four major river drainage systems. The South Platte river basin, 15 km due east of the tower, flows northeast after

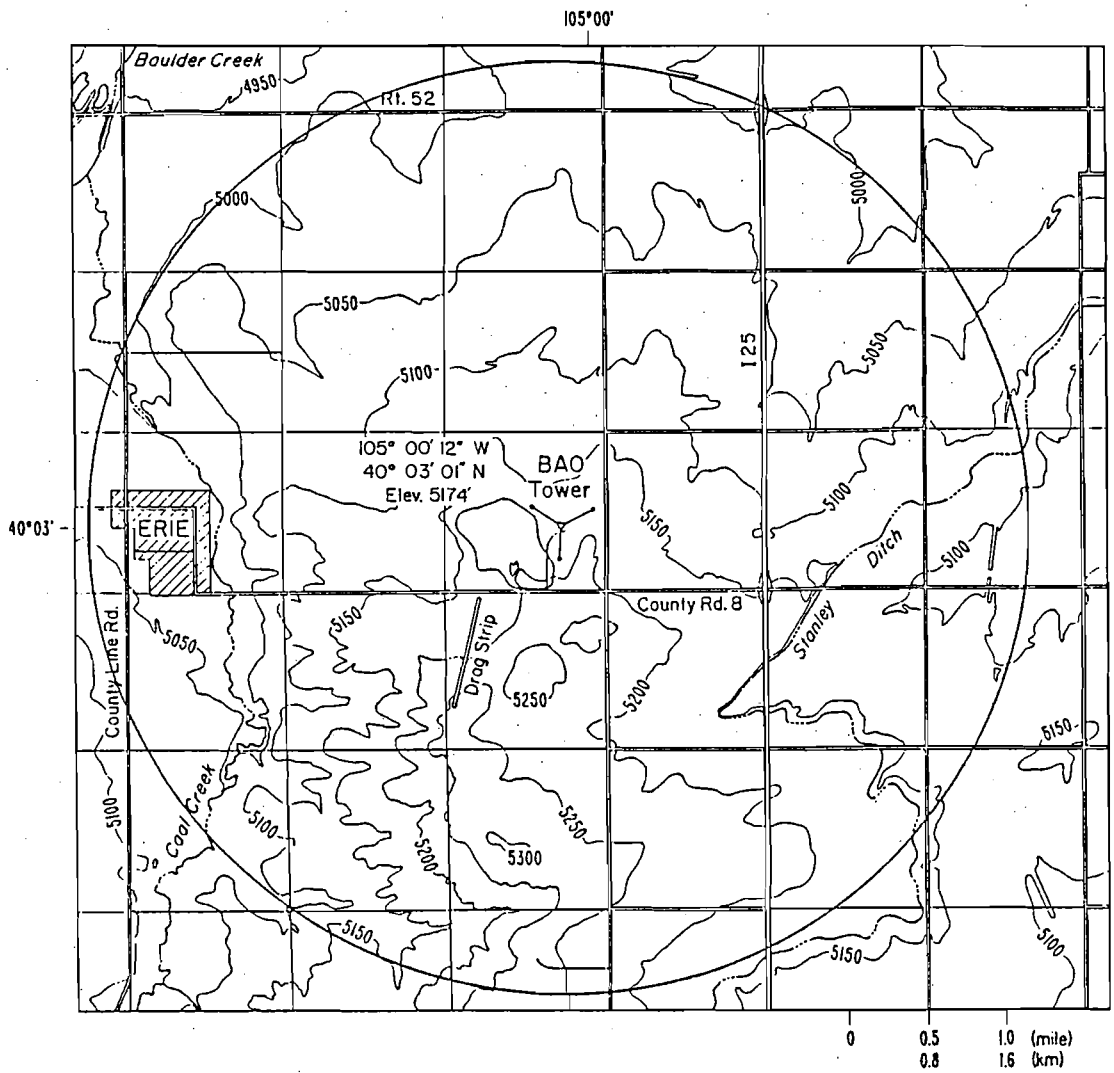

Fig. 5. Contour map of local BAO terrain (circle = 5 km radius).

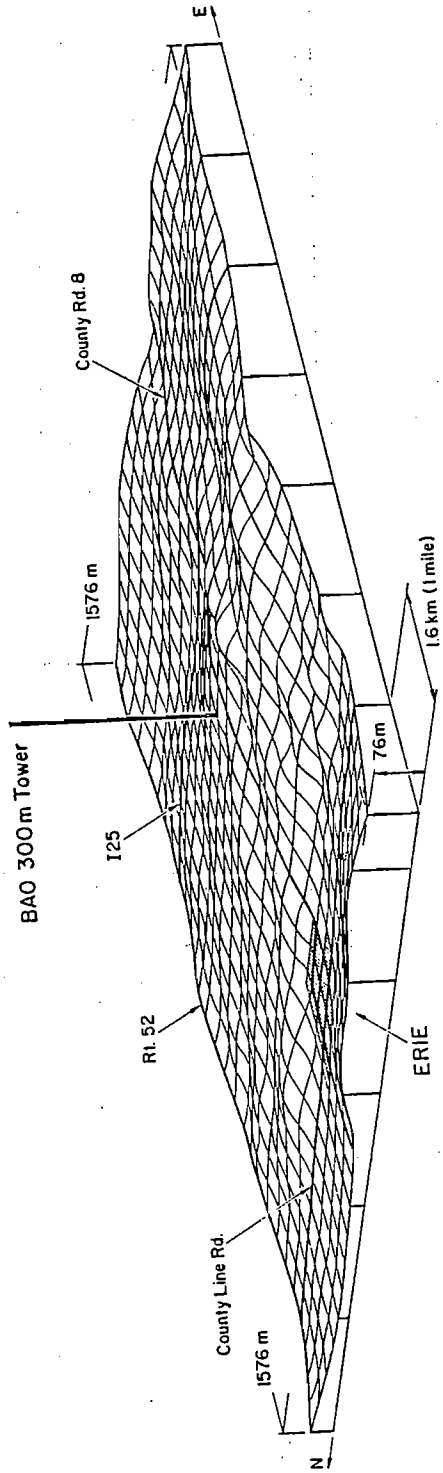

Fig. 6. 3-D view of BAO (w/exaggerated vertical scale).

running through Denver. The remaining three rivers are oriented east-west and located north of the BAO (Fig. 7). Horizontal cross-sections in Fig. 8 depict the four points of the compass extending out 30 km from the BAO. The local terrain around the tower slopes gently downward from the south to north, east and west with a relative flat grade on the order of 2%.

3.3 Instrument Design and Tower Structure Considerations

Due to certain principles of instrument operation and structural configuration of the instruments and tower, some subjective interpolation of the data was necessary.

Cooled mirror dew point sensors use minute hygroscopic particles as a basis for condensation to form on the mirror and thereby measure dew point temperature. Too many particles or particles too large contaminate the mirror producing false or oscillating readings. An automatic heating cycle once every twelve hours for five to fifteen minutes in the dew point sensors eliminates a good portion of this problem. The heating cycle was not synchronized at each tower level but was evident in the time series of the dew point temperatures. When this cycle was found in the data, a linear interpolation was used to extract meaningful data points.

Not all temperature profiles at the BAO appear as expected and at times have "kinks". This is especially evident when the mixed layer encompasses the tower. Parts of the descrepancy are explainable by real atmospheric conditions or bad data, while others are possibly due

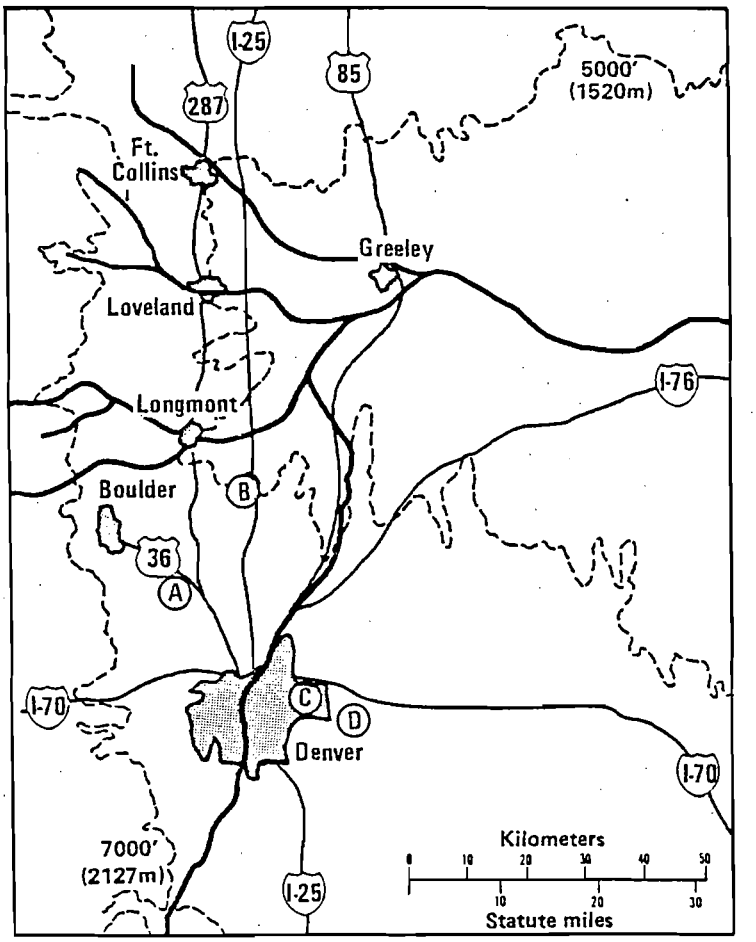

Fig. 7. BAO location relative to the Rocky Mountain Front Range, Denver and major river drainage systems.

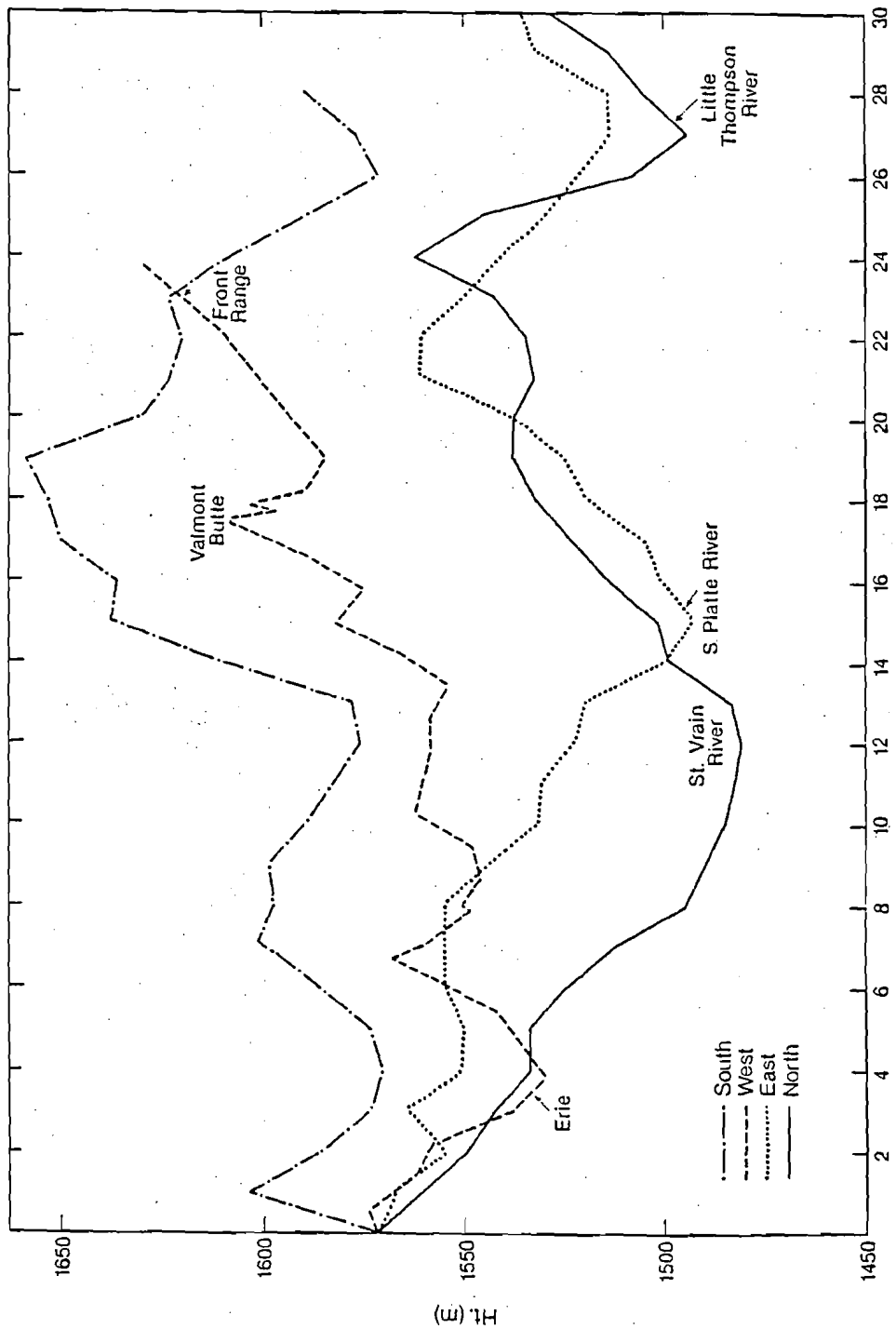

Fig. 8. Horizontal cross-section extending out from BAO at the four major points of the compass.

to the way temperature is measured. Recent studies by Wolfe (not published) on the response characteristcs of temperature sensors at the BAO and work by McTaggart-Cowan (1976) and Slob (1978) on measuring temperature bring to light many unanswered questions. Aspiration rate, shape of the air intake and radiation shields (primary and secondary) are all known to be important when measuring temperature. Side by side tests of BAO temperature sensors show there are also effects due to individual sensor time constants and even 20 min averages of two closely mounted sensors are not free of these effects. Most of the effects are small and can't be easily distinguished from the others. When comparing two or more like sensors one must be aware of their relative accuracies because of these physical processes.

At the BAO the sonic and propeller-vane anemometers are located on opposite sides of the tower (see Fig. 1.2, Kaimal et al., 1980, BAO Report No. 2) to provide useable winds for all directions. Because of this configuration, a computer program was written to determine which sensor was on the lee side and to perform some additional data quality checks. The sonics were tested first for tower shadowing (Gill et al., 1967 and Cermak and Horn, 1968) and used when possible. If the sonics were shadowed, the propeller-vanes were used after examining the data for any 0-360° phase shift problems. BAO software uses a phase analysis routine on each 1 Hz sampled point, but even this does not eliminate erroneous readings for the propeller-vanes when winds are light and variable. If only one of the instruments was functioning properly

it was used regardless of positioning on the tower. Analysis of tower shadowing effects at the BAO indicate that 20 min mean directions and speeds do not differ significantly for the two sensors. This fact is also evident by agreement of the wind data found in this thesis.

The following BAO calculation was also considered when using sonic and propeller-vane 20 min data. The sonics measure two horizontal wind components (u,v) and from each 20 min mean of u and v a speed and direction are calculated. This type of calculation produces a vector average rather than a scalar average like that obtained from the propeller-vanes. The need for recalculating 20 min means in a consistent fashion was not deemed necessary as the two types of averaging produced only minor differences.

3.4 Tower Data Set

The time period chosen for analysis is from just prior to sunrise at 0400 Mountain Standard Time (MST) until 1140 MST. Table 4 shows the 20 min data set for the thirteen days during June and July of 1981 and 1982 with a '1' indicating data present and a '0' meaning no data available. Eight of 13 days chosen have continuous data, 2 days are missing data near the end of the analysis period and the 3 other days are missing no more than 2 non-consecutive 20 min periods out of 24 possible. Missing data toward the end of the analysis period is not considered significant as the boundary layer was above or nearly above the height of the tower by this time. Single missing points were

Table 4. BAO Data Synopsis

DATE YYMMDD	HOUR (MST)							
	4	5	6	7	8	9	10	11
810622	111	111	111	111	111	100	000	000
810625	101	110	111	111	111	111	111	111
810711	111	111	111	111	111	111	111	111
810728	111	111	111	111	111	111	111	101
820604	111	111	111	111	111	111	111	111
820616	111	011	111	111	101	111	111	111
820620	111	111	111	111	111	111	111	111
820621	111	111	111	111	111	111	111	111
820708	111	111	111	111	111	111	100	000
820720	111	111	111	111	111	111	111	111
820721	111	111	111	111	111	111	111	111
820724	111	111	111	111	111	111	111	111
820731	111	111	111	111	111	111	111	111

1 = data available
0 = data missing

linearly interpolated by using both vertical and time series data. Individual days and the criteria for their choosing are presented in the following two chapters.

Twenty 20 min averages used provide two advantages. First they serve to smooth out small scale changes that may not be important to the overall boundary layer growth. Secondly they allow for interpolation of missing points with minimum impact on the complete data set. Times of all BAO data points are the start time of the 20 min averaging period. All times are MST unless otherwise stated.

3.5 Sodar Data

Monostatic sodar facsimile records were available on 8 of the 13 days (Appendix B). The NOAA, WPL Mark VII sodar (Owens, 1975) was located at three different positions around the tower on these days. Smaller spatial scales eliminated by sodar volume averaging and tower time averaging make the spatial separations between sodar and tower of little consequence. Positions and specifications of the BAO system are given in Fig. 9 and Table 5. Sodars operate in a manner very similar to micro-wave radars by transmitting a sound pulse that is scattered off small scale acoustic refractive index fluctuations in the atmosphere. These fluctuations are usually areas of turbulence associated with inversions or convective regions that affect the temperature structure. The sodar records in this thesis were produced by a 2 KHz signal pulsed every 5 sec reaching a height of 850 m (based on an

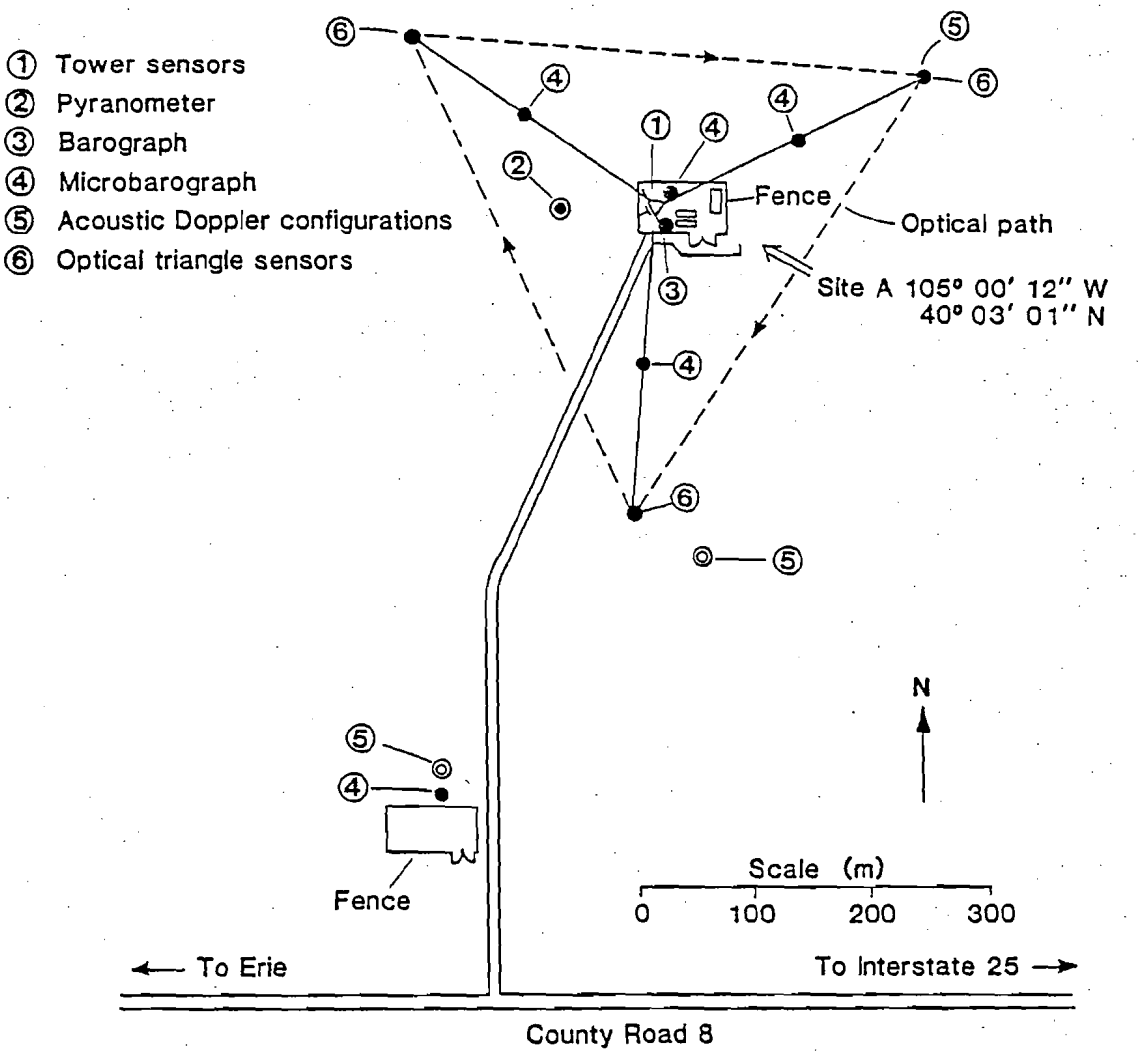

Fig. 9. BAO site showing sensor positions.

Table 5. Sodar Specifications

A)	Frequency (f)	2000 Hz (w/100 Hz bandwidth)
B)	Pulse width (pw)	.04 s
C)	Pulse repetition rate (pr)	5 s
D)	Beam pattern (b)	4° from center of beam
E)	Speed of sound (c)	340 m s^{-1} (at 14°C)
F)	Receiver delay (d)	~.117 s
	Maximum height	(pr•c)/2 = 850 m
	Minimum height	(d•c) = 40 m
	Vertical resolution	(pw•c) = 13.6 m

Ht (m)	Sample Area[1] (m^2)	Sample Volume[2] (m^3)
300 m	1381	18788
200 m	614	8350
100 m	153	2087

1 Area = πr^2 r = tan 4°•Ht

2 Volume = Area • vertical resolution

average speed of sound of 340 ms^{-1}). Minimum height, restricted by system design to eliminate pulsed signal feedback, is 40 m. The facsimile record actually represents an integrated volume because of the nature of sodar measurement techniques. This volume increases with height as a direct function of beam width while the height resolution remains a constant 13.6 m. Although the original sodar records extend up to 850 m, Appendix B depicts traces of only 425 m in height. Reasons for this are the physical properties (molecular absorption and attenuation) of sound in the atmosphere and the changes in the temperature structure with time which combine to limit acoustic scatter at higher altitudes. An excellent quantitative reference on sodars is found in Neff (1975).

3.6 Other Supporting Data

Additional data are used to provide a synoptic picture and extend the vertical profiles of potential temperature, dew point temperature and the wind. Synoptic summaries in this thesis are based on data taken from NOAA's "Daily Weather Map" series (Appendix C) and three hourly surface maps available from the National Climatic Center in Asheville, NC. Rawinsonde flights (12Z /05 MST; Appendix D) from Denver are used along with WBAN-11 daily surface observations to provide additional sky cover, pressure and wind information.

3.7 Data Reduction

Nearly all BAO-related data were useable for analysis with minimal processing. The exceptions were potential temperature (θ) and specific humidity (q). The BAO software calculates 20 min means of wind speeds and directions, dew points and absolute temperatures. All other parameters were calculated especially for this thesis. Data processing was done on the BAO PDP 11/70 computer.

To calculate θ, it is first necessary to obtain an absolute pressure at each of the eight tower heights using the hypsometric equation. Inputting these pressures and their corresponding temperatures into Poisson's equation we obtain θ. Specific humidity calculations also use the absolute pressure found for each level to extract vapor pressure (e_p) from the dew point temperatures. The equation for calculating e_p was taken from Murray (1967). Dew point temperatures are used in place of the ambient temperature in the equation which then calculates e_p rather than saturation vapor pressure. Once e_p is determined it is converted to q using Murray's approximation. The equations for finding θ, e_p and q are found in Appendix E.

It should be noted here that virtual (T_v) temperature and virtual potential (θ_v) temperature are not used or calculated. This could be important if there are either large mixing ratios or changes in the gradient of the mixing ratio. High levels of moisture in the atmosphere can contribute significantly to the buoyancy or lifting of a

parcel. Moist air is less dense than dry air (at the same pressure and temperature) and therefore more buoyant. Where large moisture gradients exist the interpolation of the stability will be affected if the virtual temperature is not considered. A significant decrease in moisture with height will indicate more stability with respect to the environment than actually exists if using a simple "dry" temperature curve. As will be seen later in the data analysis, moisture levels and gradients are not of the magnitudes to produce changes worthy of this additional calculation.

IV. SELECTION OF DAYS

Five basic criteria were used to select observational cases. These criteria are as follows:

1. Sky cover ≤0.3 (at Denver) in the early morning
2. Continuous data available from the BAO
3. Solar radiation data available at the BAO
4. Nocturnal inversion existing at the tower at sunrise
5. Undisturbed synoptic conditions

This list represents the hierarchy used to obtain a quality data set.

4.1 Sky Cover

Clear skies or opaque cloud cover less than or equal to 0.3 at 0750 MST was the initial guideline. Cloud observations from Denver are a subjective measurement, especially at night or near sunrise and because of this, reports were analyzed both as an individual observation and as a total picture of the sky conditions. Clouds reported to the west over and along the foothills were not regarded as important to early morning boundary layer growth. Denver hourly sky conditions (opaque/total) are given in Table 6 from 0400-1200 with an example of actual cloud types observed at 0750 listed in Table 7. Evidence of correlation between mixed layer growth and cloud cover is discussed in

Table 6. DEN Sky Cover

Time (MST)	0400	0500	0600	0700	0800	0900	1000	1100	1200
Date									
810622	0/2	0/2	0/0	0/0	0/0	0/0	0/0	0/0	0/0
810625	0/0	0/0	0/0	0/0	0/0	0/0	0/0	0/0	1/1
810711	2/3	5/7	3/4	2/2	0/0	0/0	1/1	2/2	1/3
810728	0/0	0/0	0/0	0/0	0/0	0/0	0/0	0/0	0/0
820604	0/0	0/0	0/0	0/0	0/0	0/0	0/0	1/1	1/1
820616	0/0	0/0	0/0	0/0	0/0	0/0	0/0	0/0	0/0
820620	0/0	0/0	0/0	0/0	0/0	0/0	0/0	0/0	0/0
820621	0/1	0/1	1/1	0/1	0/0	0/0	1/1	1/1	2/2
820708	0/0	0/0	0/0	0/1	1/2	2/2	3/3	5/5	7/7
820720	0/0	0/0	0/0	0/0	0/0	0/0	1/1	3/3	3/3
820721	0/0	2/8	2/8	0/0	0/0	0/0	0/0	1/1	3/3
820724	0/0	0/0	0/0	0/0	0/0	0/0	0/0	0/0	0/0
820731	0/0	0/0	0/0	0/0	0/0	0/0	0/0	0/0	0/0

opaque/total (1/10's)

Table 7. DEN (0750 MST) Sky Cover

Date	L	M	H	Total opaque	Total
810622			0 Cs	0	0
810625	0 Cu			0	0
810711		0 Ac	0 Ci	0	0
810728				0	0
820604				0	0
820616				0	0
820620	0 Sc			0	0
820621	0 Cu			0	0
820708	0 Sc	0 Ac	2 Ci	1	2
820720				0	0
820721	0 Cu			0	0
820724				0	0
820731	0 Cu			0	0

(1/10's)

Holzworth (1967) and shown by Schewe (1975). Cloud cover as a rule reduces the intensity of the surface heat flux which slows or stops the growth of the mixed layer. Stull (1976b) believes that CBL growth stops when a balance between entrainment, synoptic scale subsidence and convective cloud induced subsidence is reached. Representativeness of the Denver data was verified by comparison with Buckley Air Base and Broomfield (Jefferson County Airport) observation stations (Fig. 7) and solar radiation data from the BAO. Total sky conditions were also examined using hourly satellite imagery.

4.2 Data Continuity

To provide an adequate picture of the CBL evolution, nearly continuous operation of the BAO tower was required during the early morning. Chapter III Section 4 describes the data and Table 4 indicates data availability. Only four individual 20 min periods are missing and require interpolation of all the tower parameters. Three of these periods are in the initial sunrise transition period where changes are small and erratic but it is felt that a combination time series and height linear interpolation is able to reproduce an accurate 20 min mean. The remaining missing period occurred after the mixed and superadiabatic layers have already formed. Interpolation here may create a false inversion rise, but should not affect the overall growth pattern.

Individual instrumentation problems are unavoidable and handled in the same manner as entire missing periods. Dew point heating cycle

points are easily corrected for because dew point 20 min values do not exhibit rapid changes that make interpolation difficult. Wind data has two sensors making the chances of missing data small. Problems encountered with the temperature sensors were confined to the 300 m level on three days when the aspirator motor failed. Because tracking the mixed layer depth above 250 m was not possible these points were left out of the analysis.

4.3 Solar Radiation

The BAO pyranometer measures both direct and diffuse short wave solar radiation. Solar radiation data are then used in conjunction with cloud observations to confirm sky conditions at the BAO. The data of 11 July 81 and 8 July 82 are two periods in which BAO solar radiation data are given priority over Denver cloud observations. A time series (Fig. 10) of 11 of the 13 days extending beyond the 24 analysis periods shows both early morning similarities and afternoon differences of the incoming solar radiation at the BAO. These differences are not unexpected since cumulus clouds form along the front range and move slowly eastward as the days progress. Toth and Johnson (1983) shows a similar time series of solar radiation data for several PROFS (Program for Regional Observing and Forecasting Services) stations in 1982 over northeastern Colorado.

Some cloud build-up does occur out over the plains, but normally develops too late in the day to affect the morning boundary layer

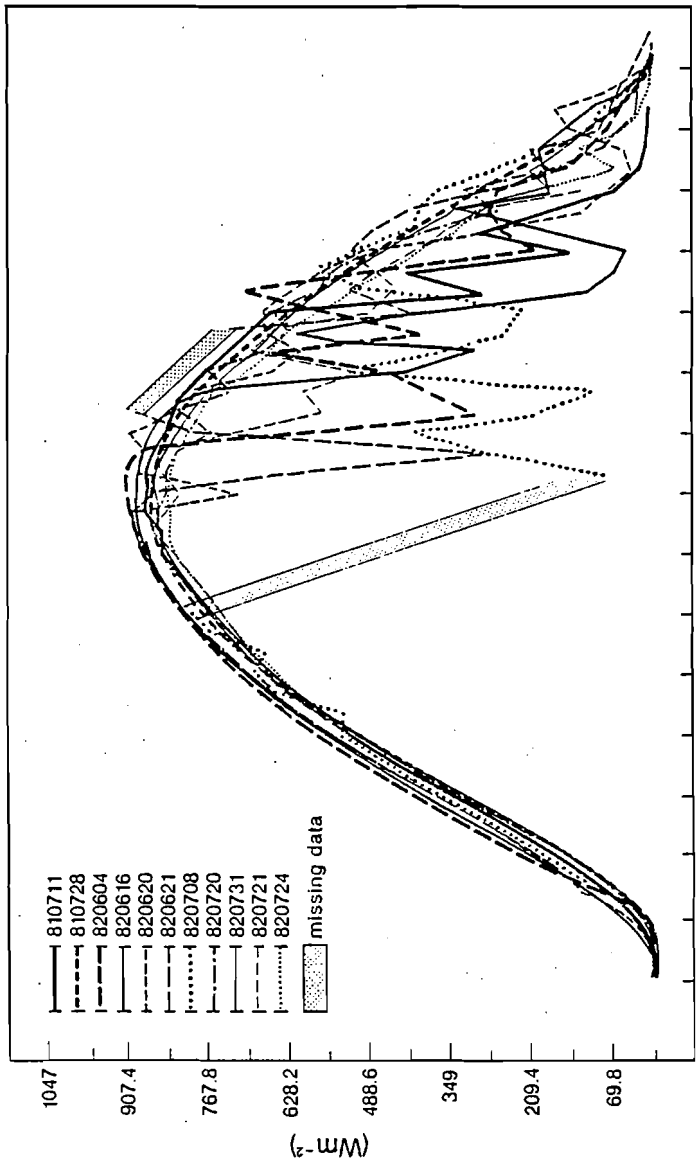

Fig. 10. BAO solar radiation time series of 20 min means (direct and diffuse) 0400-2000 MST; 11 days.

growth. Johnson and Toth (1982a) look at the interrelations of mesoscale flow patterns, heating of the sloping terrain and preferred areas of convective activity over northeastern Colorado.

A nearly unobstructed horizon greets sunrise, with gradually sloping terrain east of the BAO. Artifical horizon tests at the BAO show minimum elevation angles of less than 2 deg. Sunrise varies a maximum of 27 min for all cases and produces some minor differences in the initial solar radiation data (Fig. 10). These differences are insignificant in affecting the overall boundary layer growth because of other physical processes taking place at the surface (e.g., evaporation, surface heating) that essentially control the growth rate. Surface albedo, conductivity and moisture all play a part in how this incoming energy is distributed. Mean daily values taken from climatological data for June (Trewartha and Horn, 1980) and July (Climate of the United States, 1974) indicate lower cumulative amounts (2.09×10^5 Wm^{-2}) of solar radiation present by 1140 than the average of the 13 observational days (2.22×10^5 Wm^{-2}). Approximately 47% of the total daylight occurs by 1140 during June and July. This difference in total incoming energy can be explained by the fact that the comparison is between individual "clear" days and monthly averages taken from several years of data.

4.4 Nocturnal Inversion

Radiation inversions, as mentioned earlier, have an effect on boundary layer growth. The stonger the initial stability at the surface, the slower the CBL grows all other factors being equal. Strong surfaced based radiation inversions might be expected on all selected days from our initial criteria of clear skies. This is true for the 13 observation days, but not for all days originally surveyed (as a consequence of other factors, e.g., strong winds, cloud cover, etc.).

In Fig. 11 are θ profiles at 0400 presented as departures from the lowest tower temperature (10 m) for each 20 min period. These 20 min mean profiles for each day show inversions, but they are not all identical in structure. Soundings from Denver at 12 Z/05 MST (Fig. 12) are used for extention of the vertical profiles, but the question again arises of how representative Denver's conditions are to the BAO. Comparisons of tower profiles to Denver soundings are not expected to produce compatible results based on their spatial separation, 20 min tower averaging versus rawinsonde individual sample points and vertical resolution. Standard rawinsonde ascent rates are 300 $mmin^{-1}$ which translates into only two to three data points within the 300 m tower height. Taking into account the additional factors of horizontal advection, local terrain features and sometimes poor signal levels during the first minutes of a rawinsonde flight, comparisons with the BAO tower are not likely to be good. Despite these differences Fig. 13 shows good agreement in all cases but one (8 July 1982) and even the

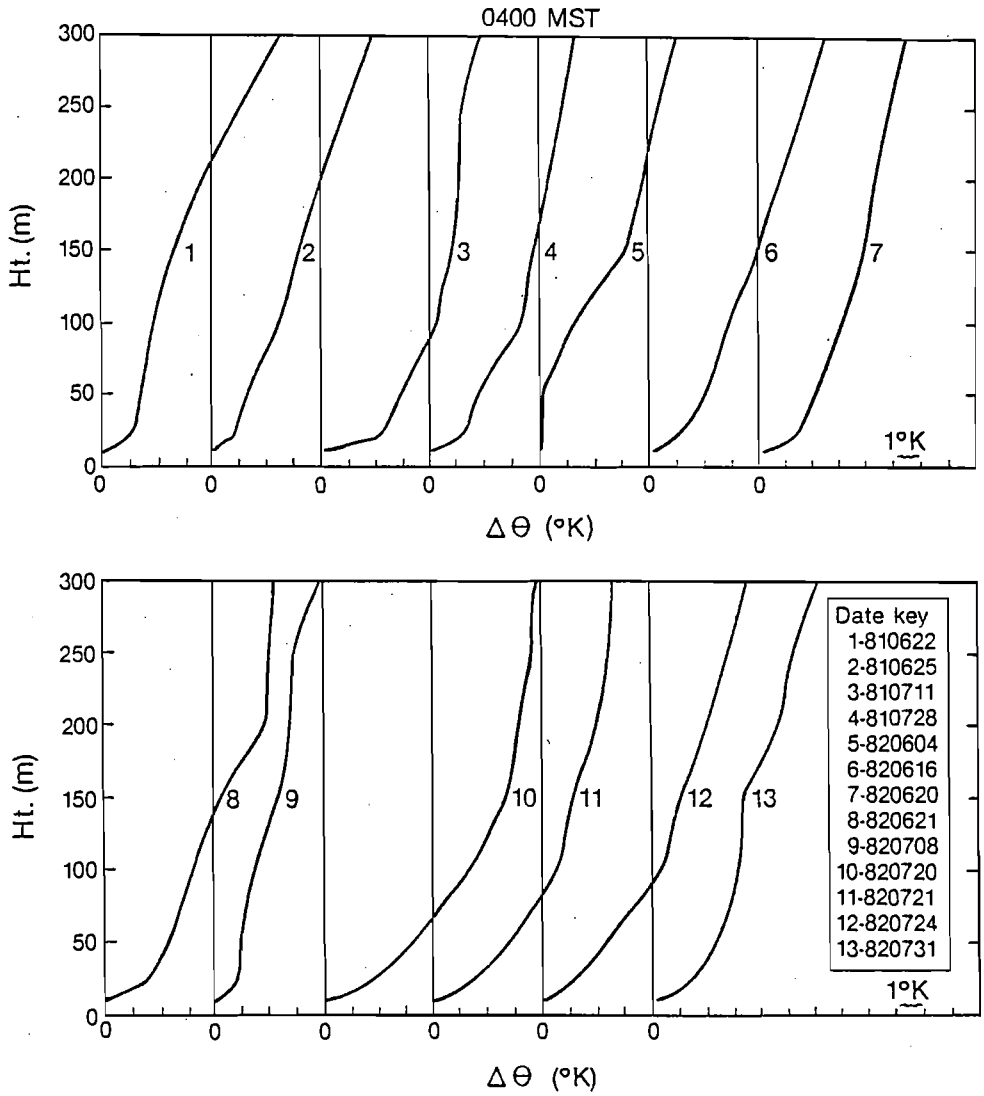

Fig. 11. BAO 0400 MST $\Delta\theta$ profiles of 20 min means ($\Delta\theta = \theta_z - \theta_{10\ m}$); 13 days.

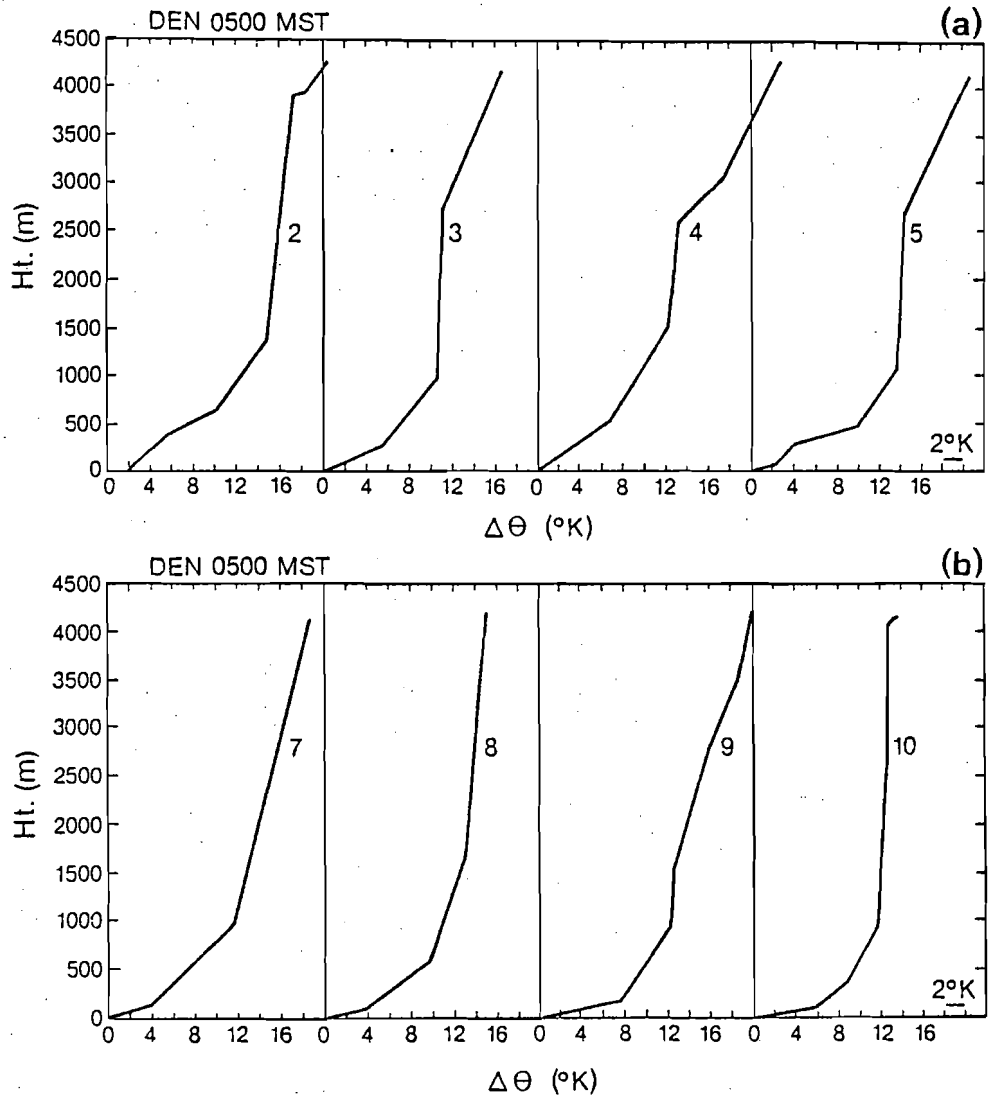

Fig. 12. DEN 0500 MST rawinsonde $\Delta\theta$ profiles ($\Delta\theta = \theta_z - \theta_{sfc}$); 10 days.

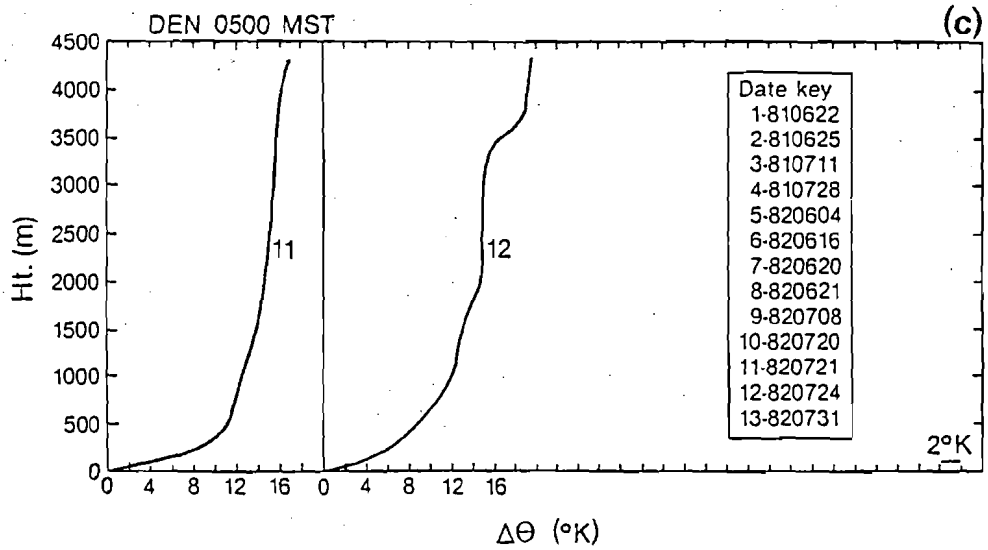

Fig. 12. (continued)

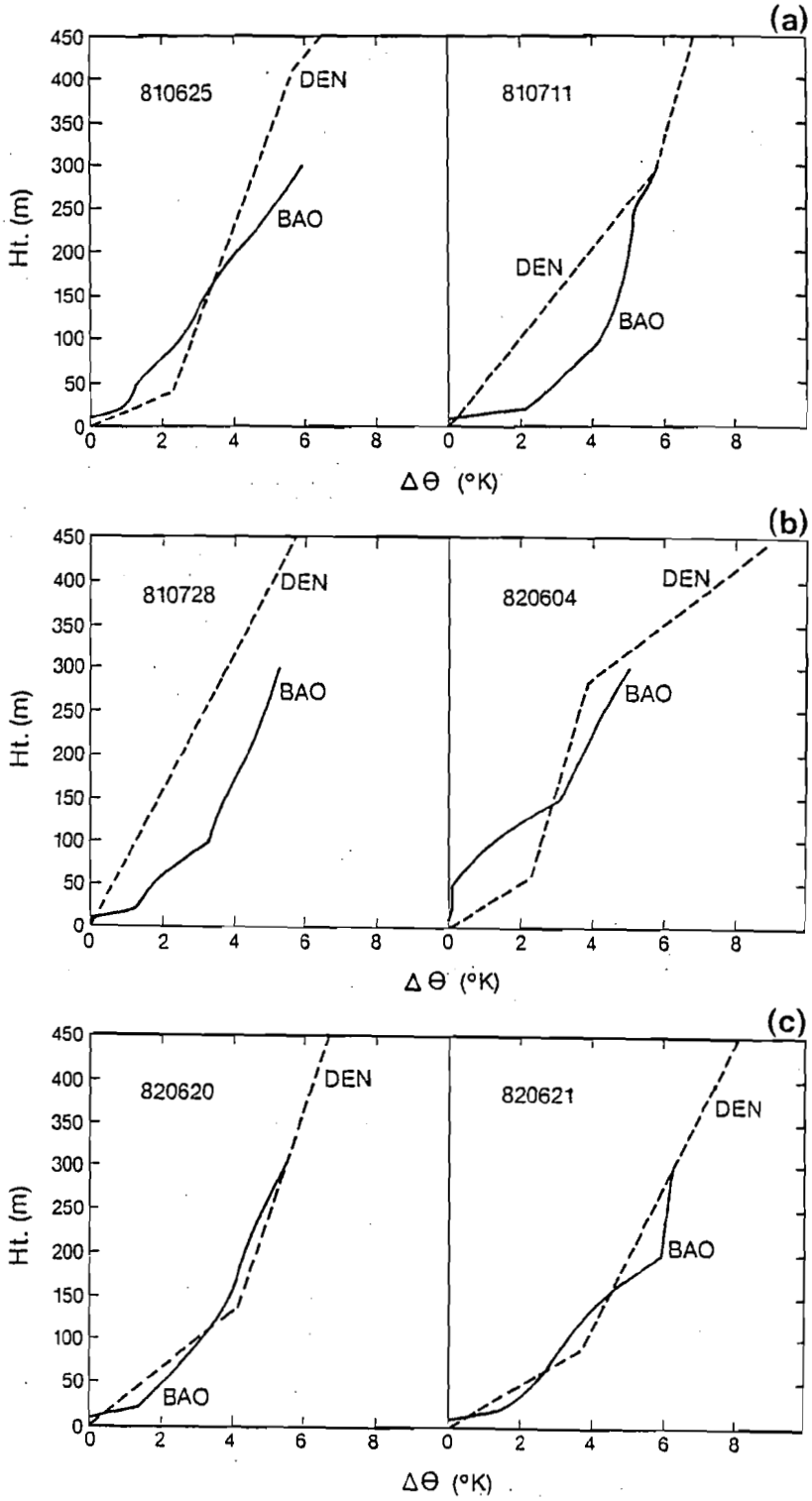

Fig. 13. BAO (0400 MST) vs. DEN (0500 MST) $\Delta\theta$ profiles; BAO $\Delta\theta = \theta_z = \theta_{10\ m}$ and DEN $\Delta\theta = \theta_z = \theta_{sfc}$; 10 days.

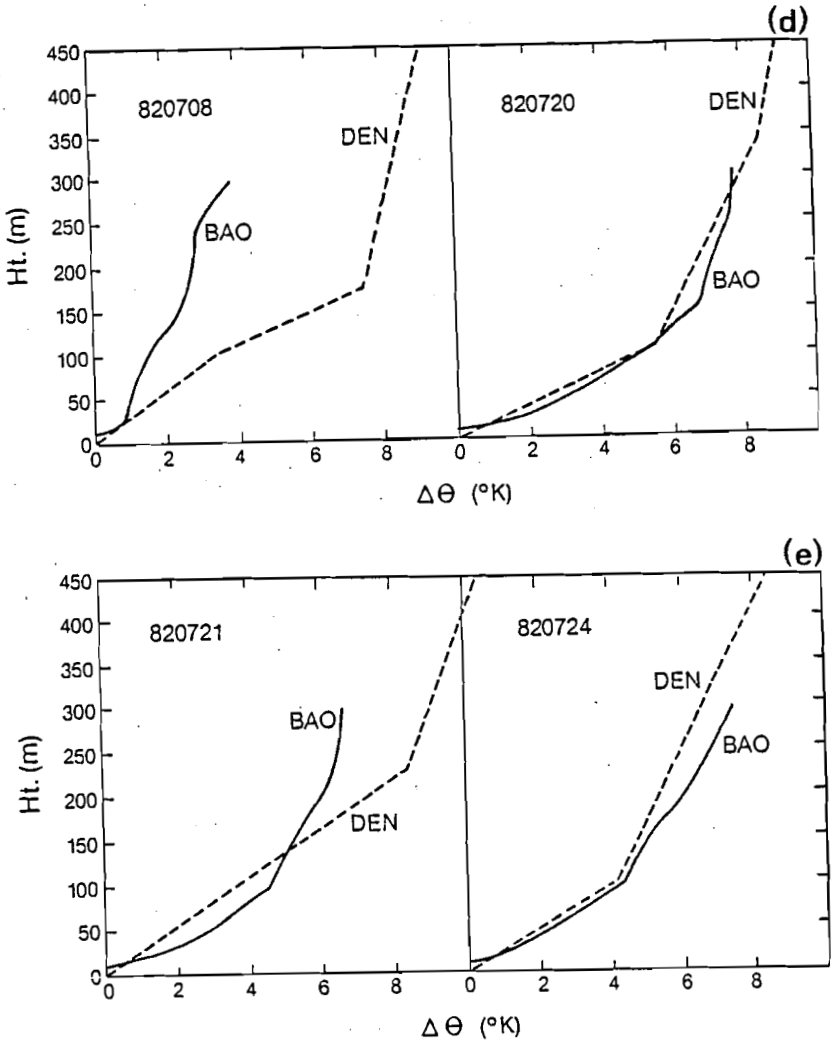

Fig. 13. (continued)

sharp inversion structure in the lowest levels compares better than expected. It should be noted that 0500 MST (12Z) is the approximate time that rawinsonde data is transmitted while actual release times are about 60 min prior to this.

Features in addition to the surface inversion are visible in the Denver skew-T/Log P plots up to 500 mb (Appendix D); dew point temperature and wind profiles. The surface based inversions extend to an average depth of 308 m varying from 91 m at the shallowest to a maximum of 530 m. The stability is greatest near the surface and weakens upwards to 1372 m on the average or nearly 700 mb in all cases. From this point up to 500 mb (~4200 m AGL) there are both adiabatic lapse rates and some instances with slight stability. On three of the days an increase in stability accompanied by a layer of rapid drying is found near 500 mb. Upper regions such as these are often indicative of high pressure with subsidence warming and drying aloft. As synoptic conditions show, all three days do have high pressure to the north. Yoshino (1975) and André and Mahrt (1982) discuss similar profiles and some reasons for their formation.

Rapid and continual drying with height exists on four of the eight days available. On three other days drying just above the surface evolves into a constant mixing ratio profile. Surface values of the dew point and air temperatures are very close due to radiational cooling of the air overnight.

The wind profiles are in good agreement with the overall synoptic situations. Seven of the eight days have light winds up to 500 mb. Even though light and mostly variable, there is a tendency for southerly surface flow consistent with the local and South Platte river drainage effects and synoptically forced WNW winds near 500 mb. The absence of strong westerly downslope winds and any significant veering (counter-clockwise rotation) with height precludes significant warming or increasing stability due to orographically induced subsidence.

4.5 Synoptic Conditions

Synoptic controls, though last on the list, are a dominant factor in final selection of the days. It was the goal of this selection process to collect a set of data based on the first four criteria that were then found to be undisturbed synoptically. Typically, an upper level ridge in conjunction with a strong high pressure system positioned over the region would be considered ideal. As it turned out, several days had to be discarded because of unwanted synoptic disturbances even after meeting the first four criteria. Table 8 is a meteorlogical summary showing a comparison between the days and Appendix C contains the 0500 surface and 500 mb charts for each day. It should be noted that the winds plotted for Denver on 21 July 1982 at 0500 are not consistent with Denver's original observation form (WBAN-11). The observed winds are 210° at 10 kt compared to 210° at 20 kt for the plotted data. Winds recorded in the log are assumed correct and seem to fit in with the local gradients and surrounding stations.

Table 8. Meteorological Summary

Date	DEN (0500 MST) sfc P (mb)	DEN (0500 MST) 700 mb Ht (m)	DEN (0500 MST) 500 mb Ht (m)	DEN (0500 MST) Lowest 100 mb average moisture (g/kg)	BAO (0400 MST) sfc T (°C)	BAO (0400 MST) sfc q (g/kg)	BAO (0400 MST) Precip. last 24 hr. (mm)	BAO (0400 MST) Sunrise (MST)	BAO (0400 MST) Solar* Radiation ($Wm^{-2} \times 10^5$)
810622	1010.0	--	--	--	15.35	9.99	0	0432	--
810625	1018.1	3215	5940	7.89	15.21	10.61	0	0433	--
810711	1008.8	3217	5960	7.81	22.65	8.14	1.8	0441	2.18
810728	1014.2	3138	5890	8.74	13.49	9.43	0	0455	2.16
820604	1006.3	3095	5740	4.87	7.43	7.58	0	0433	2.38
820616	1011.7	--	--	--	8.41	6.38	2.8	0431	2.36
820620	1013.4	3132	5800	5.12	12.98	5.97	0	0432	2.31
820621	1010.5	3132	5810	4.93	12.90	6.67	0	0432	2.32
820708	1009.1	3147	5850	4.96	16.41	6.79	0	0439	--
820720	1011.4	3175	5890	3.27	20.64	5.35	0	0448	2.13
820721	1013.9	3202	5940	3.50	22.01	5.95	0	0449	2.10
820724	1011.6	3187	5930	4.56	19.09	6.99	0	0451	2.10
820731	1016.1	--	--	--	16.51	10.58	0	0458	2.11

* Cummulative amount from 0400-1140 MST

Table 8. Meteorological Summary (continued)

	Satellite synopsis	500 mb spd (kt)	500 mb dir (deg)	Surface synopsis	500 mb synopsis
810622	CLR	25	290	weak upslope gradient 1017 H to N	zonal
810625	CLR	10	310	weak upslope gradient 1027 H to N	weak ridge to W
810711	CLR	10	250	weak downslope gradient 1005 L to NE	weak ridge over eastern 2/3 of U.S.
810728	CLR	10	270	southerly gradient weak winds 1023 H to NE	weak trough to E
820604	CLR	30	260	southerly gradient 1003 L over Salt Lake City	short wave moving on coast Pac. N.W.
820616	CLR	15	330	weak southerly flow 1018 H in eastern Colorado	trough in mid-west
820620	CLR	10	270	northerly gradient cold front in eastern Wy. 1004 L over N. Wis.	trough over Great Lakes moving NE
820621	CLR	15	310	very weak southerly gradient stationary front in NE Colo.	slight ridging
820708	CLR	25	260	weak southerly gradient stationary front to SE 1020 H to E	weak ridge along front range
820720	CLR	5	300	center of weak High 1013 H over Colorado	zonal
820721	CLR	25	350	weak NW gradient 1017 H in central Wy.	weak short wave in mid-west
820724	CLR	25	240	weak southerly winds cold front in NE Colorado	slight ridging over central U.S.
820731	CLR	20	310	western side of broad High over central U.S.	weak ridging along Rockies

Review of the summary and Appendix C finds strong high pressure the exception rather than the rule. Weak pressure gradients and light winds dominate the synoptic pattern. Several days originally considered were dropped because of advective cooling behind a cold front. Days with high winds were also eliminated because of the strong advection present. By choosing undisturbed situations, large-scale synoptic forcing can be almost completely eliminated as one control of the tower mixed layer growth. Previous work by Hahn (1981) with BAO data and Johnson and Toth (1982b) with the PROFS data along the front range show that in the absence of large scale synoptic controls, a well defined diurnally-forced mesoscale circulation pattern takes over.

Upper level winds and ridge/trough patterns as seen on the 500 mb charts serve to support the clear skies and weak surface conditions found. No major troughs or storm systems are evident on any of the 13 days, nor is strong ridging present. Zonal flow and weak ridges are the preferred patterns.

V. OBSERVATIONAL RESULTS

5.1 Potential Temperature

5.1.1 Pre-growth (Inversion)

With data included 40 to 60 min prior to sunrise, we are able to observe the final stages of the nocturnal inversion and atmospheric conditions not yet affected by surface heating. Inversions seen at the tower and Denver are influenced by two mechanisms, turbulent heat flux divergence (mechanical mixing) and radiative cooling both at the surface and in the atmosphere. Near the ground the effects of wind shear and friction induced mechanical mixing on deepening the NBL are several times larger than the effect of radiative cooling.

Inversions form at night when the surface cools to below the temperature of the overlying air. From this time until morning the air just above the surface also begins to cool by radiating energy upward and downward creating a low-level inversion. Without vertical mixing the inversion remains sharp and shallow. Mixing of the cold air through mechanical processes (wind shear) reduces the strength of the inversion at the same time it deepens. Holzworth (1967) and Schewe (1975) find a general correlation between increased wind speed and decreased inversion frequency. A fixed relationship of wind speeds to inversion frequency has not been found, but it seems logical that

stronger cooling near the surface can tolerate higher winds and larger shears before the inversion is mixed out. In the atmosphere above the turbulent region radiative cooling along with heat transfer by molecular diffusion are small relative to mechanical mixing and cooling near the surface. It is the combination of these different cooling and mixing rates that determines the Denver 0500 potential temperature profile (Fig. 12). Negative buoyancy and downward heat flux work against upward mixing, making the height of the NBL much less than its daytime counterpart (CBL).

The remnance of the mixed layer from the previous day are also seen in elevated regions of the soundings where the vertical gradient of θ approaches zero. Results in this thesis (to follow later) are consistent with those of Carson (1973) showing that the actual lapse rate of θ remains slightly positive even in well mixed areas of the daytime CBL.

5.1.2 Growth Processes in the Early Morning

As surface heating begins, there is no noticeable warming of the air or formation of a mixed layer. A certain amount of warming of the ground takes place depending on surface conditions. Water at the surface and in the soil absorbs a portion of the incoming solar energy and eventually evaporates if the air is subsaturated.

In a semiarid region such as the eastern plains of Colorado, there is almost always large potential evaporation. Available moisture begins to change phase very quickly after sunrise. Local moisture at the tower is limited to irrigation ditches, condensation forming at the surface during the night and moisture remaining from isolated summer showers. It is just after sunrise when the incoming solar energy is small and relative amounts of liquid water are at their maximum that the evaporation and evapotranspiration (physical exchange of heat and moisture between the vegetation and atmosphere) are most likely important. During this period a large portion of the available energy is often not used for warming the atmosphere.

Considerable work in the field of climatology by Geiger (1965), Sellers (1965) and Yoshino (1975) examines the effects of surface conditions and heating on the overlying atmospheric boundary layer. Local vegetation at the BAO, except for the immediate tower area, consists of natural grasses and fields of wheat and corn separated by rows of bare soil. During midsummer to late summer when the wheat and corn are ready for harvest, evapotranspiration normally drops off. Rosenburg et al. (1983) have examined the microclimate of fields similar to those surrounding the BAO. A term they call the "internal" boundary layer is described and represents the layer of air downwind of the leading edge of a new underlying surface. The internal boundary layer, for practical purposes the same as the surface layer, is being affected by a change in the surface conditions. Three such effects possible at the

BAO are evaporation in near-by irrigated fields, air flow parallel versus perpendicular to planted rows and regional sensible heat advection ("oasis effect").

Recent work by Lenschow et al. (1979) examine the morning boundary layer growth over complex terrain in northeastern Colorado and the effects of cold air drainage and mechanical mixing. Cold air forming close to the ground during the night and horizontal density differences along with uneven terrain force the heavier air to seek the lowest point (equilibrium). On a small scale this is called "pooling" and differs from "katabatic" drainage type flow off the Rocky Mountains analyzed by Hootman and Blumen (1983).

In the morning uneven heating of the earth's surface begins. Differential heating and the convergence of turbulent heat flux are not believed sufficient to produce the large temperature changes (12°C) over a short period of time reported by Lenschow. What does appear to take place is that these pockets of stabily stratified cold air act like a separate boundary layer with turbulent transport of properties across the interface inhibited. A parameter used to examine whether turbulent mixing is present or possible is the Richardson number (Ri). Ri is a ratio of the vertical gradient of θ to the vertical wind shear (Appendix E). As this ratio approaches a critical value ($Ri<0.25$), either from a decreased $d\theta/dz$ and/or an increased dU/dz, turbulent mixing is enhanced. Calculations of Ri within the NBL reveal values very close to critical creating periods of momentary internal turbulence.

At the same time heating of cold air pockets is taking place, relatively less stable air over higher ground also warms to a point where a shallow CBL forms. Coupling these two areas of the differing stability with horizontal advection and shear stress ($-\overline{u'w'}$) can result in large temprature changes. Depending on the depth and overall stability of the cold air and the amount of stress applied, these changes may occur either very rapidly or slowly. In order to see such large temperature changes, displacement of the cold air by the warm air is favored over a mixing of the two. This process allows the cold air to retain its physical characteristics as it moves downstream for a short time. Changes are not restricted to temperature alone, but include moisture and winds with the largest changes occurring in valleys.

5.1.3 Sunrise Transition (0400-0620 MST)

Steady growth of the CBL is not readily evident until early morning horizontal gradients near the surface are eliminated through mixing. Profiles of each observational day from 0400-0620 at the BAO are presented in Fig. 14. Temperature changes of the magnitude found by Lenschow et al. (1979) are not seen due in part to the 20 min smoothing and also the fact that the BAO is on a slope rather than in a depression where cold air can collect and then be displaced. Displaced pockets of cold air may advect by the tower though.

Examination of the sunrise transition period shows moderate consistency between the 13 days. In eight cases formation of a mixed

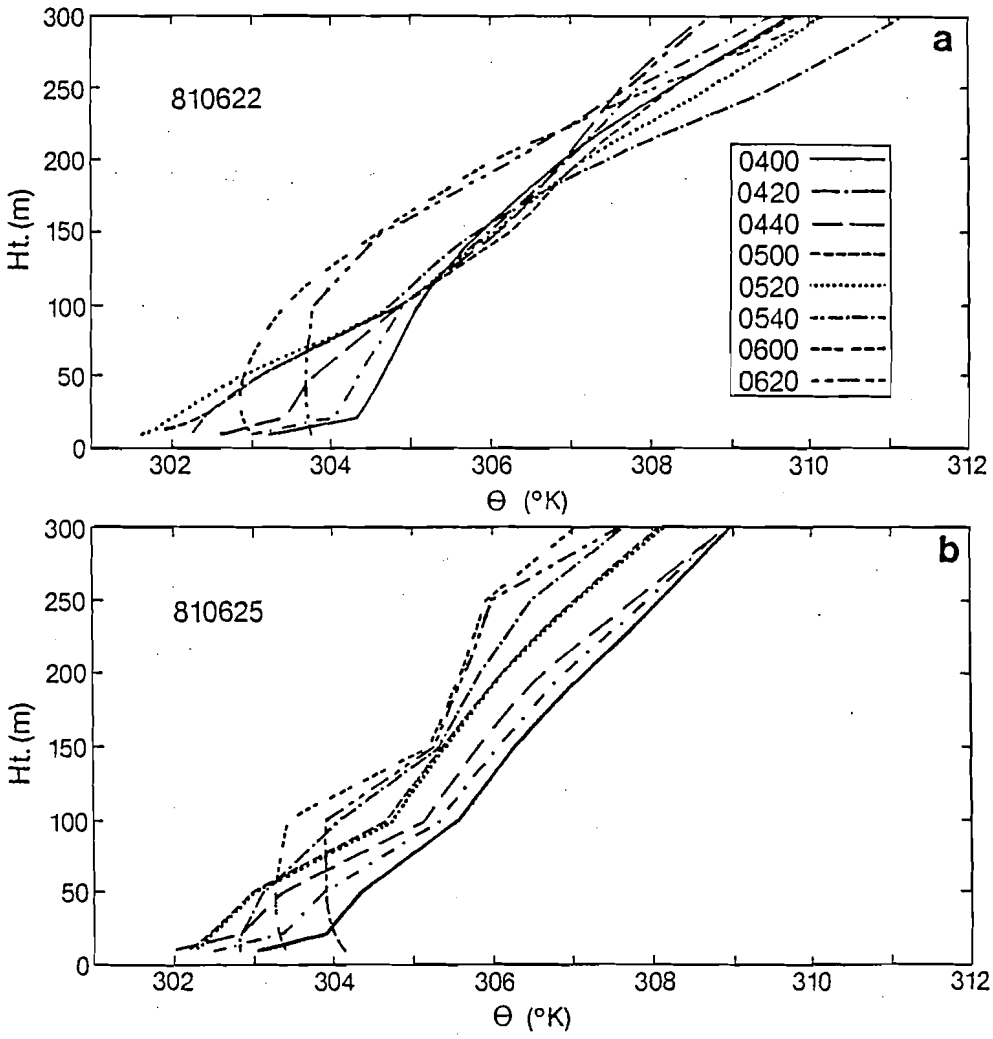

Fig. 14. BAO θ time series profiles of 20 min means (0400-0620 MST); 13 days.

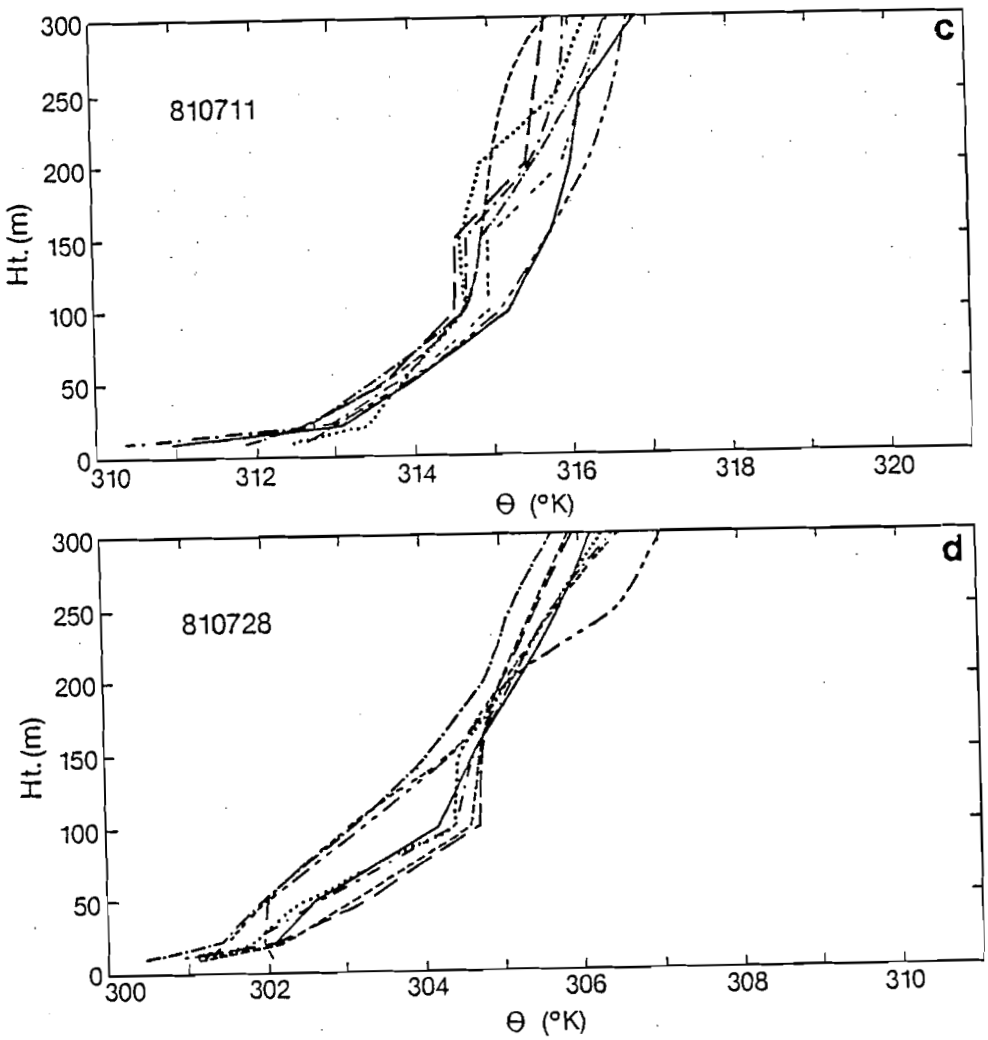

Fig. 14. (continued)

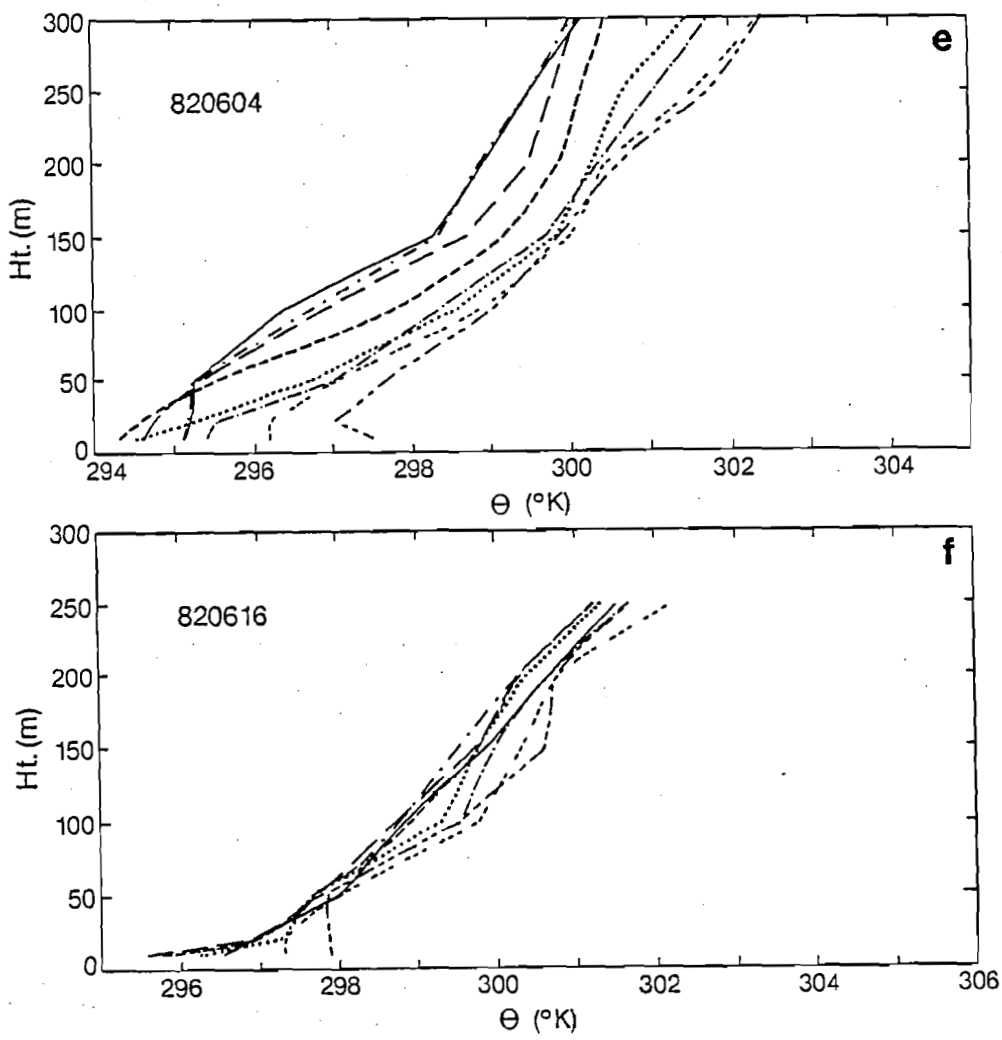

Fig. 14. (continued)

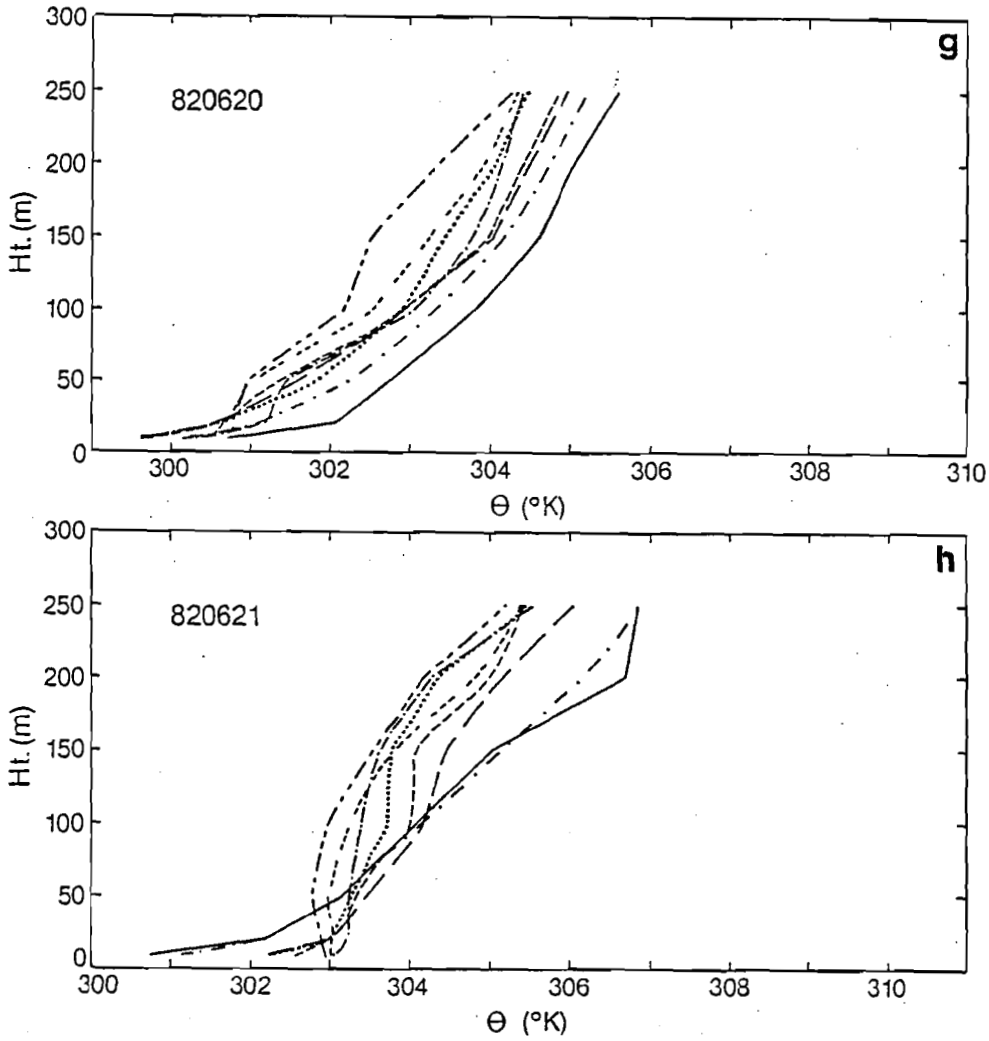

Fig. 14. (continued)

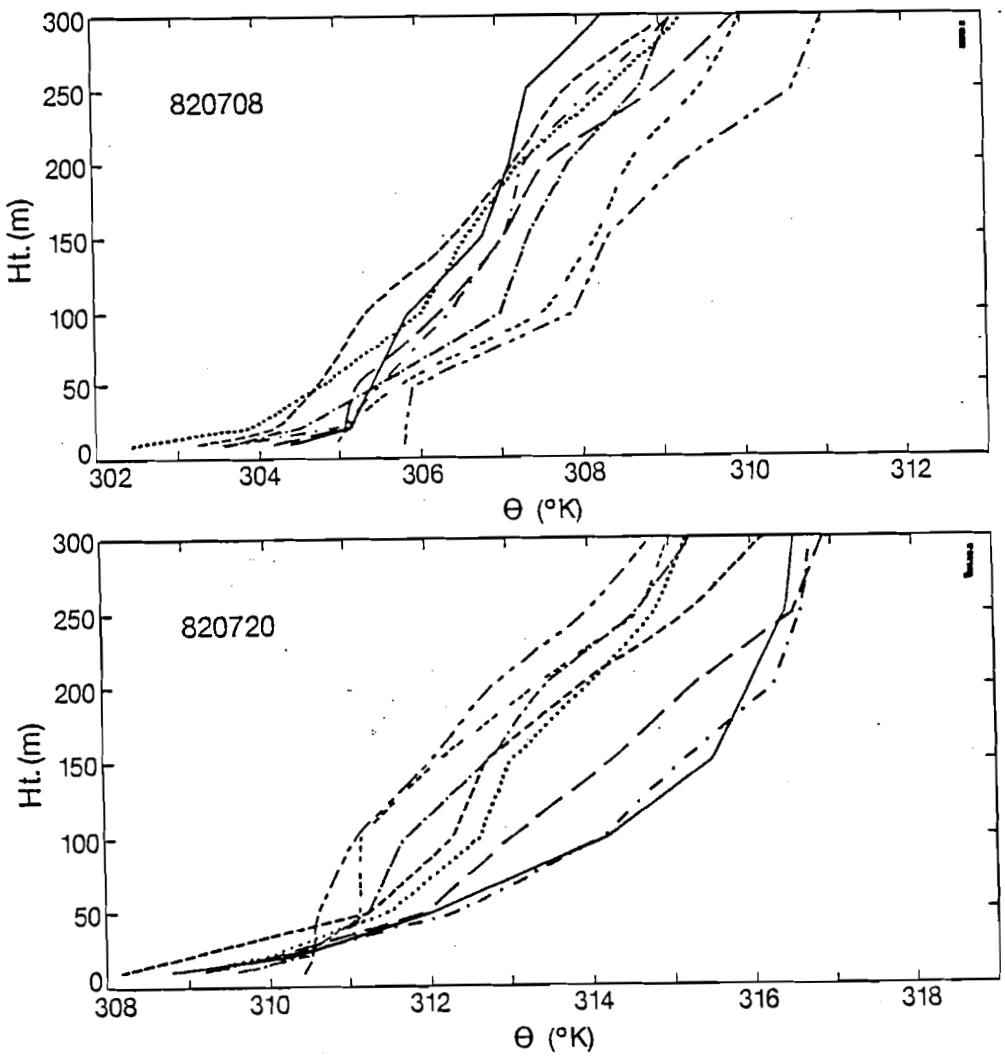

Fig. 14. (continued)

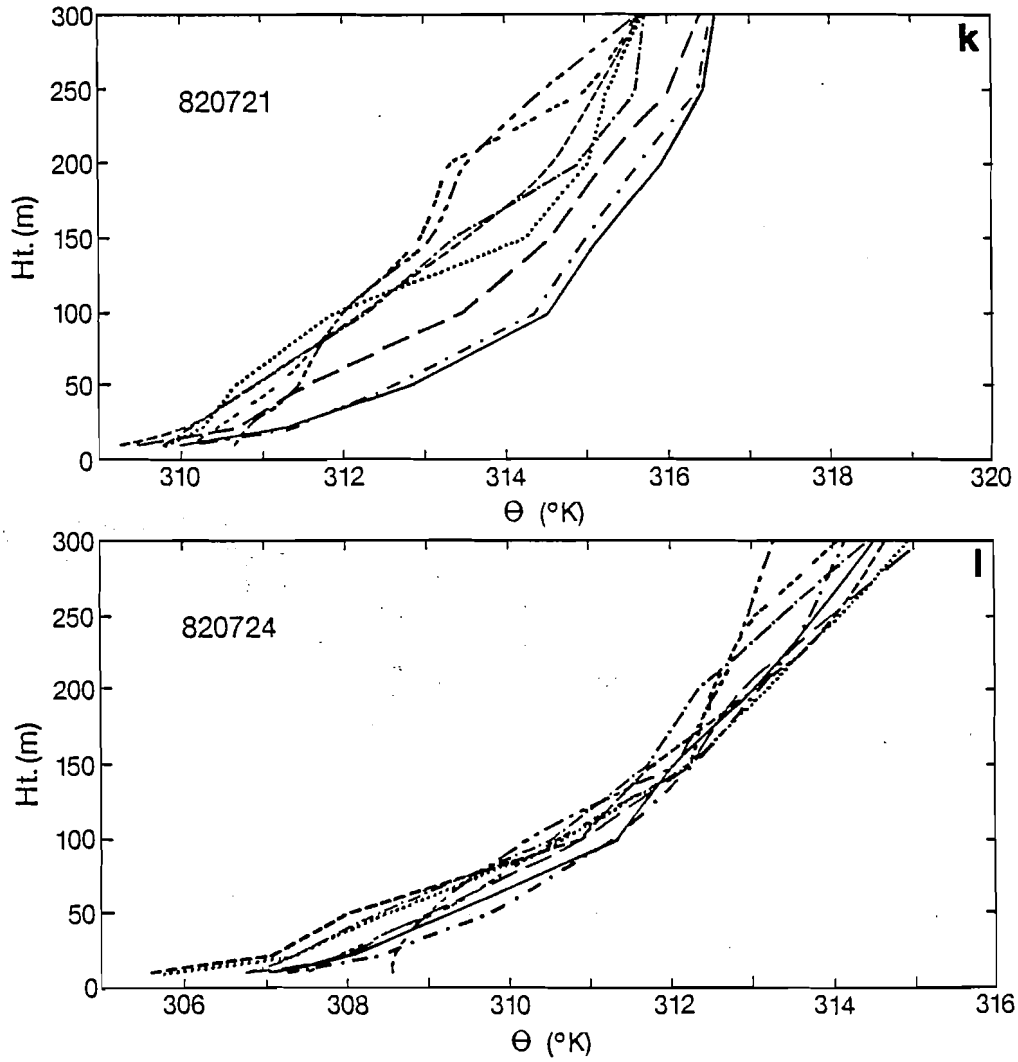

Fig. 14. (continued)

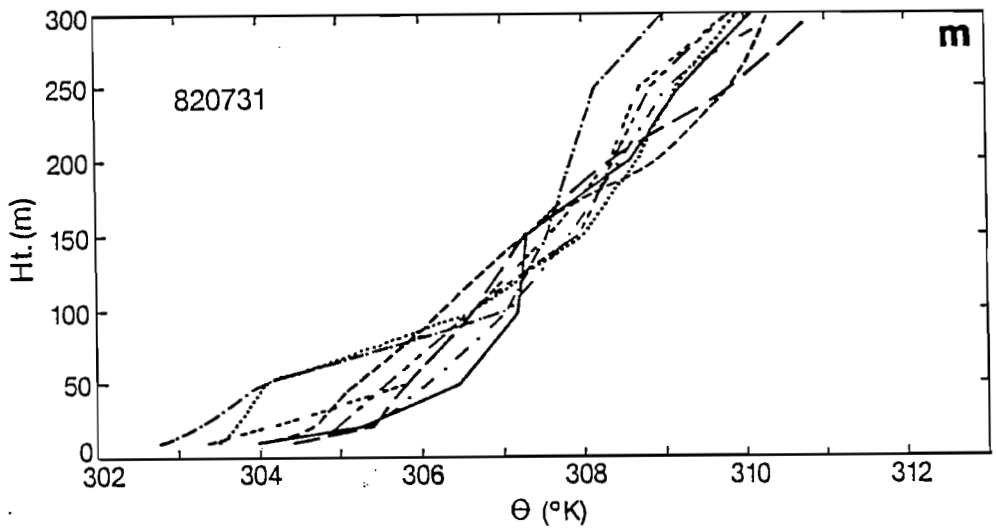

Fig. 14. (continued)

layer is evident, some only 40-60 min after sunrise and in two cases reaching a maximum depth of 100 m. Five of these days show signs of a superadiabatic layer forming, which is an indication of strong surface heating unable to mix upward rapidly enough. Of the five remaining days, four show no significant change of θ and the last day (4 June 1982) warms at a nearly constant rate over the entire depth of the tower. Common growth patterns start to appear once a definite mixed layer forms.

We find more inconsistency in the upper 2/3's of the tower profiles where cooling (7 days), warming (3 days) and no significant change (3 days) in θ occur, apparently independent of mixing below. Mid-levels at times have a tendency toward less variation which, combined with the warming below and cooling above, gives the θ profiles in Fig. 14 an hour glass appearance. On several days there is cooling throughout the entire tower depth even as the CBL evolves below (25 Jun 1981). If the boundary interface is at 50 m, it is not logical to assume that cooling at 300 m can be attributed to entrainment.

Fluctuations in θ at the top of the tower are at times as large if not larger than those at the surface though they may be opposite in sign. Sodar data indicate elevated layers that oscillate in a wave-like fashion up and down the tower. Gossard et al. (1983) analyzes the detailed structure of such layers at the BAO using a moveable instrument carriage. Results shows that these layers are correlated with small regions of turbulence mixing and sharp temperature gradients. It

is likely that the layers seen by the sodar are a partial answer to the unorganized appearance of the early morning evolution and the temperature fluctuations at the upper levels of the tower.

Potential temperature profiles for the entire 0400-0620 period do not always present similar growth patterns, but in almost all instances changes in θ, regardless of the sign, maintain the existing stability. Only two consecutive days (20, 21 July 1982) with sharp inversions in the lowest levels show a noticeable change in stability. Both are days with cooling (as much as 3°K) above the lowest 22 m coupled with a decrease in the stability (Figs. 14j,k).

Closer examination of the transition period finds cooling a dominant feature in the middle to upper levels of the tower. Figures 14j,k are two of seven cases where a maximum of 3°K cooling at 50 to 100 m is observed. Reasons for this large decrease in θ are not readily evident, but speculations can be made from the available data. The sodar facsimile record for 21 July 1982 (Appendix B) shows evidence of some type of irregular temperature structure occurring at the same time as the cooling (note dark region peaking at 0500). Structures like these usually indicate an area of increased turbulent mixing. The 20 min mean wind profiles (summarized later in Chapter VI, Fig. 23) reveal direction and velocity shear in the lowest levels. This shear could be in part responsible for mixing cooler air near the surface upwards. The lack of corresponding warming, if mixing is indeed taking place, leads one to look for additional explanations.

From Fig. 18 it is evident that westerly flow is generally downslope (warming) and northerly flow upslope (cooling). At sunrise, between 0400 and 0500 the winds shift from a westerly to northerly component. The vertical motion and resulting adiabatic cooling accompanying such a shift (for average conditions on 20 July 1982) are 0.03 m s^{-1} and 3.6 K hr^{-1}, respectively. This cooling rate is comparable to that observed. Thus, it is possible that the upper level cooling may be a consequence of adiabatic cooling associated with shifting slope circulations early in the morning. This process is taking place while sensible fluxes at the surface are still quite small.

Cold air drainage off the mountains as described by Hootman and Blumen (1983) is not consistent with the cooling at this time period. Results of Hootman and Blumen show the strongest cooling occurring in the early evening at the outset of the drainage flow. The effects of cold air pockets early in the morning (Lenschow et al., 1979) can not be ruled out as a factor. The tower is located on a slope though, and because of this the processes analyzed by Lenschow may relate in an "indirect" way to the BAO. For a more complete explanation, the effects of advection and the local terrain need further study.

5.1.4 Mixed Layer Development (0640-0900 MST)

Development of the CBL continues between 0640 and 0900 (Fig. 15). On 2/3's of the days mixing extends above 300 m by 0900. As stated in

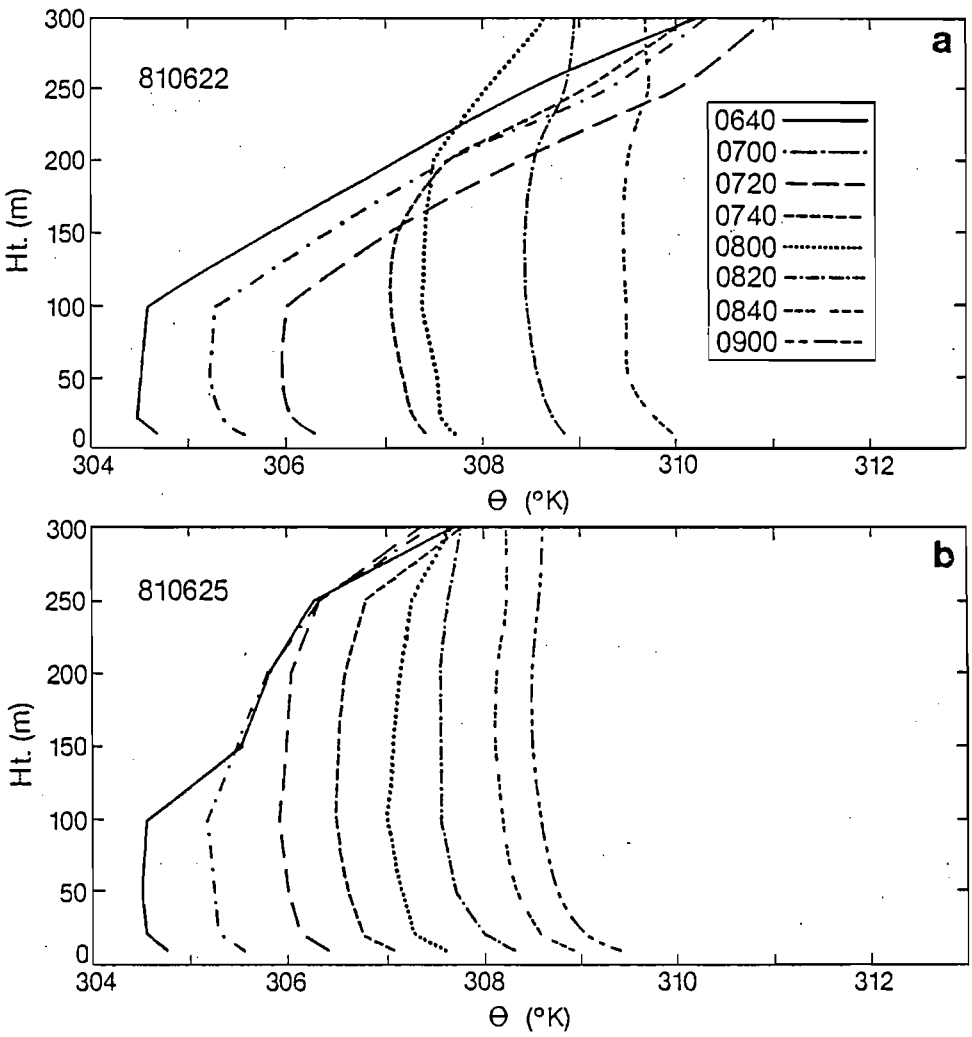

Fig. 15. BAO θ time series profiles of 20 min means (0640-0900 MST); 13 days.

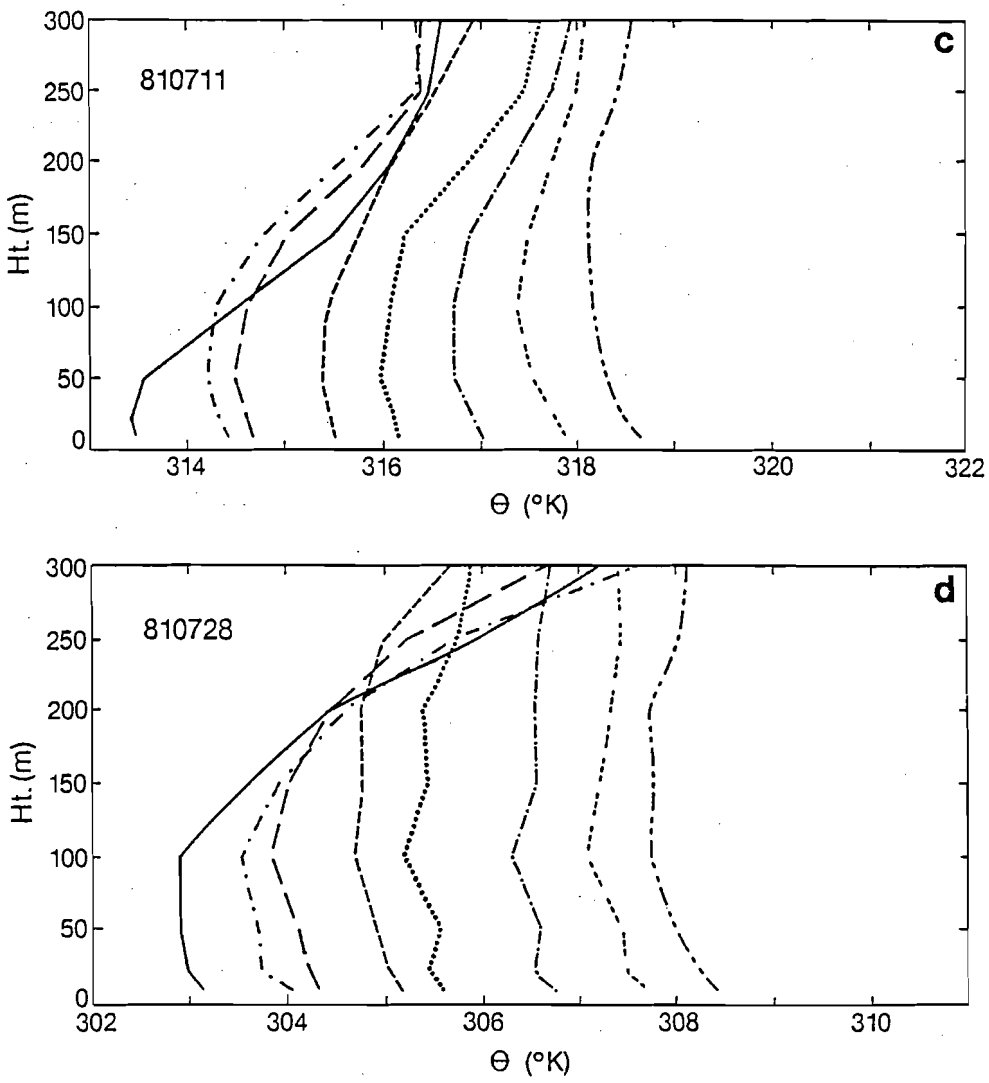

Fig. 15. (continued)

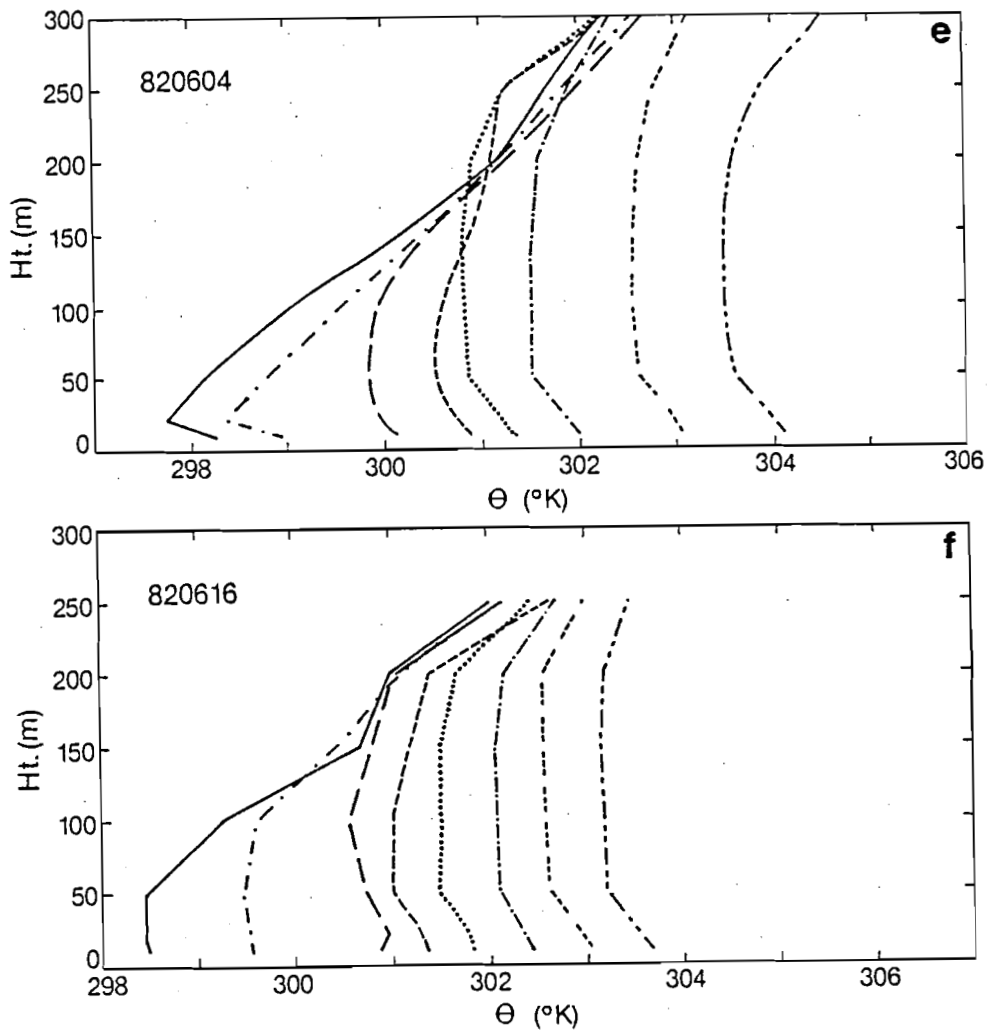

Fig. 15. (continued)

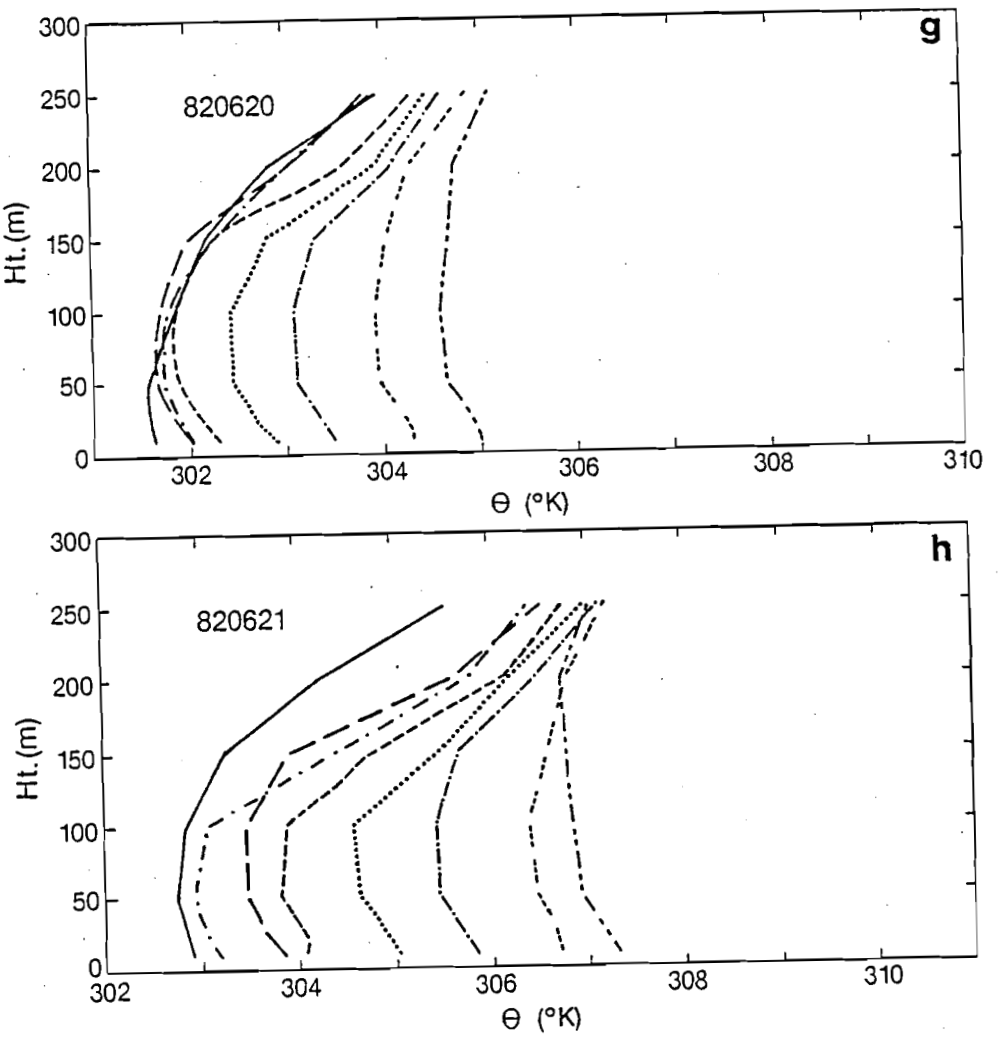

Fig. 15. (continued)

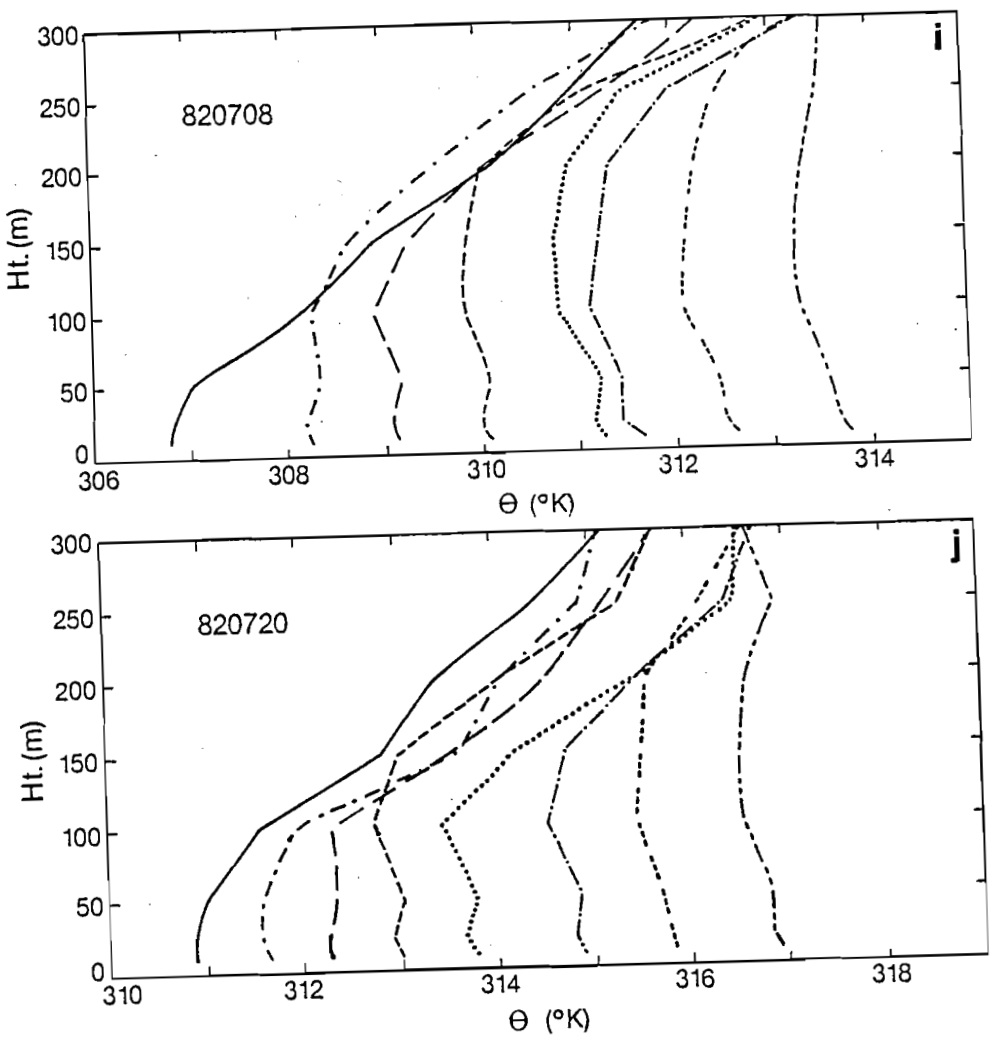

Fig. 15. (continued)

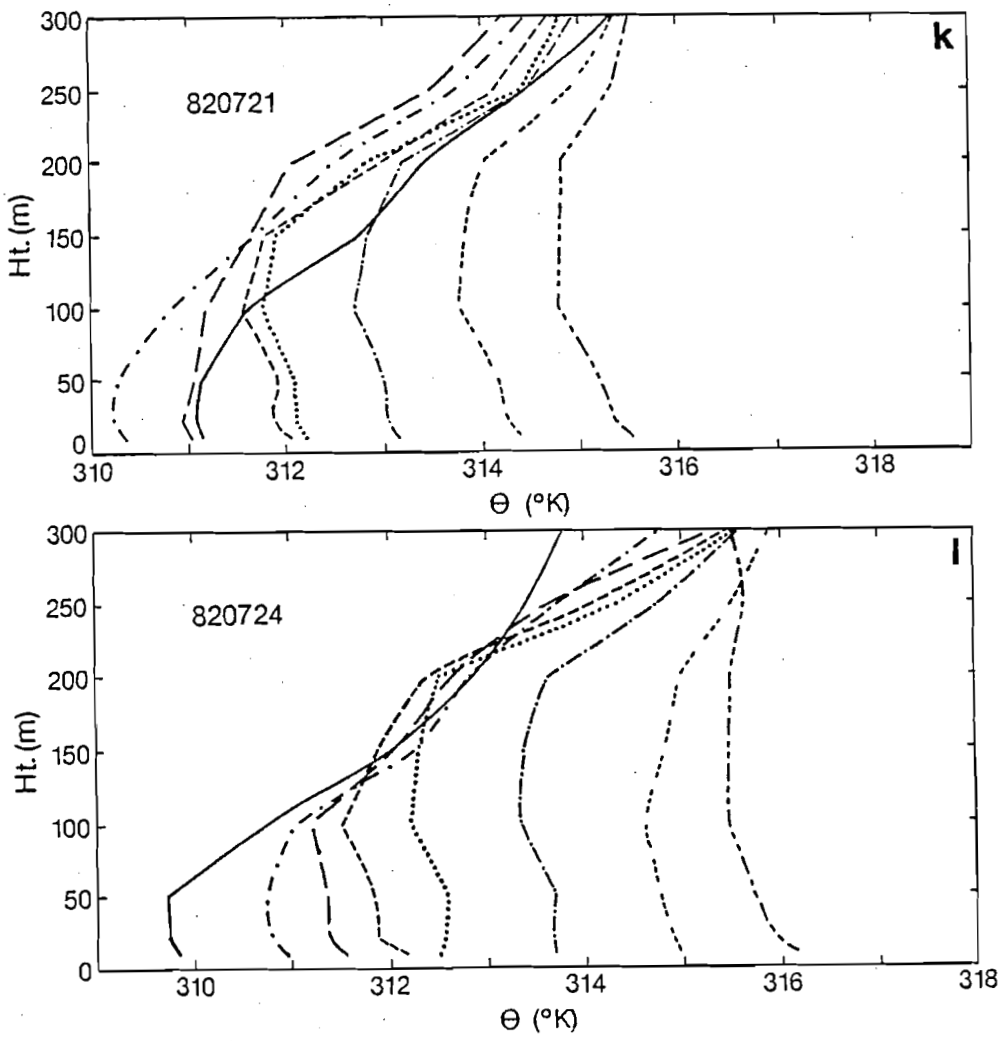

Fig. 15. (continued)

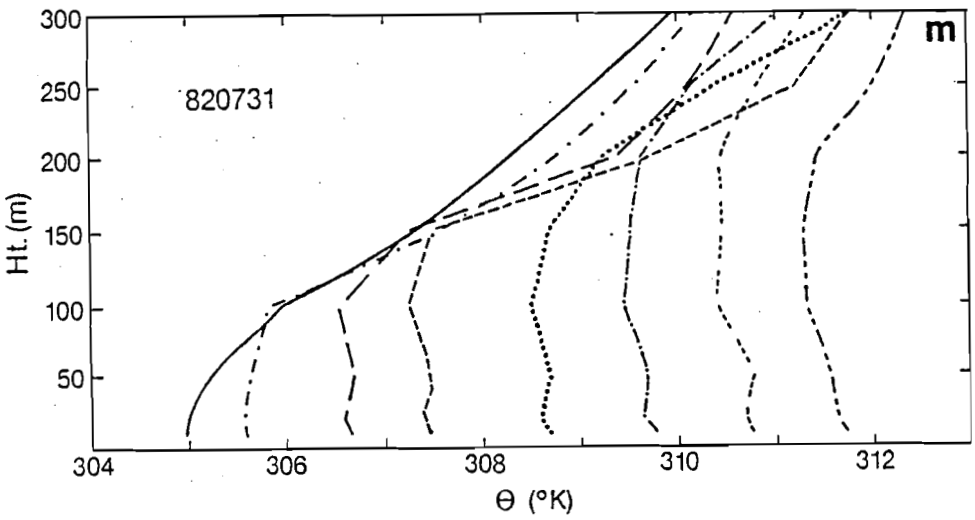

Fig. 15. (continued)

the previous section, when the lower CBL mixes out early morning gradients of θ, overall growth patterns become evident. The superadiabatic layer is also increasing in depth.

If examining CBL growth through surface heating and mixing alone, one might expect a smooth steady rise over a homogeneous surface. This assumes horizontal advection is negligible, surface conditions are nearly identical and a larger and larger volume of air is being warmed as the mixed layer grows. At the BAO we do not see this consistent pattern for several reasons.

Thermal penetration and entrainment are possible partial explanations of the erratic growth. Entrainment is dependent on vertical stability, with increased stability in the capping inversion retarding entrainment. Determining the stability of the lifted air in relation to its surroundings can be done in a similar manner to the "parcel" theory. For an unsaturated atmosphere the parcel is lifted dry adiabatically and it is assumed that there is no mixing between the parcel and the atmosphere through which it moves. Comparison of the virtual temperatures between the parcel and its surroundings determines the stability. Higher virtual temperature (lower density) than the surrounding air means the parcel has positive buoyancy and continues to accelerate vertically. In terms of a rising thermal, once it penetrates the inversion its virtual temperature is lower (higher density) than the capping stable layer. A negative buoyancy now exists and the parcel tries to return to an equilibrium point. During entrainment the

same overall ideas apply and, in addition, the lifted parcel does mix with its environment which in turn affects the buoyancy. Conceptually, the virtual temperature of air penetrating and then mixing above the capping region increases, thereby reducing the amount of negative buoyancy. Air displaced by rising thermals is compensated for by locally subsiding air due to the conservation of mass. This downward moving air must also be envisioned as part of the entrainment and is governed by the same thermodynamic processes. These complicated processes along with vertical tower resolution and data averaging appear to be some of the reasons for the erratic growth of the mixed layer found in the BAO tower data.

Figure 16 (Kaimal, 1976) represents vertical velocity and heat flux data over a ten minute period obtained from tower and tethered balloon data in a summertime experiment in Minnesota. The top of the figure is the location of z_i and the curved vertical lines are the outline of the rising thermals. Though the figure depicts a much deeper mixed layer than analyzed in this thesis, the upper portion still shows the rising thermals and the corresponding areas of subsidence as would be found on the BAO tower. Downward moving air carries with it momentum from above and if there exists a large wind shear, the downward extent of this air can be substantial. Stull (1973) presents an illustration of the "dome-wisp" concept in the entrainment region. The dome is a penetrating thermal plume and the wisp is thought of as air from above pushing down between the plumes.

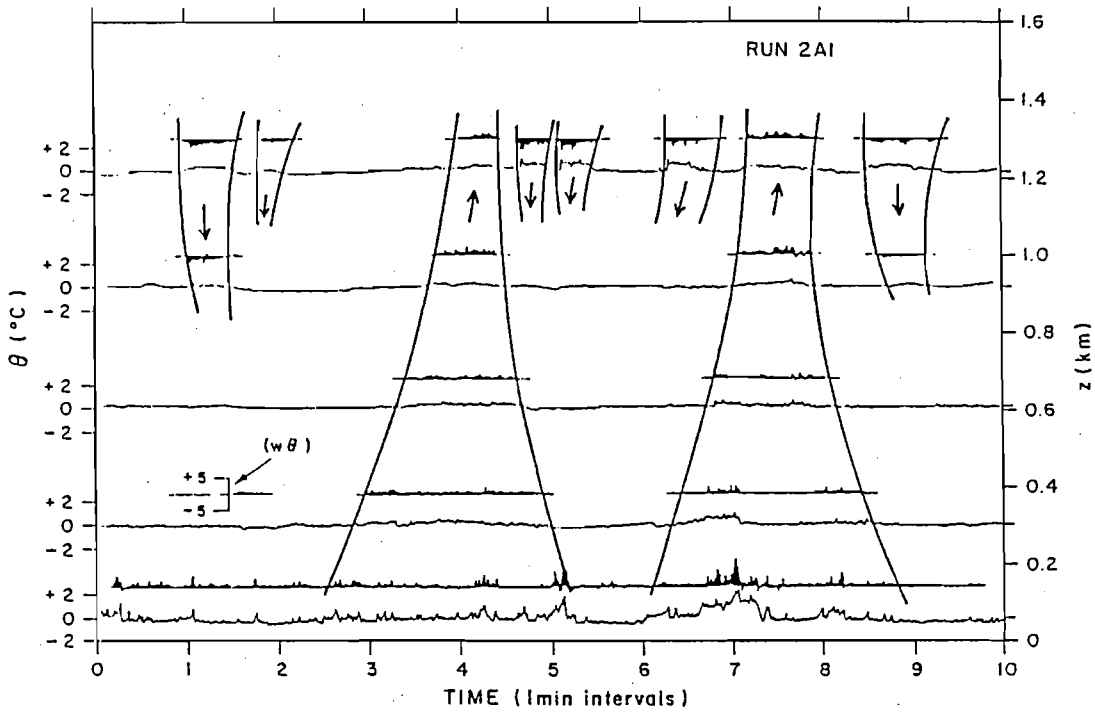

Fig. 16. Temperature fluctuations (horizontal lines) and vertical heat flux (shaded regions) during a 10 min period (Kaimal, 1976).

Mixing by entrainment is not instantaneous and an oscillating motion (internal gravity waves) is often set up along the upper mixed layer boundary. This is similar to orographic lifting generating the waves found on the lee side of the Rocky Mountains but on a much smaller scale. The periods of these oscillations are at the Brunt-Väisälä frequency (N). N, also known as the buoyancy frequency, is a measure of the static stability where, if N equals zero, a state of eqilibrium exists with no oscillations. A series of three papers by Stull (1976 a,b,c) examines the dynamics of entrainment, entrainment in a mixed layer model and finally the internal gravity waves generated by thermal plumes.

Elevated layers not seen by ground-based sensors are depicted in sodar records as they oscillate and advect through the tower. Fig. 17 is a comparison of the tower mixed layer depths to those measured by the sodar. BAO data points are based on 20 min average θ profiles, where as the sodar data are individual points taken at 00, 20, 40 min after each hour from the facsimile records (Appendix B). Tower points lack vertical resolution and averaging of the data may shift the actual growth pattern or smooth vertical gradients into weak undefinable interface zones. Sodar records represent time height cross sections of backscatter smoothed over the scattering volume. There is often a discrepancy in defining z_i as measured by a sodar and z_i from a θ profile. Panofsky and Dutton (1984) state differences of z_i as large as 10% are possible because the turbulence region seen by the sodar

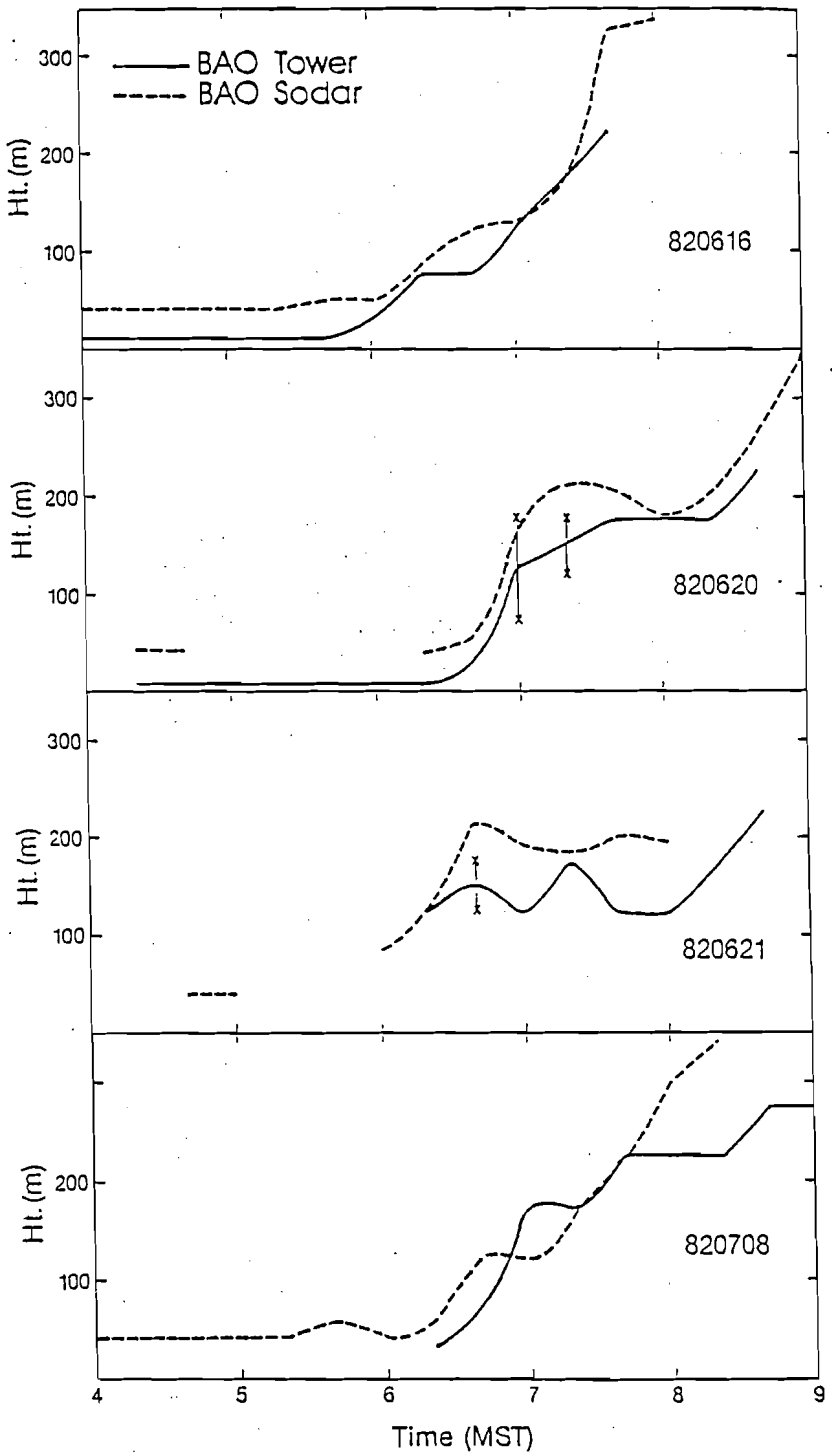

Fig. 17. BAO z_i (20 min mean) vs. sodar record z_i (single point) (0400-0900 MST); 8 days. BAO plots bracketed by 'X' are areas of uncertainty when z_i is not well defined. Missing portions of BAO tower data are when z_i is below 10 m (early morning) or above the tower. Missing sodar data are points where z_i is below minimum resolution or a clear z_i is not evident.

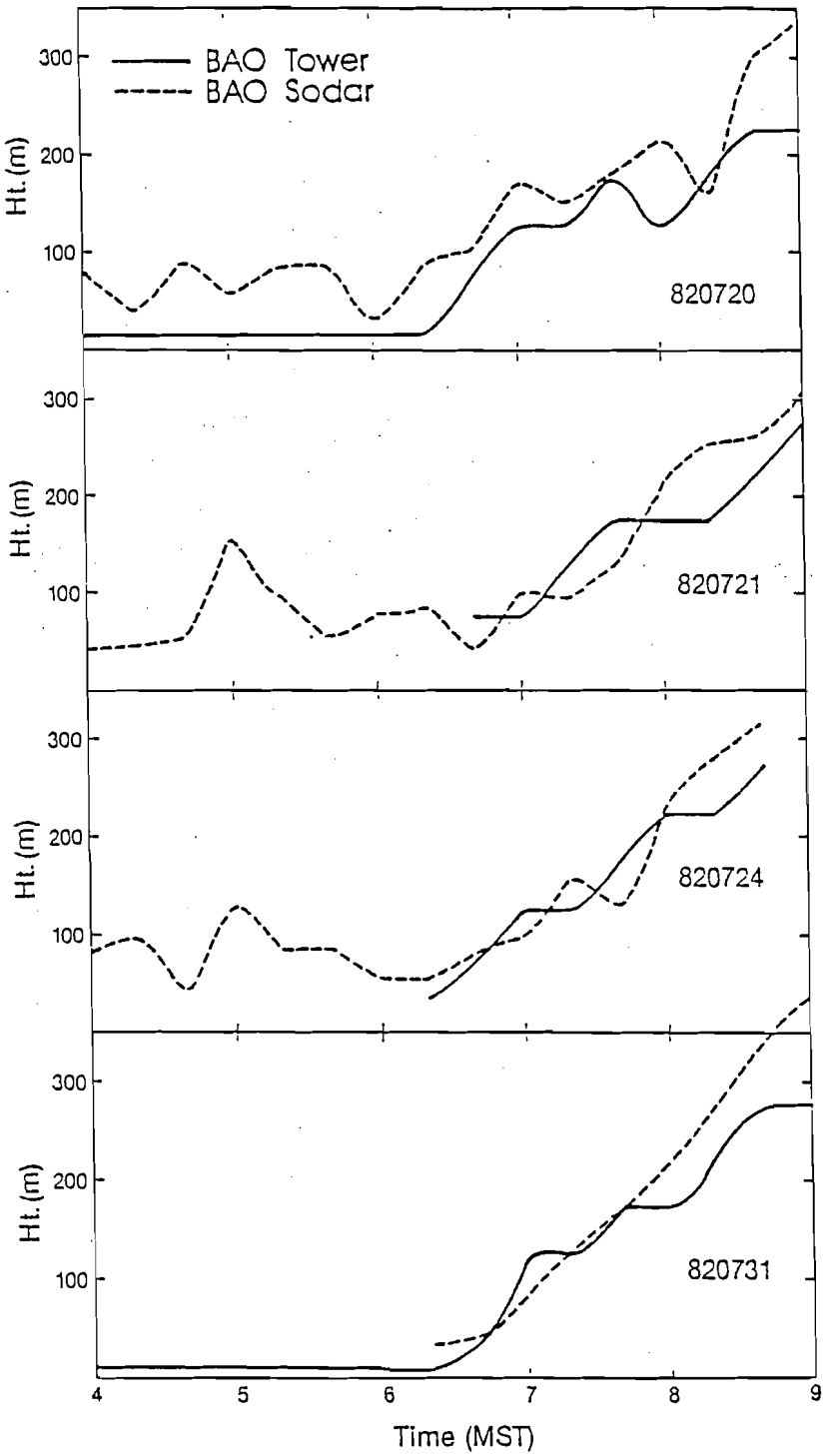

Fig. 17. (continued)

extends above and below the lowest point of the inversion found in the θ profile. Nevertheless, the agreement between the two independent estimates of z_i is quite good.

Appendix B also pictures how mixed layer growth stagnates when in the presence of elevated layers. In particular cases on 8 July 1982 around 0630 and 20 July 1982 from 0640 until 0730 are examples of these layers. Also seen on 20 July 1982 is the correlation of the oscillation of multiple elevated layers and the inversion rise profile. Trough portions of the wave appear to produce a subsidence type lid.

Days with a mixed layer forming in the initial period (0400-0620) continue a similar pattern during the next stages of growth. Examining all the profiles in Fig. 15 we find two major features; a superadiabatic layer which grows in depth and intensity and a layer above the mixed layer with both absolute cooling and warming (decreases or increases in θ). Changes in the stability of the capping inversion and entrainment are the most likely causes. Growth of the superadiabatic layer continues at a rate and to a depth dependent on surface roughness, vertical wind shear and sensible heat flux. Maximum depth approaches 100 m in an exponential like profile.

Overall there are three recognizable growth patterns: 1) mixing below and entrainment above (Stull, 1973), 2) mixing below only "Pattern 1" (Whiteman, 1982a) and 3) a combination of (1) and (2) or undefinable growth. The preferred pattern for θ above z_i is toward

cooling (5 days; Figs. 15a,c,d,j,m) and is consistent with Stull (1973). Stull uses a model to simulate growth and compares his results to the O'Neill data. He finds not only cooling, due to entrainment, but an increase in stability above z_i in the transition layer. This change in stability (also found in the BAO data) should in turn modify the entrainment rate.

Four days (Figs. 15b,e,f,i) follow Benkley and Schulman's (1979) idea which is very much like Whiteman's (1982a) "Pattern 1" for the destruction of inversions in mountain valleys. Here boundary layer growth is accomplished predominately through convective mixing generated at the surface while the temperature in the stable layer above remains constant. The last four cases (Figs. 15g,h,k,l) are a combination of processes. A common factor here appears to be that at some time during these periods z_i either remains constant or drops in height over several periods.

Figure 18 is a comparison of observed tower mixed layer depths and those calculated from the simple equation (Tennekes, 1973):

$$z_i = \left(\frac{2(1+2k)}{\gamma} \int_0^t A \sin\omega t\right)^{1/2} . \qquad (6)$$

It is assumed in (6) that the surface heat flux is closely approximated with a sinusoidal function, where ω is the period and A the amplitude. The initial lapse rate (γ) is calculated from tower θ profiles near sunrise, an average maximum surface heat flux (A) is determined from

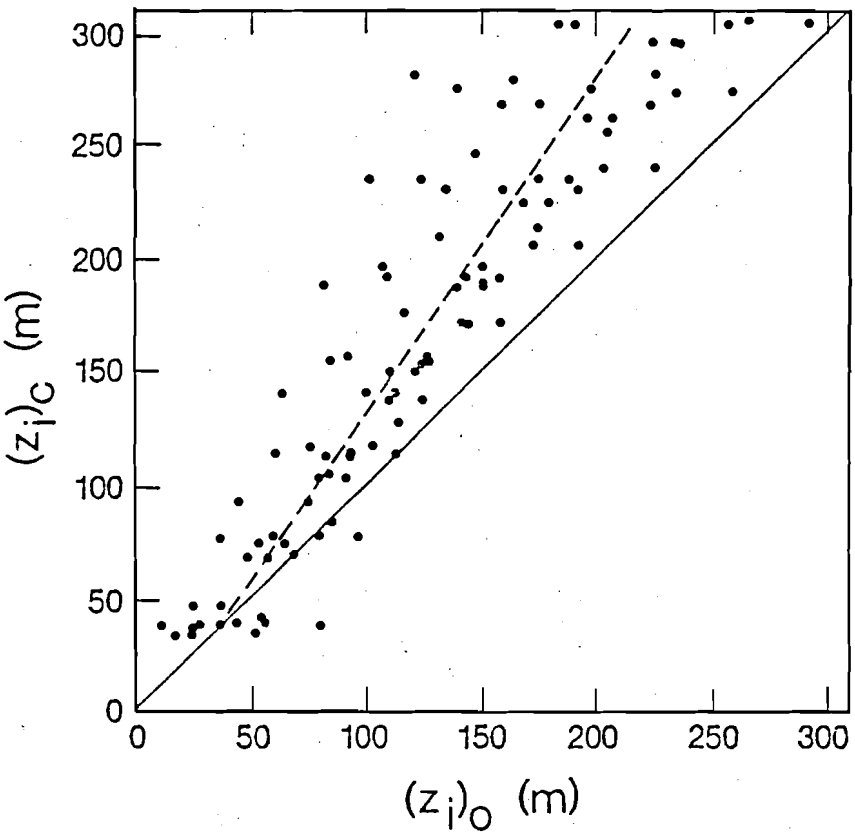

Fig. 18. Calculated mixed layer depths $(z_i)_c$ versus observed BAO tower depths $(z_i)_o$, solid line (——) is perfect fit and dashed line (---) is mean fit; 13 days.

past measurements at the BAO and the entrainment coefficient (k) is replaced by a constant (0.2). Horizontal advection is neglected and the initial input of surface heat flux is taken as the point where z_i is first observed to grow on the tower. This delay is an unrefined way of allowing for variations in surface heating and evaporation from day to day and early morning low sun angles. Observed values of z_i are smoothed linearly for each day before comparison because, variations seen are due in part to the averaging and vertical resolution of the data.

Sensitivity studies of equation (6) show that the mixed layer prediction depends significantly on the assumed evolution of the heat flux. Changes in the entrainment (k) have almost no effect on the growth of z_i. Increasing A or decreasing γ by the same percentages has nearly an identical influence on z_i. These points help to confirm the importance of an accurate heat flux measurement.

Results in Fig. 18 show calculated values larger for a majority of the cases. Assumption of a sine profile gives more rapid growth to the heat flux and in turn z_i than is probably really present (due to evaporation and thermal lag for example). This could account for the differences seen in Fig. 18. Vertical motion and mechanical mixing are additional terms not incorporated in equation (6) that could further influence the comparison.

5.1.5 Maturing Mixed Layer (0920-1140 MST)

Two of the 13 days are not used in this section because of lack of data points (22 June 1981 and 8 July 1982). In all cases but one (31 July 1982) the boundary layer is already above the tower by 0920 (note sodar records: Appendix B). We find in Fig. 19 a deepening of and in some cases an increase in strength of the superadiabatic layer with time. This continued development is not unexpected because surface heating is near its maximum.

Again each day shows continual warming but not at a constant rate. Incoming energy is nearly identical, and with similar wind flow patterns one would not expect substantial variability. Inspecting the area surrounding the BAO it becomes evident how important local surface conditions might be. Strip planting creates alternating rows of bare soil with wheat or corn. These contrasting surfaces and even the difference between newly sprouted wheat and that ready for harvest produce significant surface heating differences (Rosenburg et al., 1983). Vertical extent and strength of thermals generated over these dissimilar surfaces are also affected. Lenschow et al. (1981) while examining fluxes from aircraft data taken just north of the BAO sees similar results.

Average total increase of θ in the mixed layer is 4.0°K with the largest increase 7.0°K (4 June 1982) and the smallest increase 1.5°K (11 July 1981). Increases in θ per 20 min period are fairly consistent on nine of the days but only relative to each individual day.

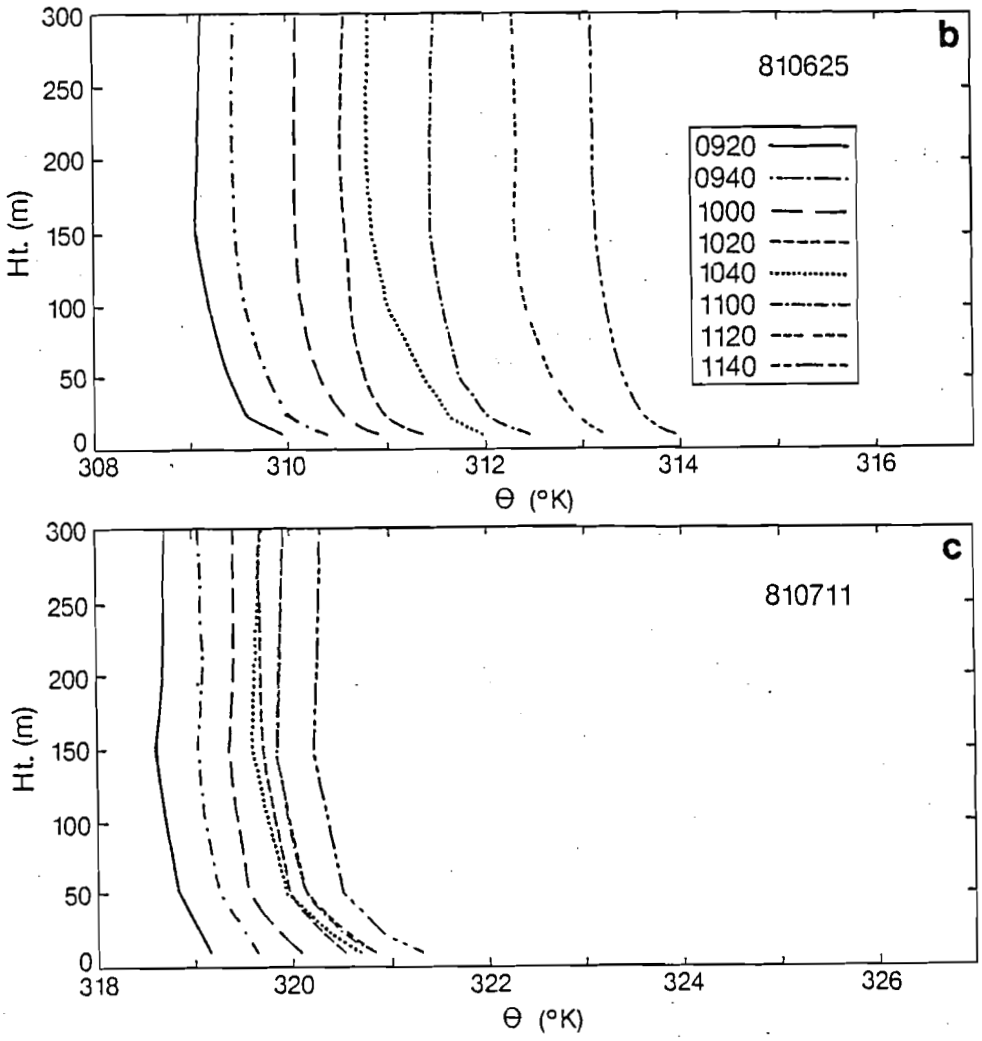

Fig. 19. BAO θ time series profiles of 20 min means (0920-1140 MST); 12 days.

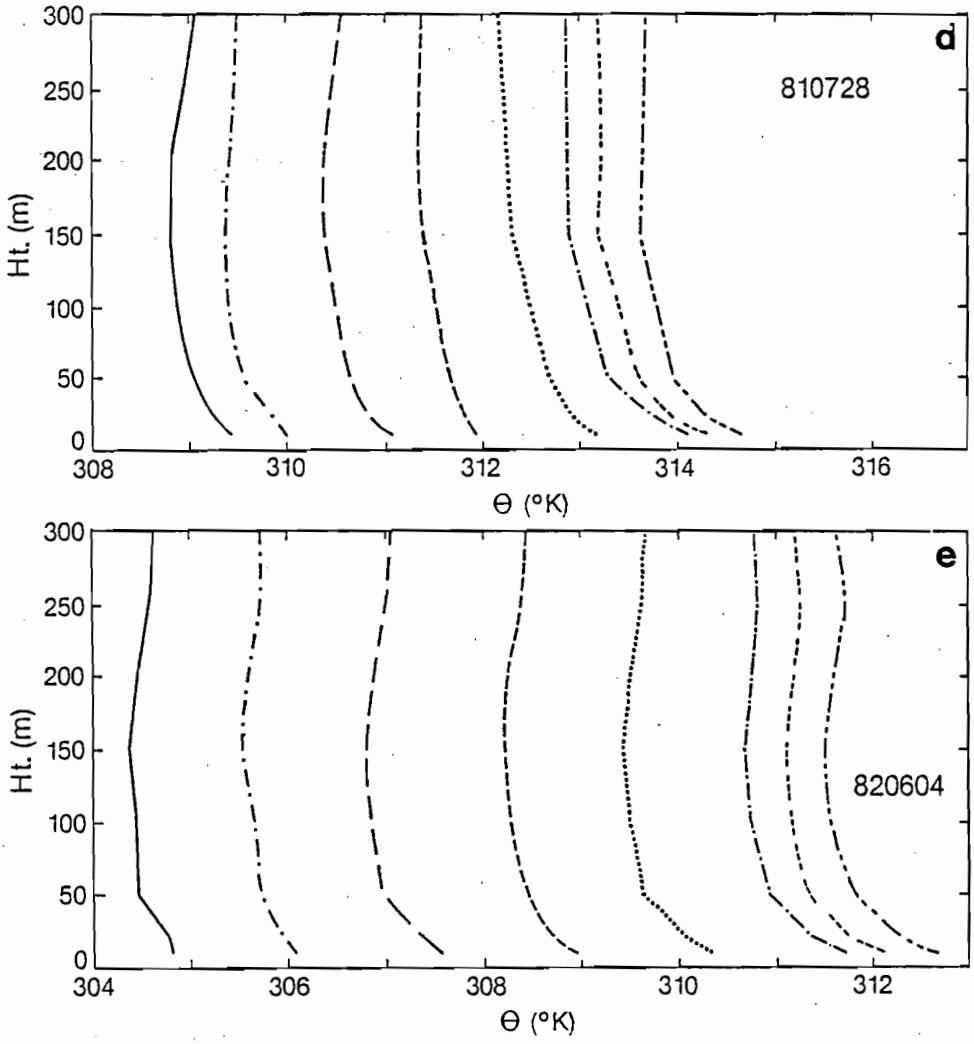

Fig. 19. (continued)

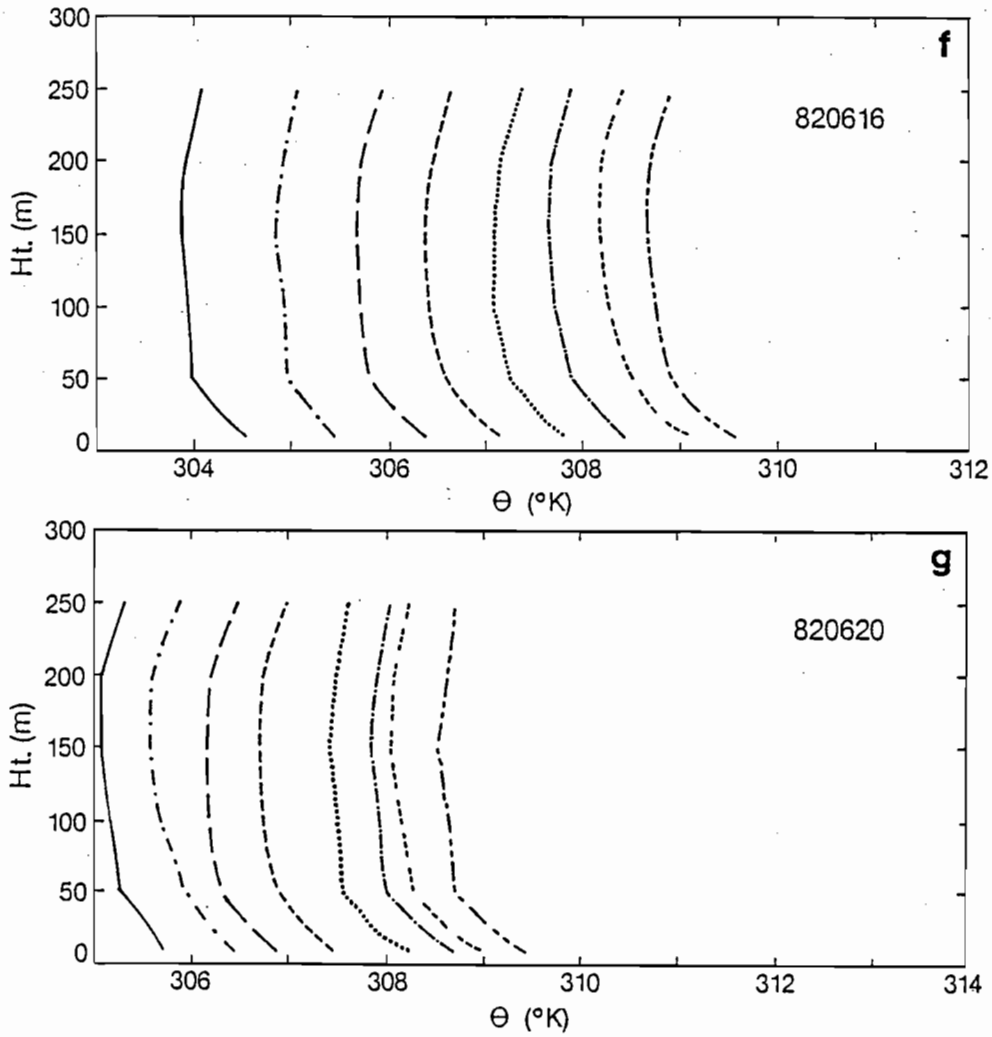

Fig. 19. (continued)

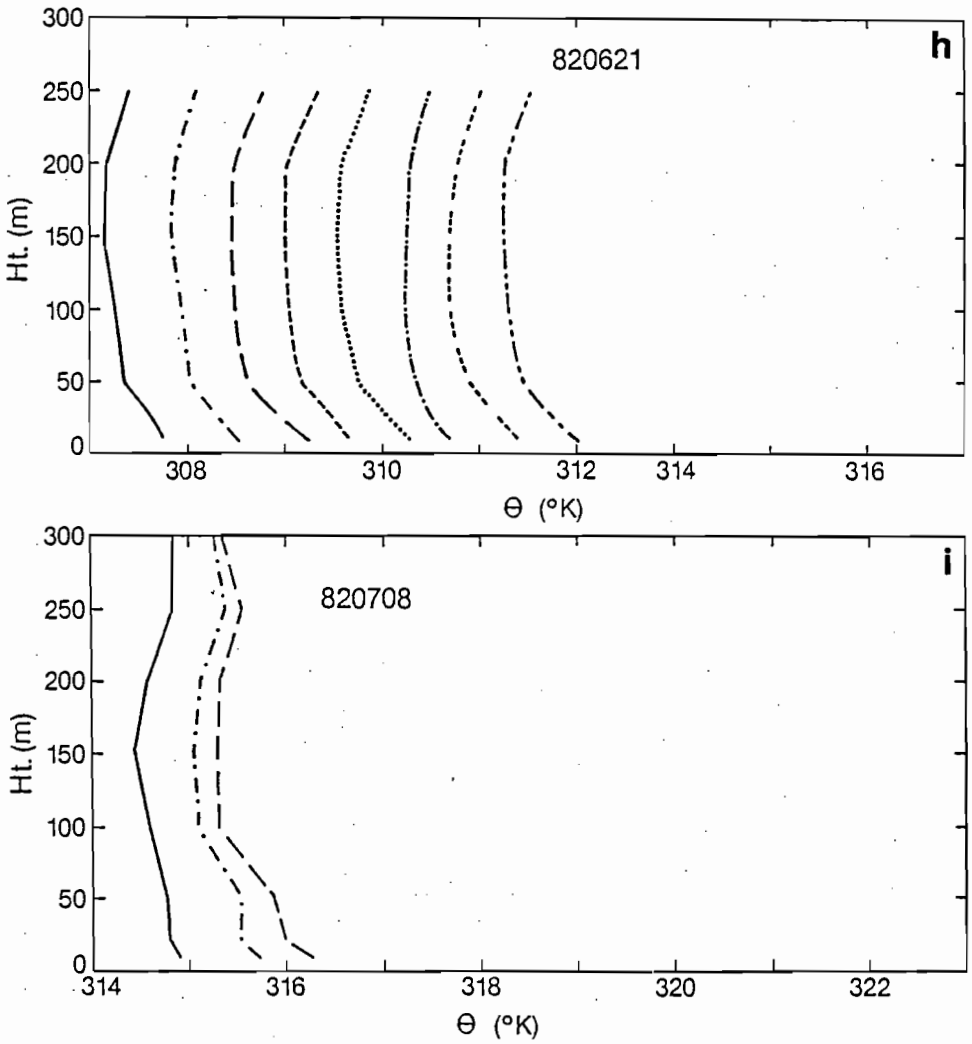

Fig. 19. (continued)

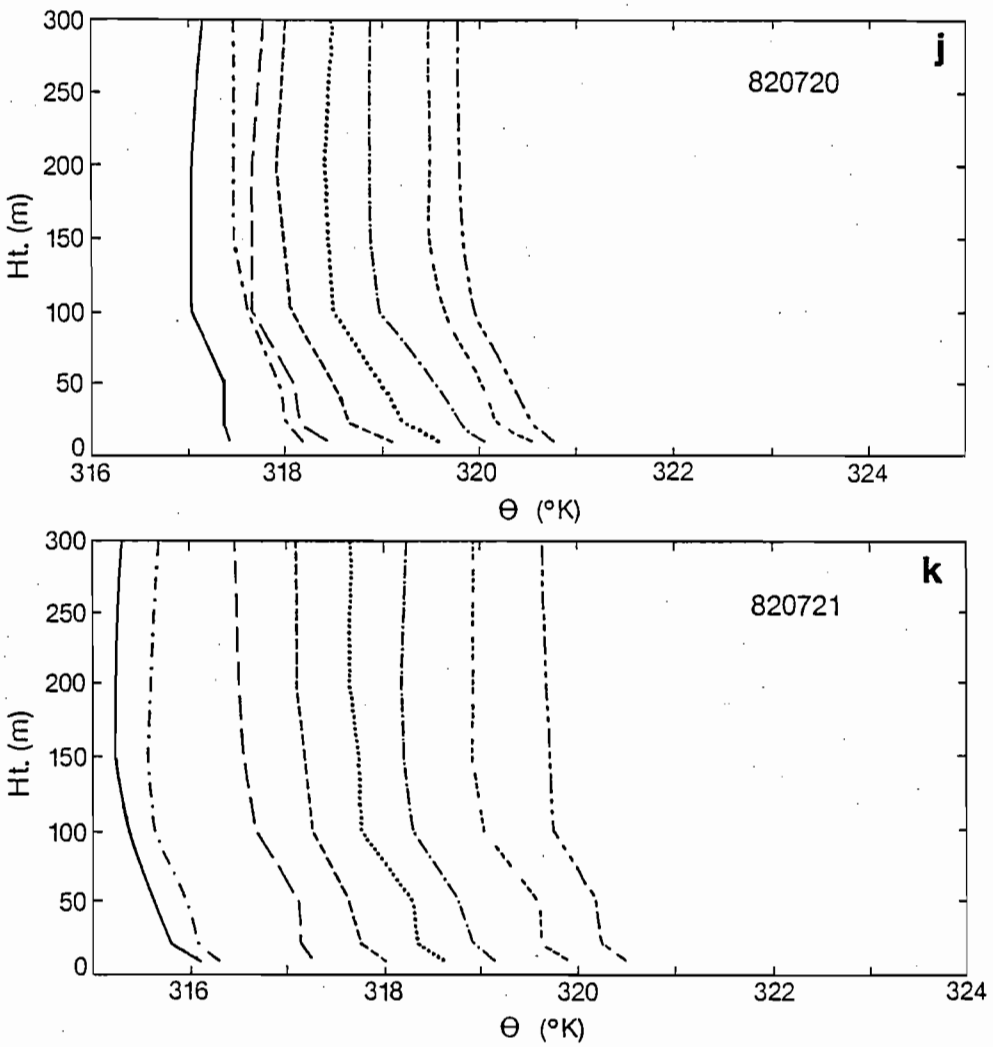

Fig. 19. (continued)

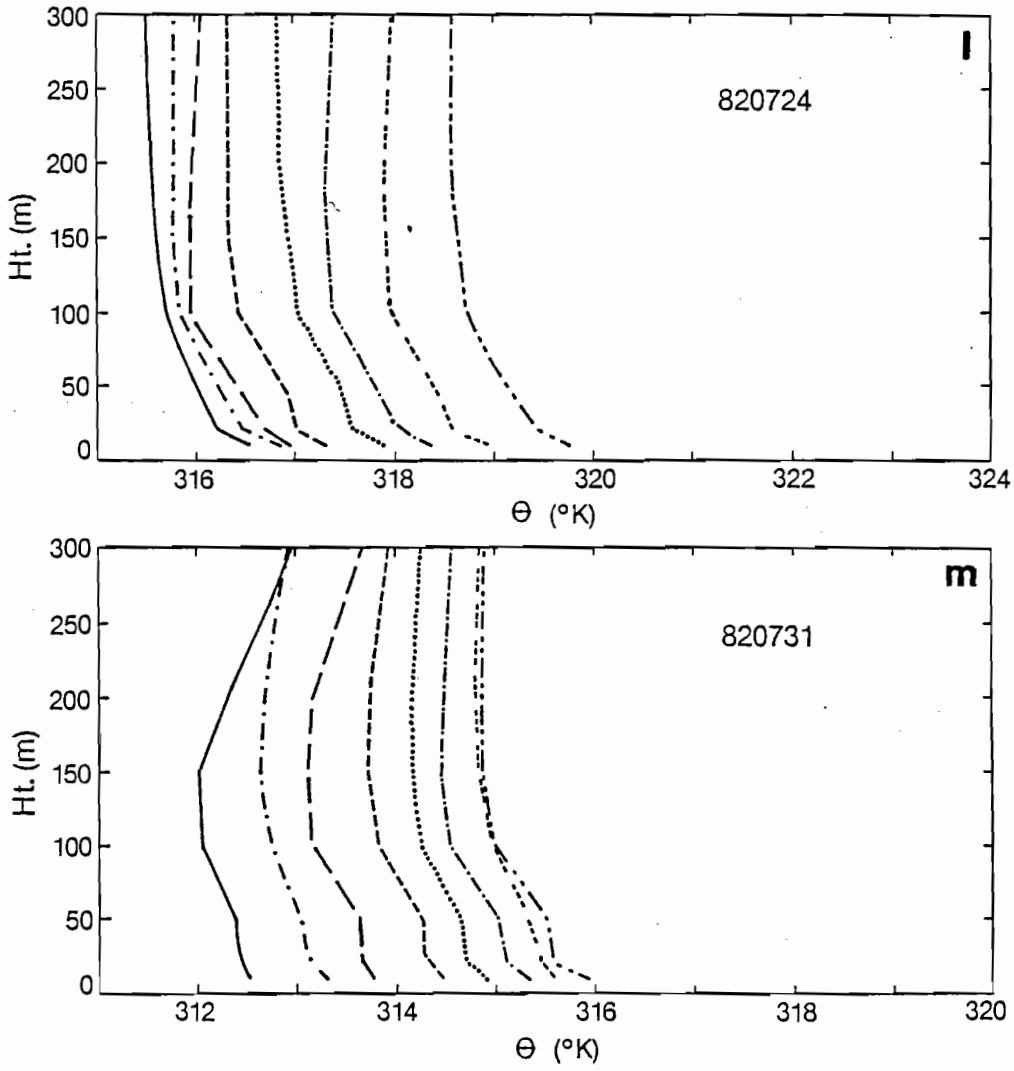

Fig. 19. (continued)

Maximum depth of the superadiabatic layer now lies somewhere between 100 and 150 m and has the appearance of two layers with different stabilities. Because gradients in the upper portions of this layer drop off slowly and the gradients in the mixed layer are slightly positive (Carson, 1973), there is not a sharp cut-off between the superadiabatic and mixed layers. Vertical tower resolution and averaging may also give a false appearance to the superadiabatic layer.

A simple equation can be written for $d\overline{\theta}_v/dt$. Using an expression similar to Tennekes (1973)

$$\frac{d\overline{\theta}_v}{dt} = \frac{(\overline{w'\theta_v'})_s - (\overline{w'\theta_v'})_i}{z_i} \tag{7}$$

and rewriting it in terms of entrainment ratio and breaking horizontal advection out of the total derivative we get

$$\frac{\partial\overline{\theta}_v}{\partial t} = \frac{(\overline{w'\theta_v'})}{z_i}(1+k) - \vec{\overline{V}} \cdot \vec{\nabla}\,\overline{\theta}_v \quad , \tag{8}$$

where $(\overline{w'\theta_v'})_i = -k(\overline{w'\theta_v'})_s$. Examining this equation provides a little better understanding why the profiles in Figs. 19 c and e show such large differences.

From equation (8) it is evident that a number of factors can affect the rate at which the CBL warms: advection, surface buoyancy flux, the depth of the mixed layer (z_i) and processes that influence the entrainment (discussed earlier). The 13 cases were deliberately chosen so that advective effects were small. Assuming that $(\overline{w'\theta_v'})s$ and k are within 30-50% of their average values for these days, it is apparent that the factor of 4 difference in observed $\overline{\partial\theta v}/\partial t$ is most likely a consequence of widely varying mixed layer depths on the various days. These depths and their variations in time could not be determined after approximately 0900 because the mixed layer depth was generally above the top of the tower and sodar records as explained in Section 3.5 no longer are able to identify z_i.

Without further study and more detailed information on the variability of $(\overline{w'\theta_v'})_s$, z_i, entrainment or advective processes it is not possible to determine precisely the contributions of all of the terms in equation (7).

5.2 Winds

Winds in general are more variable than θ. Figures 20 and 21 are speed and direction time series composites at 3 levels on the tower (10, 150, 300 m). Included with the tower direction plots are hourly averaged PROFS mesonet data July 1981, interpolated from Johnson and Toth (1982b). While intercomparison of tower and PROFS speeds is not made, it is noted that speeds from the mesonet are less than those for

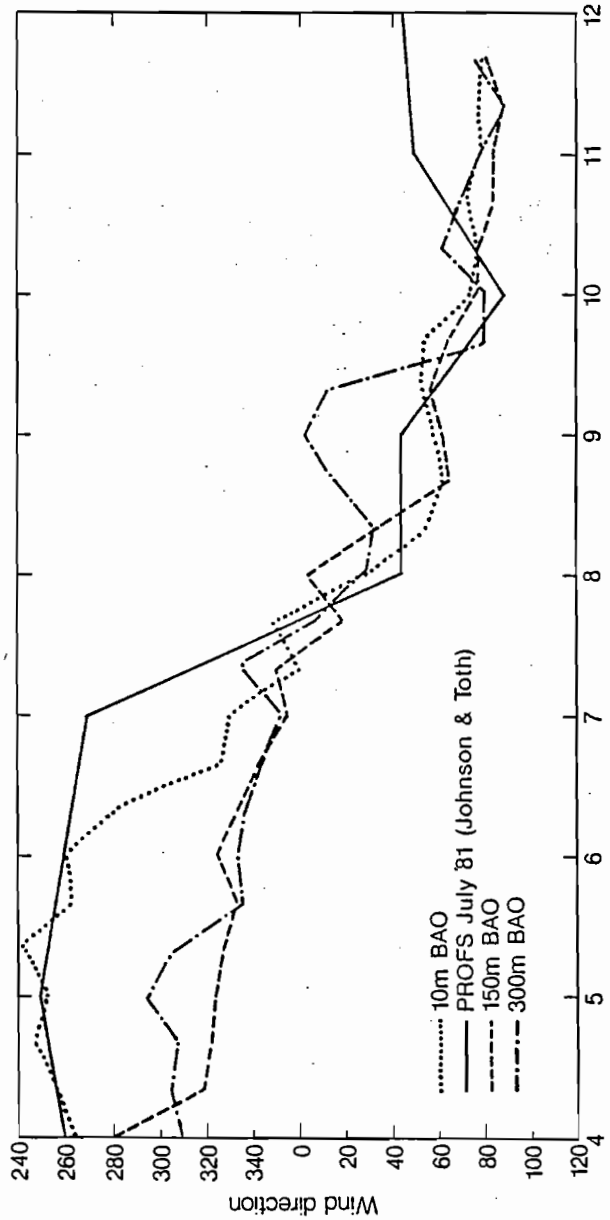

Fig. 20. Wind direction time series composite of BAO 20 min means (0400-1140 MST) and Johnson and Toth (July 1981) hourly averages (0400-1200 MST).

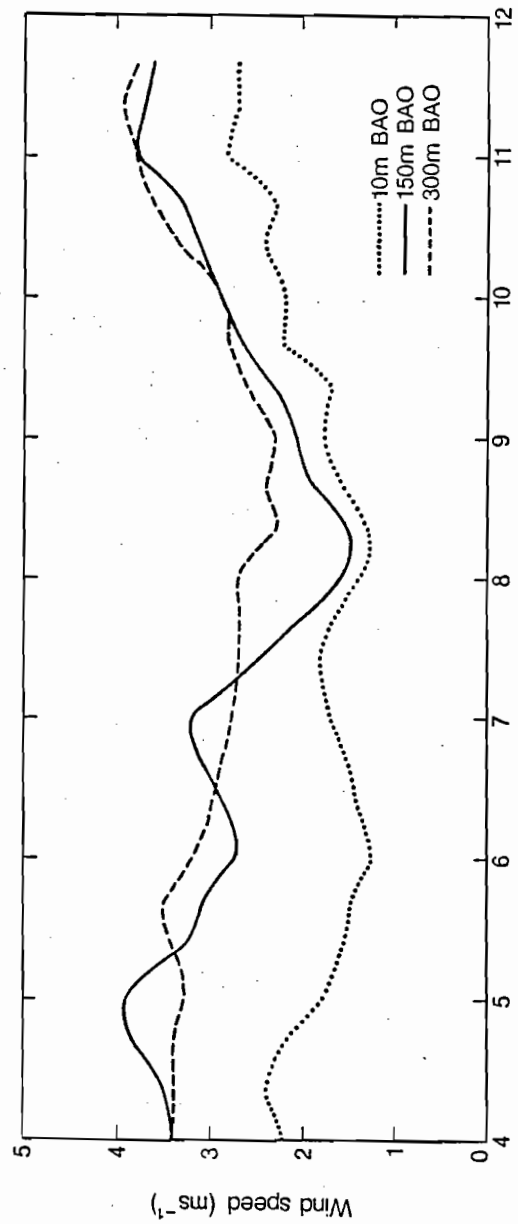

Fig. 21. Wind speed time series composite of BAO 20 min means (0400-1140 MST).

the tower. This fact is due in part to the height of the measurement level and hourly averaging of the PROFS data over an entire month. For the cases chosen in this thesis a PROFS mesonet station was not yet located at the BAO.

Consistency of the BAO 10 m and PROFS directions helps to confirm the local mesoscale influence discussed by Johnson and Toth. Early morning drainage winds out of the southwest are consistent with the local terrain. Winds above 50 m on the tower appear influenced by larger scale drainage off the front range as well as the synoptic pattern. Clockwise turning of the wind begins at the lowest levels around 0620. It is at 0720, when the wind direction at 10 m reaches 340°, that all levels on the tower begin to turn as one. Clockwise rotation of the wind is believed to be a combination of horizontal forcing brought about by changes in the surface pressure field and the Coriolis force (Toth and Johnson, 1983).

The composite of the BAO wind speeds are similar in trend to that of the directions. Early morning light winds (drainage) are evident at 10 m. As the wind turns at all levels, speeds decrease until 0820 when the direction reaches approximately 40°. This minimum in the wind speed appears to correlate with the shift from nighttime drainage to upslope flow caused by heating. Winds at all levels then gradually increase in speed starting at 0820 reaching a maximium of 4 ms^{-1} at 300 m by the end of the analysis period. Tower wind profiles show less variability as winds become vertically "mixed" over the height of the

tower. Johnson and Toth (1982b) in their hourly streamline analyses show how the entire front range behaves in a similar manner.

Two studies on wind characteristics and profiles present results from the BAO using similarity and surface layer theory. Schotz and Panofsky (1980) using

> "results derived under ideal conditions at locations where actual conditions are somewhat more complex"

conclude three things. First they find that after defining a term called "effective" roughness, west winds at the BAO closely fit the surface layer theory even though they move up a slight hill. Effective roughness differs from true roughness in that it is significantly larger because it takes into account the rolling terrain. Next, useful estimates of winds up to 150 m are derived from 10 m winds using the effective roughness lengths and stability measurements. The higher the height at which the winds are estimated the larger the area that must be used in determining roughness lengths. Finally, values of the von Karman constant are calculated from observations. These numbers are consistent with previous findings in near neutral conditions, but do show a direction dependence. Korrell et al. (1982) reconfirms the work of Schotz and Panofsky, adding new data for different seasons, stabilities and wind directions.

The wind contribution to the development of the CBL is primarily in two ways that are both a result of wind shear (mechanical turbulence). Wind shear at the surface is a major factor early in the

morning when convective mixing has not fully developed. As the evolution process continues its importance decreases. The other region of wind shear is at z_i. Comparison of Figs. 20 and 21 (wind time series composites) with Figs. 14 and 15 (θ time series profiles) shows there is vertical wind shear on the tower until almost 0800 MST while the mixed layer is growing.

A recent study at the BAO (Phoenix II; data and results not yet published) collected slow ascent rawinsonde profiles of a growing CBL. What is seen in these profiles is that by late morning the upslope easterlies (mesoscale controlled) are capped by westerlies (synoptically forced). This direction shear can be very important to entrainment at the boundary layer interface. Driedonks (1982b) examines both types of wind shear in relation to entrainment.

5.3 Moisture

Moisture and its role in the CBL evolution is the least understood and possibly the least important of the three variables examined in this chapter. What makes it more difficult are the problems encountered in accurately measuring moisture, especially in dry regions, and its large horizontal variability. Figure 22 shows plots of q relative to the 10 m level comparing vertical profiles for each day at 0400, 0840 and 1140. Pre-sunrise transition q profiles indicate erratic variations in the lowest levels with drier air above. In contrast to θ, q does not show signs of vertical homogeneity at 0840, i.e., there

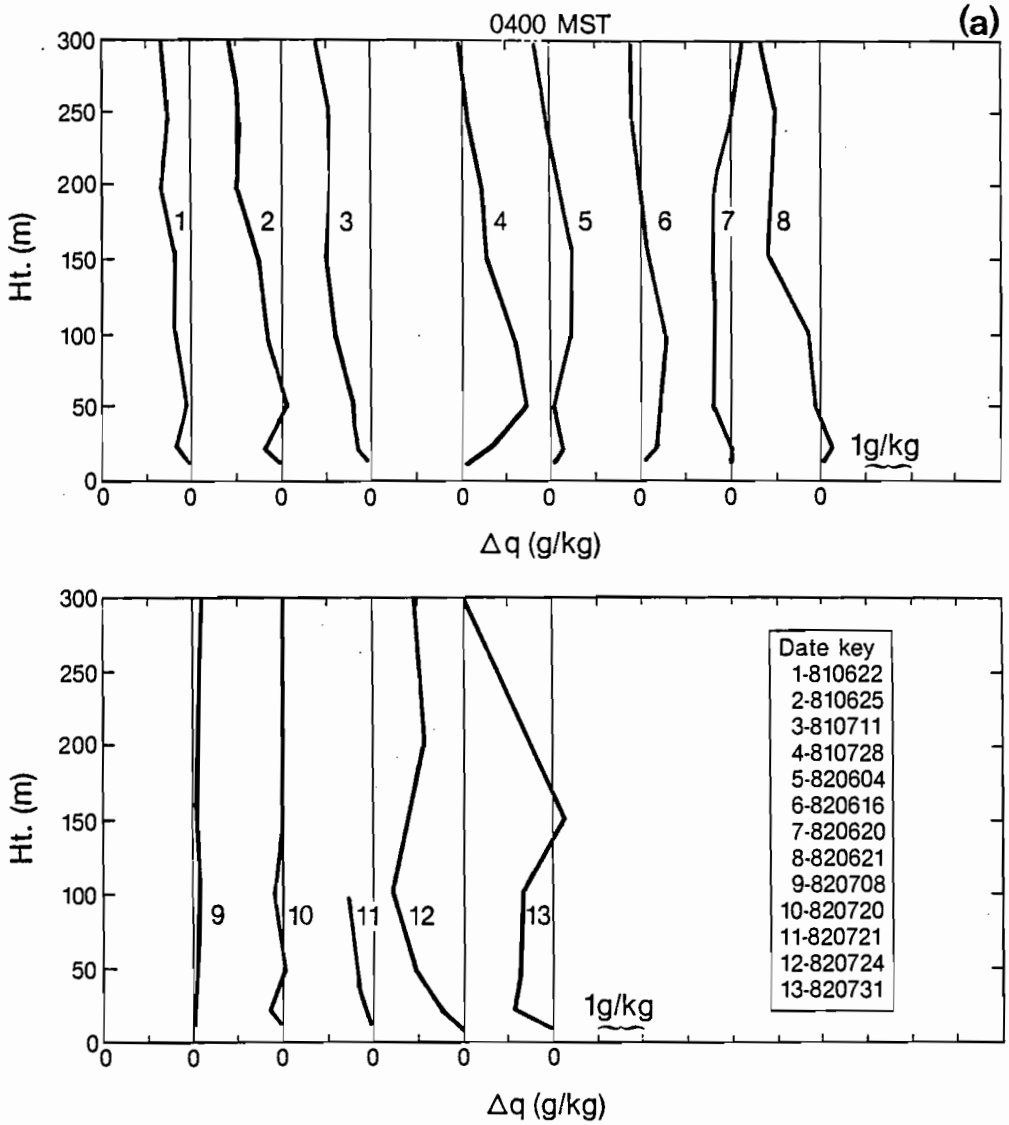

Fig. 22. BAO Δq profiles of 20 min means (0400, 0840, 1140 MST) ($\Delta q = q_z - q_{10\ m}$); 13 days.

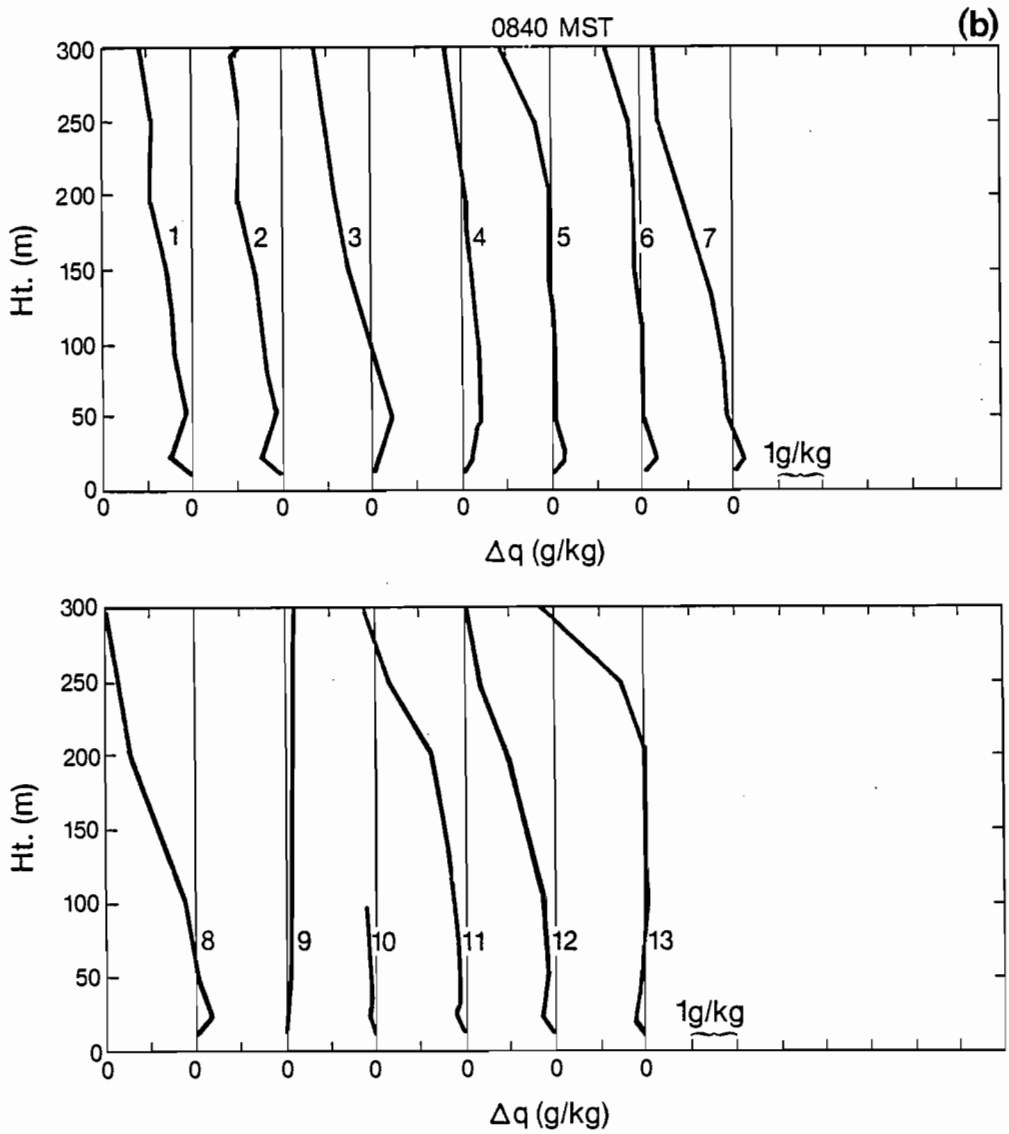

Fig. 22. (continued)

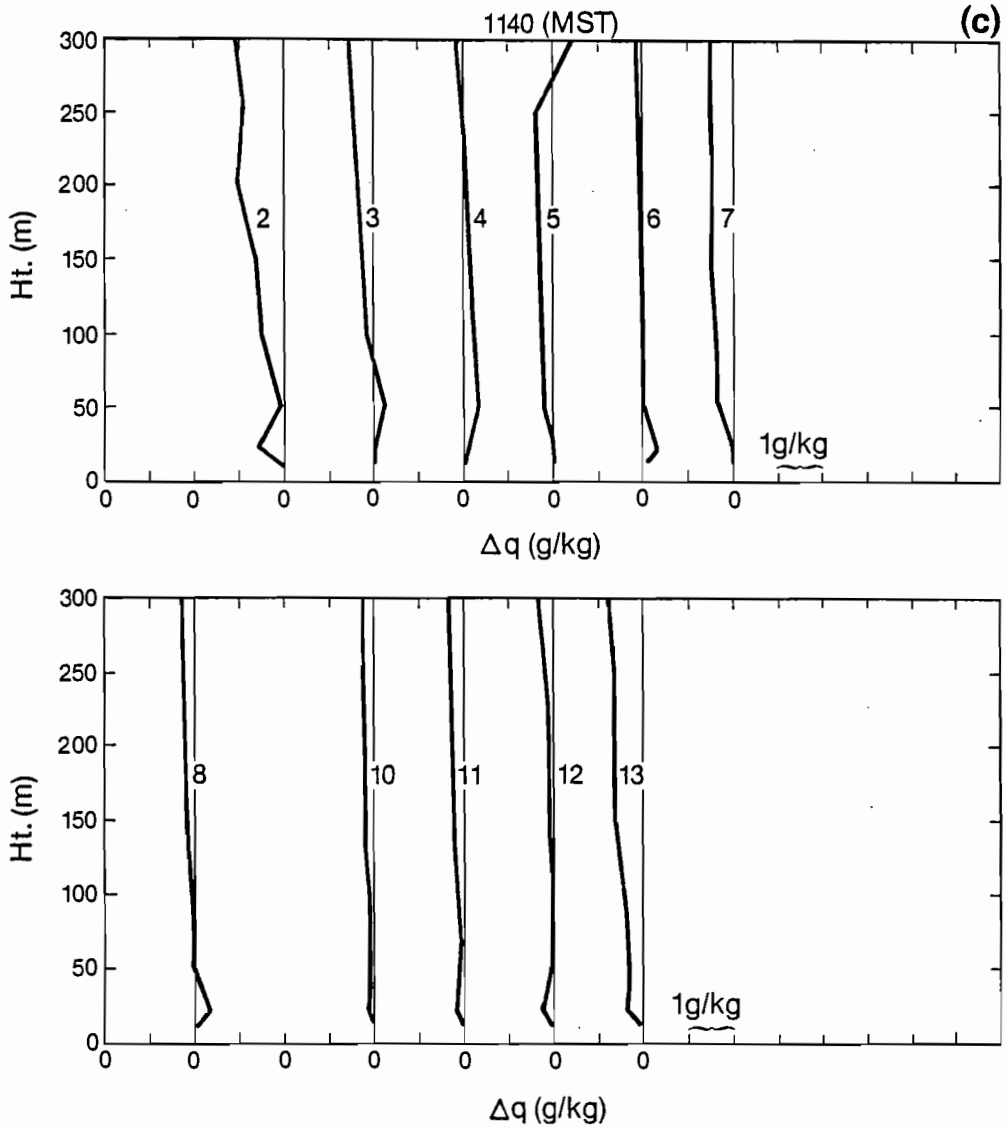

Fig. 22. (continued)

is a gradual decrease of q with height. Furthermore, gradients on all days are now more consistent. Profiles at 1140 still have a few discontinuities in the lowest 22 m with gradually decreasing values above. Gradients for the most part are now only half of what they were at 0840. Specific humidity and θ often have similar profiles close to the ground (Mahrt, 1976) but q may not be as well mixed as θ above this layer.

Examining time series of the individual days at 3 heights (10, 150, 300 m; not shown), there is evidence of a limited moisture source mixing vertically. Specific humidity at 10 m increases shortly after sunrise as evaporation and mixing of surface moisture begins. At 150 m q remains constant until 0640 when it begins to increase as the surface moisture mixes vertically. A similar trend is visible at 300 m where q remains nearly constant until 0840 before slowly increasing. As the moisture mixes vertically, its increase at 10 m slows.

Unlike Mahrt's (1976) depiction of Wangara data, BAO profiles do not show a distinct drop in q corresponding to the height of the mixed layer. This comparison may be somewhat unfair since the difference in the mixing depths is quite large. The profiles do have similar characteristics at the lowest levels to that of Sterling, Co. soundings taken in 1973 during NHRE shown by Mahrt (1976). Mahrt attributes these vertical gradients at Sterling to surface evaporation and entrainment of dry air above. If boundary layer growth is rapid, mixing of dry air into the top of the boundary layer will maintain a

strong vertical gradient. Other factors that would also lead to such gradients are differential advection of moisture caused by large vertical direction shear or increased westerly flow across the top of the mixed layer. The BAO q profiles represent only a small portion of the mixed layer discussed by Mahrt and reexamining of his results is necessary before applying them directly to this data.

Wyngaard and Brost (1984) examine further the mixing of a scalar (moisture) within the boundary layer. Both "top-down" and "bottom-up" type diffusion are discussed in relation to the CBL. Under steady state conditions (without horizontal advection) Wyngaard and Brost are able to maintain the type of vertical gradients found by Mahrt.

The importance of moisture to the growth of the CBL has not been extensively studied. Driedonks (1982b) in examining models and observations of boundary layer growth analyzes the effects of humidity. Latent heat flux and buoyancy are the two factors considered. A term used to define the ratio of sensible heat flux to latent heat flux is the Bowen ratio (B). For regions similar to the BAO this ratio is small in the early morning and very large in favor of sensible heat as the CBL grows. Moist air is lighter than dry air (for the same temperature and pressure). In the early morning the effects of increased buoyancy are usually overshadowed by the large stability present. It is later in the day as the lapse rates become less stable that this buoyancy has its greatest impact.

VI. SUMMARY AND CONCLUSIONS

6.1 Summary

Evolution of the early morning convective boundary layer (CBL) at the Boulder Atmospheric Observatory (BAO) along the Colorado front range has been investigated under clear and undisturbed conditions. Twenty minute average potential temperature (θ), wind and specific humidity (q) data for June and July of 1981 and 1982 have been used. Synoptic and local conditions have been chosen in an effort to reduce the effects of large scale circulation and to treat situations with a generally uniform energy input. While an attempt has been made to strive for horizontally homogeneous conditions by selecting these days, some horizontal variations are inevitable due to the terrain and the varying surface conditions in the region.

BAO tower θ profiles have been compared to Denver, Colorado (12Z) rawinsonde flights, winds at the BAO compared to PROFS (Program for Regional Observing and Forecasting Service) mesonet analyses and q profiles compared to a limited number of moisture studies under similar conditions. Estimates of z_i (height of the lowest point or base of the temperature inversion) taken independently from BAO tower and sodar data have been presented. Several mechanisms involved in the evolution process of the CBL have been discussed along with past CBL experiments and growth studies.

Potential temperature and wind profiles for 20 July 1982, a day determined representative of the evolution of the CBL, are presented in Fig. 23. In these three periods we see many expected processes; initial mixed layer growth, superadiabatic layer development and heating of the mixed layer. Clockwise rotation of the wind is also shown, which is a result of the inertial oscillation and the diurnal heating along the Rocky Mountain's eastern slope. The influences of local terrain and surface heating should be examined before this rotation is fit to the entire front range (Toth and Johnson, 1983). Not expected is the large cooling found near sunrise. Advection, vertical mixing and adiabatic cooling are three processes that have been examined in an effort to explain this decrease in θ. Entrainment is evident at the top of the mixed layer, though not easily recognizable due to the data averaging and vertical tower resolution. Not depicted in Fig. 23 is the variability of both θ (Figs. 14, 15, 19) and the wind from day to day.

6.2 Conclusions

Comparison of BAO and Denver θ profiles showed good agreement despite their 30 km horizontal separation and the lack of vertical resolution in the rawinsonde data. Basic vertical structures had similarities even in terms of the sharp gradients in the lowest levels. Potential temperature profiles for each day were analyzed in detail for three 2 hr 40 min time blocks. The first period (0400-0620 MST)

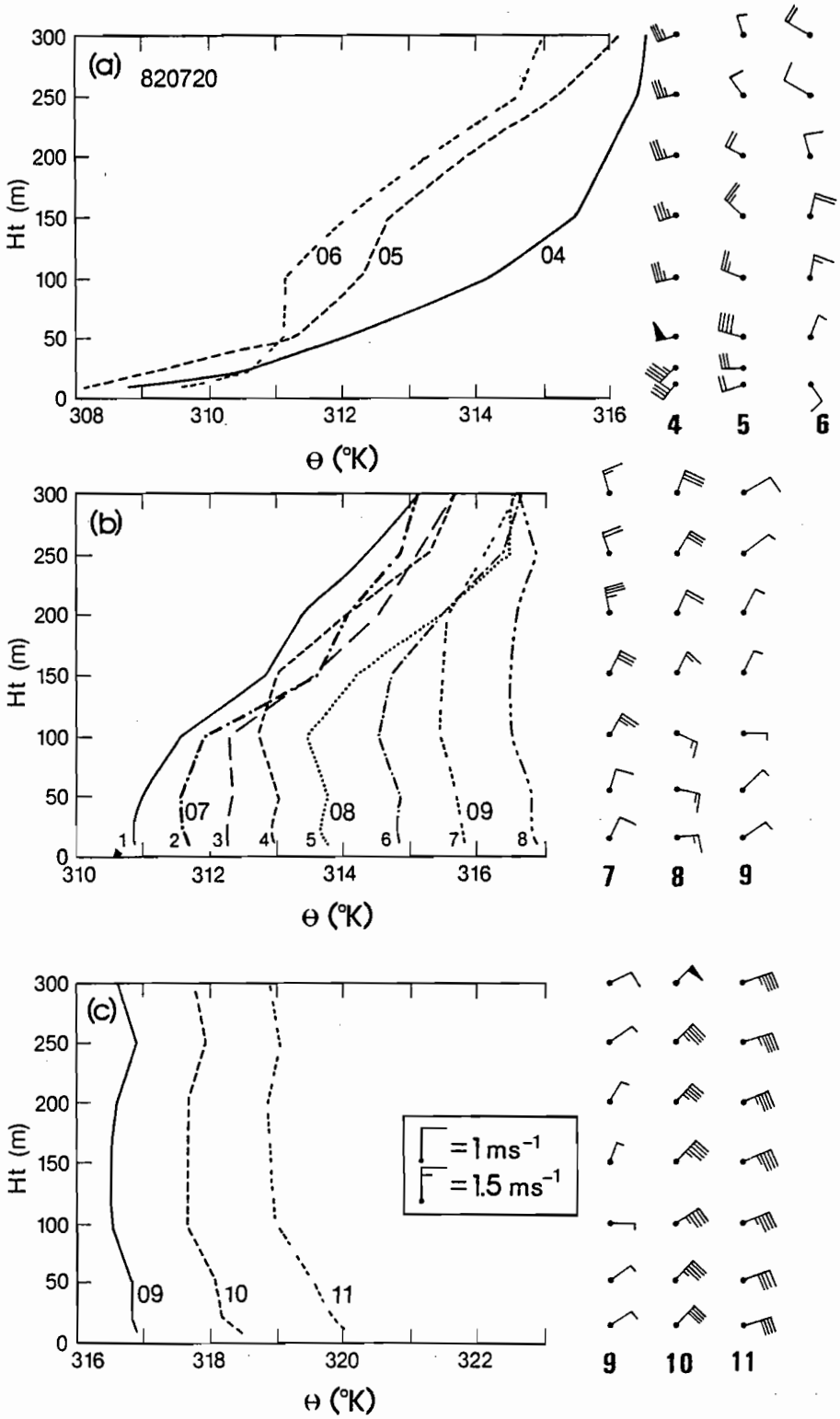

Fig. 23. BAO θ and wind profiles of 20 min means, a) sunrise transition b) mixed layer development, c) maturing mixed layer.

included the sunrise transition where horizontal gradients and changing surface conditions were important. Evidence of a developing mixed layer did appear as early as 40 min after sunrise in some instances. As the initial growth processes began in the lower 1/3 of the tower, the upper 2/3's were changing in an independent manner. Cooling and or warming in this region were at times accompanied by changes in the existing stability.

From 0640-0900 MST an evolving mixed layer was visible on the tower as well as a superadiabatic layer. Processes controlling the superadiabatic layer were not discussed, but instead these layers were examined for overall depth and shape. Exponential shaped profiles extended to a maximum depth of 100 m by the end of this period. Evolution of the mixed layer was analyzed in detail with five terms singled out from equation (5) in Chapter V as important; advection of z_i, stability, vertical motion, surface buoyancy flux and entrainment. All of these terms were affected by the complex terrain as well as by each other to some degree, but not necessarily in the same way or amount.

An attempt was made to classify the type of CBL growth found on each day. Though by no means clear-cut, two growth patterns were identified with a third covering undefined growth. The first type was classified as a combination of surface heating and mixing from below coupled with entrainment at the upper boundary interface. In the second type, growth by surface heating alone was identified.

Entrainment is also occurring here but is not changing the stability above z_i significantly. Three factors considered when examining these classifications were vertical resolution of the tower, 20 min averages and entrainment treated as a constant. Tower resolution and data averaging smoothed out the CBL growth pattern. This point combined with the fact that entrainment in a true sense could be better represented by bursts of mixing at varying rates made these classifications somewhat crude.

In the final period (0920-1140 MST) the mixed layer had grown to encompass the entire tower. What was most evident over this 2 hr 40 min period was the warming of the CBL. Because there was a large spread in the heating of the mixed layer (1.5-7°K), an attempt was made to explore the processes contributing to these differences. It was shown that the heating rate depends on advection, variability of z_i, surface heat flux and entrainment. The initial conditions set forth allowed horizontal advection to be neglected and surface heat flux was treated as a sinusoidal function, while the variability of z_i and entrainment became the unknowns. Since both z_i and entrainment were dependent on additional factors (e.g., terrain, upper-level stability), it was not possible from this analysis to directly determine their individual importance.

BAO wind profiles and time series were analyzed for the effects of local terrain and mesoscale circulation. Comparison of the BAO wind directions to an analysis of the PROFS mesonet data in July of 1981

(Johnson and Toth, 1982a) provided excellent insight into the mesoscale circulation pattern set-up along the front range. Early morning downslope drainage, both shallow flow influenced by local terrain and flow off the Rocky Mountain Front Range, was observed. This pattern shifted in a clockwise direction from downslope westerlies to easterly upslope flow over the depth of the BAO tower.

Winds influence the evolution of the CBL primarily through mechanical turbulence created by wind shear. Shear is important at the surface early in the morning when convection is in its preliminary stages and at the upper boundary interface later in the day when low-level easterlies (mesoscale) are capped by upper-level westerlies (synotpic scale).

BAO q profiles did not have the consistent mixing pattern that was found for θ. Time series at three tower levels showed evidence of vertical mixing of surface evaporated moisture. Gradients and changes in q were close to the limitation imposed by the accuracy of the instrumentation.

The main impact of moisture on the CBL is through latent heat flux and buoyancy. Latent heat flux is significant early in the morning when sensible heat flux is small. Increased buoyancy due to the moisture becomes important as the stability above the CBL weakens.

The BAO provides a continuous data platform with which to study the vertical and time variations of the CBL, while its data processing

capabilities along with the supporting data adds to the quality of the data. Not to be overlooked is the BAO's proximity to the Rocky Mountains and the surrounding non-homogeneous terrain making it a unique research site. Horizontal gradients of z_i along the front range are highly variable in all directions. This fact makes results observed at the BAO representative of a small region with mixing depths in other areas subject to local conditions.

6.3 Future Studies

As seen in this thesis, there is need for future studies and analysis of data already collected at the BAO. Increased time resolution as well as vertical resolution through the use of 10 s averages and the instrument carriage could provide additional answers to the evolution process. Lyman-alpha hygrometers are available for special experiments and would allow further study of the importance of moisture flux in the CBL, especially during the initial growth period. Direct calculation of $(\overline{w'\theta_v'})$ from tower instruments and independent measurements of z_i from sodar data would prove very valuable in future analyses. Elevated layers seen on sodars can be studied further in conjunction with tower measurements. Detailed analyses of the processes, varying strengths and time scales of entrainment are also possible while the interface region remains within the height of the tower. Knowledge of how the complex terrain interacts with boundary layer growth needs further examination under "non-ideal" conditions. And finally, because the BAO is

located within the PROFS mesonet region, the opportunity exists to combine these two data sets for a wide range of studies covering not only the CBL, but other aspects of the planetary boundary layer.

REFERENCES

André, J.C. and L. Mahrt, 1982: The Nocturnal Surface Inversion and Influence of Clear-Air Radiative Cooling. J. Atmos. Sci., 39, 864-878.

Ball, F.K., 1960: Control of Inversion Height by Surface Heating. Quart. J. Roy., Meteor. Soc., 86, 483-494.

Benkley, C.W., 1977: Model of the Planetary Boundary Layer Growth using Sodar Validation. Dept. of Meteorology, Pennsylvania State University, 110 pp.

Benkley, C.W. and L.L. Schulman, 1979: Estimating Hourly Mixing Depths from Historical Meteorological Data. J. Appl. Meteor., 18, 772-780.

Carson, D.J., 1973: The Development of a Dry Inversion-Capped Convectively Unstable Boundary Layer. Quart. J. Roy. Meteor. Soc., 99, 450-467.

Cermak, J.E. and J.D. Horn, 1968: Tower Shadow Effect. J. Geophy. Resear., 73, 1869-1876.

Clarke, R.H., A.J. Dyer, R.R. Brook, D.G. Reid and A.J. Troup, 1971: The Wangara Experiment. Tech. Paper 19, Div. Meteor. Anys. CSIRO, Australia, 341 pp.

Clarke, R.H. and R.R Brook, Eds., 1979: The Koorin Expedition. Austrailian Gov't. Pub. Service, Dept. of Sci. and Eniv., Bureau of Meteor.

Coulman, C.E., 1978: Boundary-Layer Evolution and Nocturnal Inversion Dispersal Part I. Bound. Layer Meteor., 14, 471-491.

Deardorff, J.W., G.E. Willis and D.K. Lilly, 1969: Laboratory Investigation of Non-steady Penetrative Convection. J. Fluid Mech., 35, 7-31.

Deardorff, J.W., 1974: Three-Dimensional Numerical Study of the Height and Mean Structure of a Heated Planetary Boundary Layer. Bound. Layer Meteor., 7, 81-106.

Deardorff, J.W., 1979: Prediction of Convective Mixed-Layer Entrainment for Realistic Capping Inversion Structure. J. Atmos. Sci., 36, 424-436.

Dirks, R.A., 1969: A Theoretical Investigation of Convective Patterns in the Lee of the Colorado Rockies. Atmospheric Science Paper No. 154, Colorado State University, 122 pp.

Driedonks, A.G.M., 1981: Dynamics of the Well Mixed Atmospheric Boundary Layer. Royal Netherlands Meteorological Institute Scientific Report W.R. 81-2, 189 pp.

Driedonks, A.G.M., 1982a: Sensitivity Analysis of the Equations for a Convective Mixed Layer. Bound. Layer Meteor., 22, 475-480.

Driedonks, A.G.M., 1982b: Models and Observations of the Growth of the Atmospheric Boundary Layer. Bound. Layer Meteor., 23, 283-306.

Garrett, A.J., 1981: Comparison of Observed Mixed-Layer Depths to Model Estimates Using Observed Temperatures and Winds, and MOS Forecasts. J. Appl. Meteor., 20, 1277-1283.

Geiger, R., 1965: The Climate Near the Ground. rev. ed. Cambridge, Harvard University Press, 611 pp. (translated by Scripta Technica, Inc. from the 4th German edition 1961).

Gill, G.C., L.E. Olson, J. Sela and M. Suda, 1967: Accuracy of Wind Measurements on Towers or Stacks. Bull. Amer. Meteor. Soc., 48, 665-673.

Goff, C.R. and H.R. Hudson, 1972: The Thermal Structure of the Lowest Half Kilometer in Central Oklahoma: December 9, 1966 - May 31, 1967. NOAA Technical Memorandum ERL NSSL-58, 50 pp.

Gossard, E., W.D. Neff and R. Zamora, 1983: A Case Study of Layer Fine Structure and Turbulence within Stable Elevated Layers. NOAA Technical Memorandum ERL WPL-114, 34 pp.

Hahn, C.J., 1981: A Study of the Diurnal Behavior of the Boundary-Layer Winds at the Boulder Atmopheric Observatory. Bound. Layer Meteor., 21, 231-245.

Haugen, D.A., J.C. Kaimal and E.F. Bradley, 1971: An Experimental Study of Reynolds Stress and Heat Flux in the Atmospheric Surface Layer. Quart. J. Roy. Meteor. Soc., 97, 168-180.

Hicks, B.B., G.D. Hess, M.L. Wesley, T. D.L. Sisterson, P.E. Hess, F.C. Kulhanek, R.C. Lipschutz and G.A. Zerbe, 1981: Sagamon Field Experiments: Observations of the Diurnal Evolution of the Planetary Boundary Layer Over Land. Argonne National Laboratory Report ANL/RER-81-1, 40 pp.

Holton, J.R., 1972: An Introduction to Dynamic Meteorology. Second Edition, New York, Academic Press, 319 pp.

Holzworth, G.C., 1964: Mean Maximum Mixing Depths in the Contiguous United States. Mon. Wea. Rev., 92, 235-242.

Holzworth, G.C., 1967: Mixing Depths, Wind Speeds and Air Polution Potential for Selected Locations in the United States. J. Appl. Meteor., 6, 1039-1044.

Hooke, W.H., Ed., 1979, Project Phoenix: The September 1978 Field Operation. BAO Report No. 1, 281 pp.

Hootman, B.W. and W. Blumen, 1983: Analysis of Nighttime Drainage Winds in Boulder, Colorado during 1980. Mon. Wea. Rev., III, 1052-1061.

Hosler, C.R., 1961: Low-Level Inversion Frequency in the Contiguous United States. Mon. Wea. Rev., 89, 319-338.

Johnson, N.K. and G.S.P. Heywood, 1938: An Investigation of the Lapse Rate of Temperature in the Lowest Hundred Meters of the Atmosphere. Meteorological Office Geophysical Memoirs No. 77, 49 pp.

Johnson, R.H. and J.J. Toth, 1982a: Topographical Effects and Weather Forecasting in the Colorado PROFS Mesonetwork Area. Preprint Vol.: 9th Conference on Weather Forecasting and Analysis June 28 - July 1, 1982, 440-445.

Johnson, R.H. and J.J. Toth, 1982b: A Climatology of the July 1981 Surface Flow Over Northeastern Colorado. Atmospheric Science Paper No. 342 Colorado State University, 52 pp.

Kaimal, J.C., J.C. Wyngaard, D.A. Haugen, O.R. Cote, Y. Izumi, S.J. Caughey and C.J. Readings, 1976: Turbulence Structure in the Convective Boundary Layer. J. Atmos. Sci., 33, 2152-2169.

Kaimal, J.C., H.W. Bayton and J.E. Gaynor, Eds., 1980: The Boulder Low-Level Intercomparison Experiment. BAO Report No. 2, 189 pp.

Kaimal, J.C., R.A. Eversole, D.H. Lenschow, B.B. Stankov, P.H. Kahn and J.A. Businger, 1982: Spectral Charaecteristics of the Convective Boundary Layer Over Uneven Terrain. J. Atmos. Sci., 39, 1098-1114.

Kaimal, J.C., N.L. Abshire, R.B. Chadwick, M.T. Decker, W.H. Hooke, R.A. Kropfli, W.D. Neff, F. Pasqualucci and P.H. Hildebrand, 1982b: Estimating the Depth of the Daytime Convective Boundary Layer. J. Appl. Meteor., 21, 1123-1129.

Kaimal, J.C. and J.E. Gaynor, 1983: The Boulder Atmospheric Observatory. J. Appl. Meteor., 22, 863-880.

Klöppel, M., G. Stilke and C. Wamser, 1978: Experimental Investigations into the Variations of Ground-Based Inversions and Comparisons with Results of Simple Boundary-Layer Models. Bound. Layer Meteor., 15, 135-145.

Korrell, A., H.A. Panofsky and R.J. Rossi, 1982: Wind Profiles at the Boulder Tower. Bound. Layer Meteor., 22, 295-312.

Kuo, H.L. and W.Y. Sun, 1976: Convection in the Lower Atmosphere and its Effects. J. Atmos. Sci., 33, 21-40.

Lenschow, D.H., B.B. Stankov and L. Mahrt, 1979: The Rapid Morning Boundary-Layer Transition. J. Atmos. Sci., 36, 2108-2124.

Lenschow, D. H., R. Pearson Jr. and B. B. Stankov, 1981: Estimating the Ozone Budget in the Boundary Layer by Use of Aircraft Measurements of Ozone Eddy Flux and Mean Concentration. J. Geophy. Res., 86, 7291-7297.

Lettau, H.H. and B. Davidson, 1957: Exploring the Atmosphere's First Mile, Vols. 1 and 2. Pergamon Press, New York, 578 pp.

Lilly, D.K., 1968: Models of Cloud-Topped Mixed Layers Under a Strong Inversion. Quart. J. Roy. Meteor. Soc., 94, 292-309.

Mahrt, L. and D.H. Lenschow, 1976: Growth Dynamics of the Convective Mixed Layer. J. Atmos. Sci., 33, 41-51.

Mahrt, L., 1976: Mixed Layer Moisture Structure. Mon. Wea. Rev., 104, 1403-1407.

Mahrt, L., 1983: Atmospheric Boundary Layers. Rev. Geophy. and Space Phy., 21, 1042-1048.

McTaggart-Cowan, J.D. and D.J. McKay, 1976: Radiation Shields - An Intercomparison. Atmospheric Environment Service, 8 pp.

Murray, F.W., 1967: On the Computation of Saturation Vapor Pressure. J. Appl. Meteor., 6, pp. 203-204.

National Oceanic and Atmospheric Administration: Daily Weather Maps, Weekly Series. U.S. Gov't. Printing Office.

Neff, W.D, 1975: Quantitative Evaluation of Acoustic Echoes from the Planetary Boundary Layer. NOAA Technical Report ERL 323-WPL 38, 32 pp.

Owens, E.J., 1975: NOAA Mark VII Acoustic Echo Sounder. NOAA Technical Memorandum ERL WPL-12, 71 pp.

Panofsky, H.A. and J.A. Dutton, 1984: Atmospheric Turbulence. A Wiley Interscience Publication, 397 pp.

Panofsky, H.A., 1984: Vertical Variation of Roughness Length at the Boulder Atmospheric Observatory. Bound. Layer Meteor., 28, 305-308.

Peterson, J.T. and E.C. Flowers, 1977: Interactions between Air Pollution and Solar Radiation. Solar Energy, 19, 23-32.

Quiroz, R.S., 1956: An Anotated Bibliography on Temperature Inversions in the Troposphere. Meteor. Abstr. Bibliogr., 7, 742-789.

Reible, D.D., F.H. Shair and R. Aris, 1983: A Two-Layer Model of the Atmosphere Indicating the Effects of Mixing between the Surface Layer and the Air Aloft. Atmos. Environ., 17, 25-33.

Rosenburg, N.J., B.L. Blad and S.B. Verma, 1983: Microclimate: The Biological Environment. A Wiley Interscience Publication, 495 pp.

Schewe, G.J., 1975: A Climatology of Inversions. Colorado State University Atmospheric Science Paper No. 238, 103 pp.

Schotz, S. and H.A. Panofsky, 1980: Wind Characteristics at the Boulder Atmospheric Observatory. Bound. Layer Meteor., 19, 155-164.

Sellers, W.D., 1965: Physical Climatology. Chicago, The University of Chicago Press, 272 pp.

Slob, W.H., 1978: The Accuracy of Aspiration Thermometers. Royal Netherlands Meteorological Institute Scientific Report W.R. 78-1, 17 pp.

Stull, R.B., 1973: Inversion Rise Model Based on Penetrative Convection. J. Atmos. Sci., 30, 1092-1099.

Stull, R.B., 1976a: The Energetics of Entrainment Across a Density Interface. J. Atmos. Sci., 33, 1260-1267.

Stull, R.B., 1976b: Mixed-Layer Depth Model Based on Turbulent Energetics. J. Appl. Sci., 33, 1268-1278.

Stull, R.B., 1976c: Internal Gravity Waves Generated by Penetrative Convection. J. Appl. Sci., 33, 1279-1286.

Tennekes, H., 1973: A Model for the Dynamics of the Inversion Above a Convective Boundary Layer. J. Atmos. Sci., 30, 558-567.

Tennekes, H. and A.G.M. Driedonks, 1981: Basic Entrainment Equations for the Atmospheric Boundary Layer. Bound. Layer Meteor., 20, 515-531.

Toth, J.J., and R. H. Johnson, 1983: An Observational Study of Summer Surface Flow Over Northeastern Colorado. Atmospheric Science Paper No. 2, Colorado State University, 85 pp.

Trewartha, G.T. and L.H. Horn, 1980: An Introduction to Climate. McGraw-Hill Book Co. Inc., New York, 416 pp.

Tsay, Mu-King, Ting-I Wang, R.S. Lawrence, G.R. Ochs and R.B. Fritz, 1980: Wind Velocity and Convergence Measurements at the Boulder Atmospheric Observatory using Path-Averaged Optical Wind Sensors. J. Appl. Meteor., 19, 826-833.

United States Air Force, 1969: Use of the Skew T, Log P Diagram in Analysis and Forecasting. AWS Manual 105-124.

Wallace, J.M. and P.V. Hobbs, 1977: Atmospheric Science: An Introductory Survey. Academic Press, 467 pp.

Whiteman, D.C., 1980: Breakup of Temperature Inversions in Colorado Mountain Valleys. Atmospheric Science Paper No. 328 Colorado State University, 250 pp.

Wilczak, J.M. and J.A. Businger, 1983: Thermally Indirect Motions in the Convective Atmospheric Boundary Layer. J. Atmos. Sci., 40, 343-358.

Wyngaard, J.C., Ed., 1980: Workshop on the Planetary Boundary Layer. American Meteorol. Soc., 14-18 Aug. 1978 Boulder, Co., 322 pp.

Wyngaard, J.C., 1982: Lectures on the Planetary Boundary Layer. Presented at the NATO Advanced Study Institute on Mesoscale Meteorology, France, 48 pp.

Wyngaard, J.C. and R.A. Brost, 1984: Top-Down and Bottom-Up Diffusion of a Scalar in the Convective Boundary Layer. J. Atmos. Sci., 41, 102-112.

Yamada, T. and S. Berman, 1979: A Critical Evaluation of a Simple Mixed-Layer Model with Penetrative Convection. J. Appl. Meteor., 18, 781-786.

Yoshino, M.M., 1975: Climate in a Small Area. Tokyo, University of Tokyo Press, 549 pp.

Zeman, O. and H. Tennekes, 1977: Parameterization of the Turbulent Energy Budget at the Top of the Daytime Atmospheric Boundary Layer. J. Atmos. Sci., 34, 111-123.

APPENDIX A

Whiteman (1980)

$$\frac{\partial \gamma}{\partial t} = - \vec{V} \cdot \vec{\nabla}\gamma - \frac{\partial \vec{V}}{\partial z} \cdot \vec{\nabla}\theta - \vec{w} \frac{\partial \gamma}{\partial z} - \gamma \frac{\partial w}{\partial z} + \frac{\theta}{C_p} \left[\frac{\partial}{\partial z} \frac{dQ}{dt}\right]$$

A B C D E

AWSM 105-124 (1969)

$$\frac{\partial \gamma}{\partial t} = -\vec{V} \cdot \vec{\nabla}\gamma + \frac{\partial \vec{V}}{\partial z} \cdot \vec{\nabla}\Gamma - \vec{w} \frac{\partial \gamma}{\partial z} + \frac{\partial w}{\partial z} (\Gamma - \gamma) - \frac{1}{C_p} \frac{\partial}{\partial z} \left(\frac{dQ}{dt}\right)$$

A B C D E

A) Horizontal advection of γ gradient.

B) Shearing advection of temperature gradient.

C) Vertical advection of the stability.

D) Shrinking or stretching of γ.

E) Vertical gradient of diabatic heating rate.

APPENDIX B

BAO SODAR FACSIMILE RECORDS

Note reverse time notation at the bottom of each record.

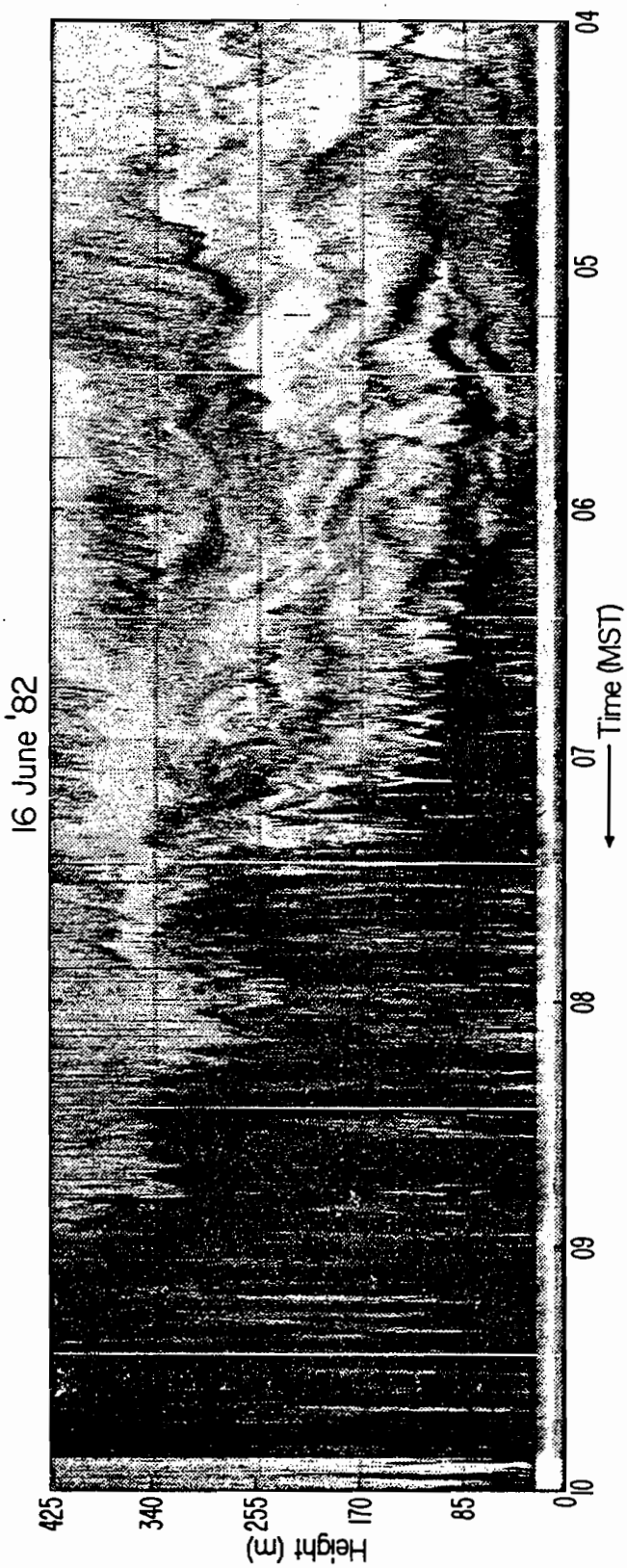
16 June '82
Height (m)
425
340
255
170
85
0
10
09
08
07
06
05
04
Time (MST)

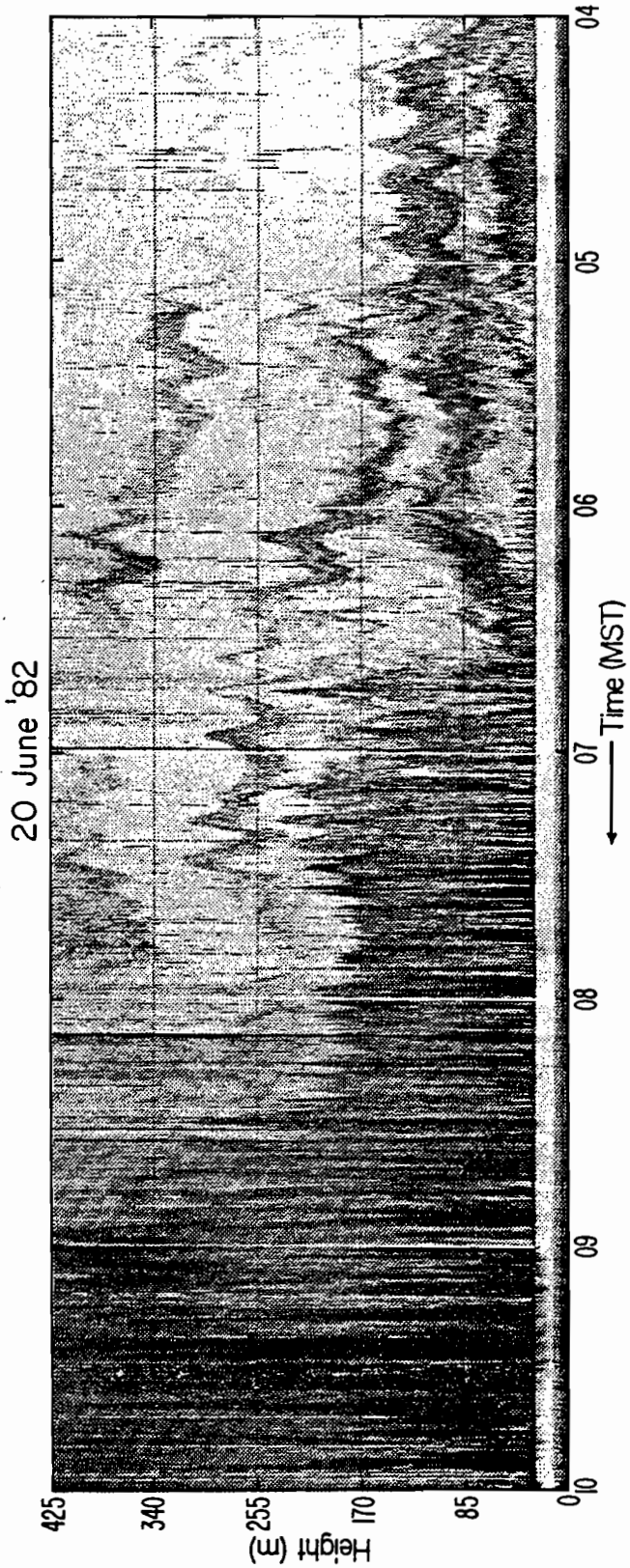
20 June '82
Height (m)
425
340
255
170
85
0
10
09
08
07
06
05
04
Time (MST)

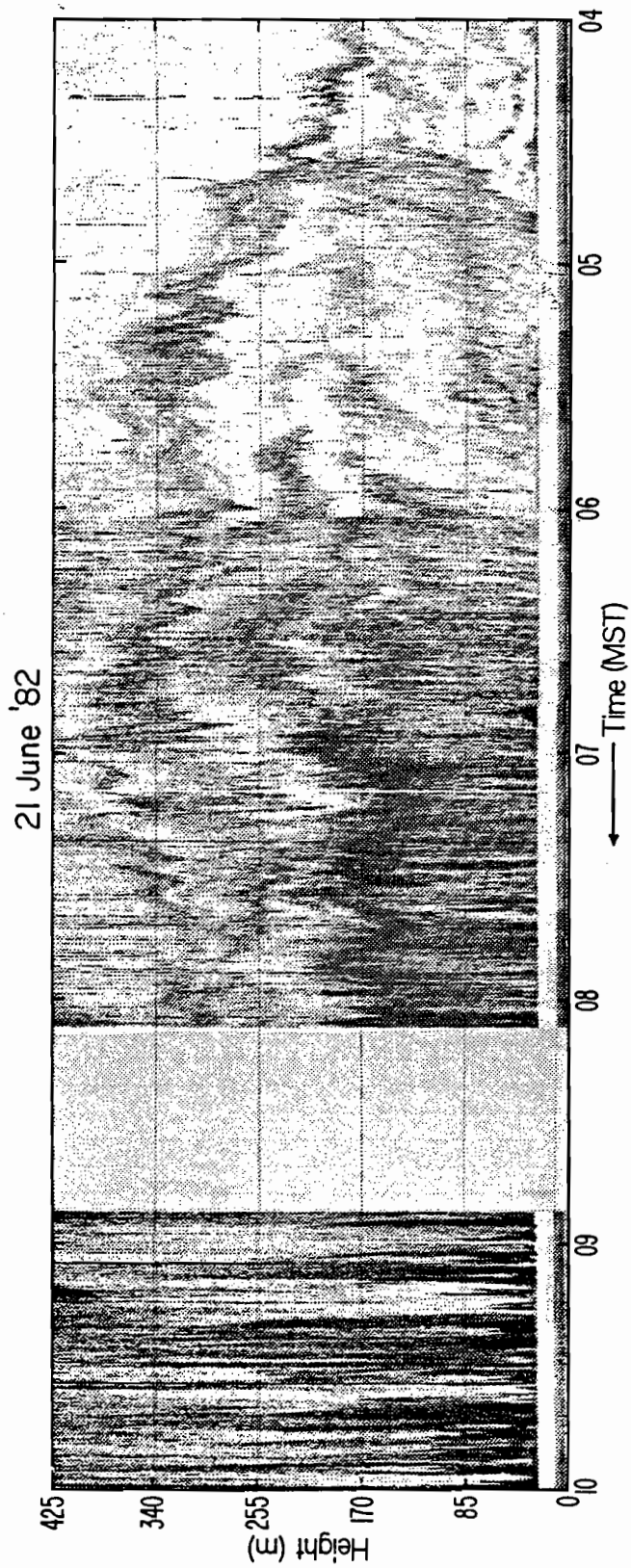
21 June '82
Height (m)
425
340
255
170
85
0
10
09
08
07
06
05
04
Time (MST)

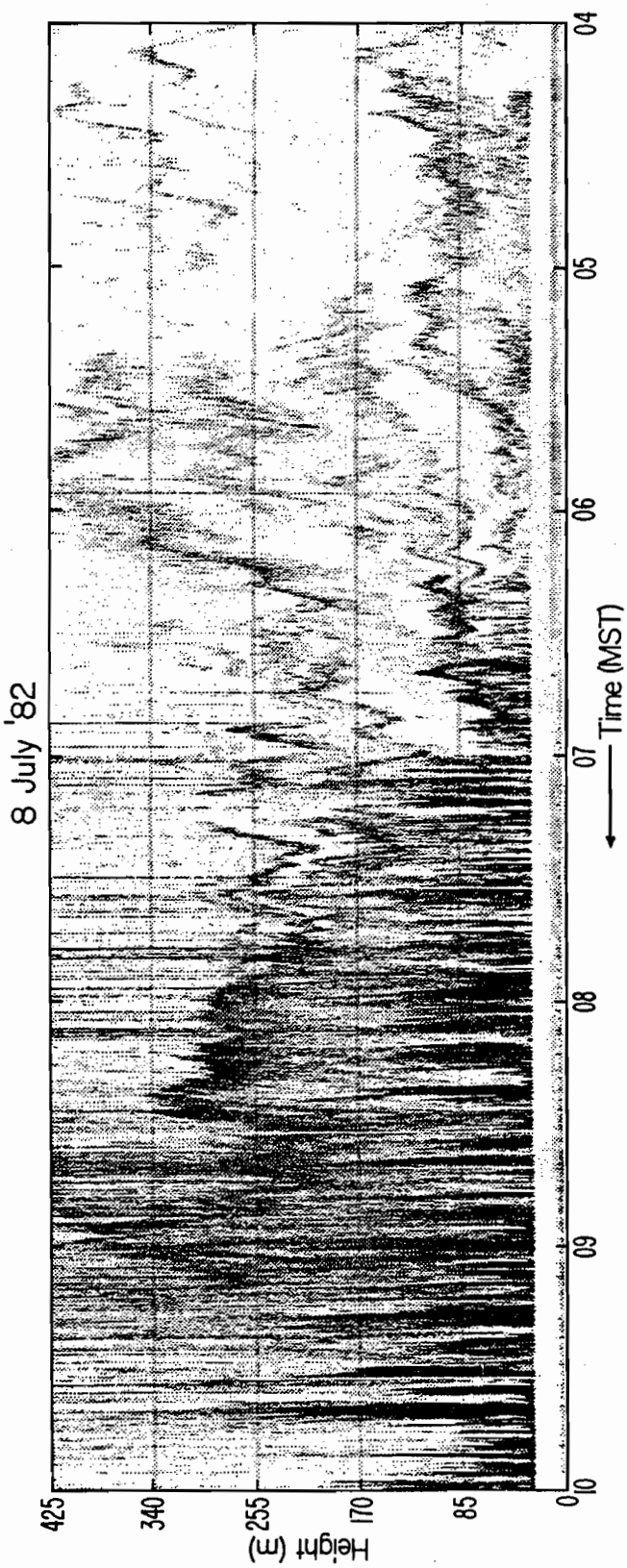
8 July '82
Height (m)
425
340
255
170
85
0
10
09
08
07
06
05
04
Time (MST)

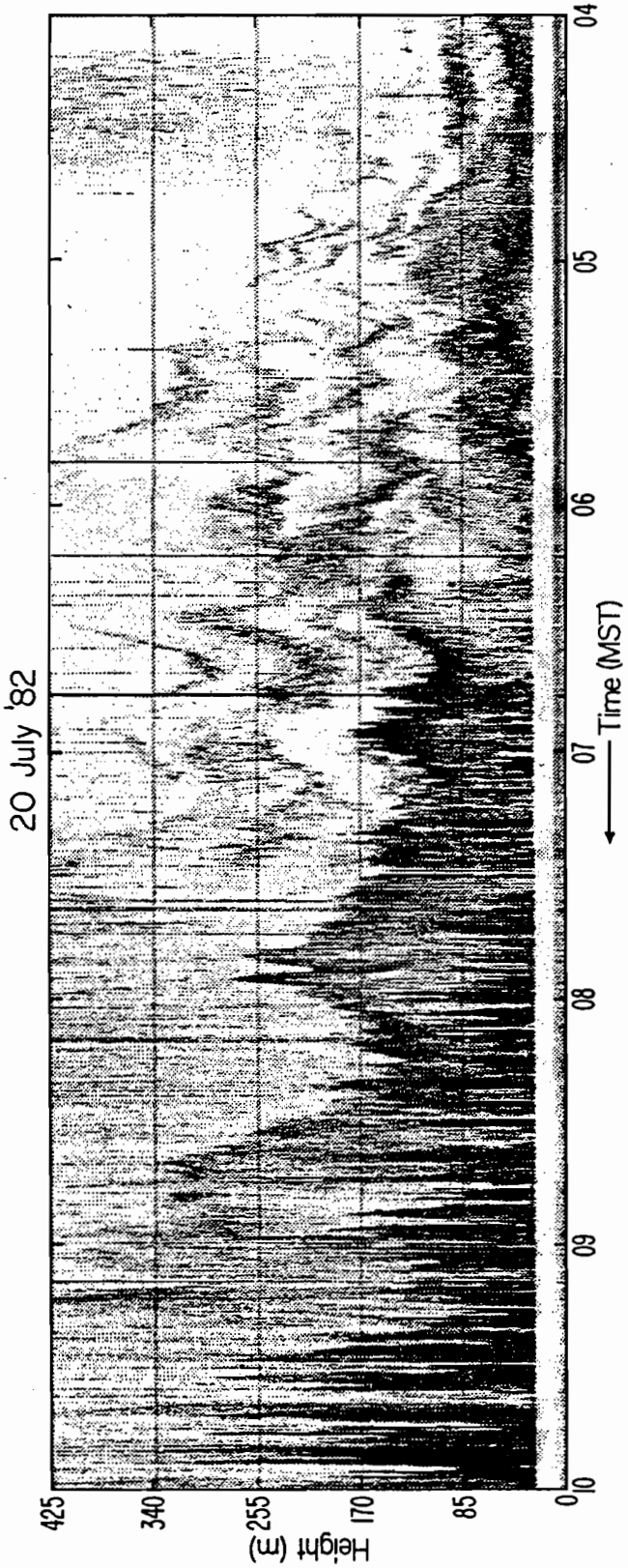
20 July '82
Height (m)
425
340
255
170
85
0
10
09
08
07
06
05
04
Time (MST)

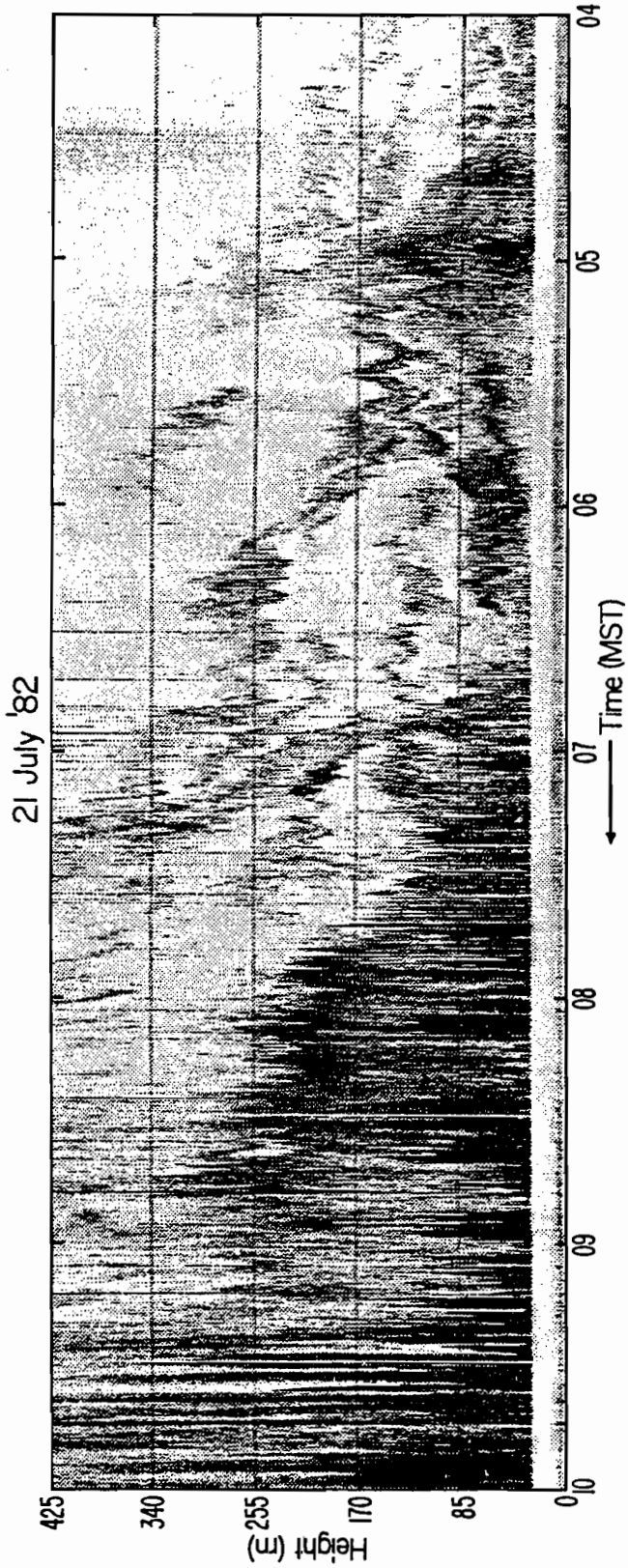
21 July '82
Height (m)
425
340
255
170
85
0
10
09
08
07
06
05
04
Time (MST)

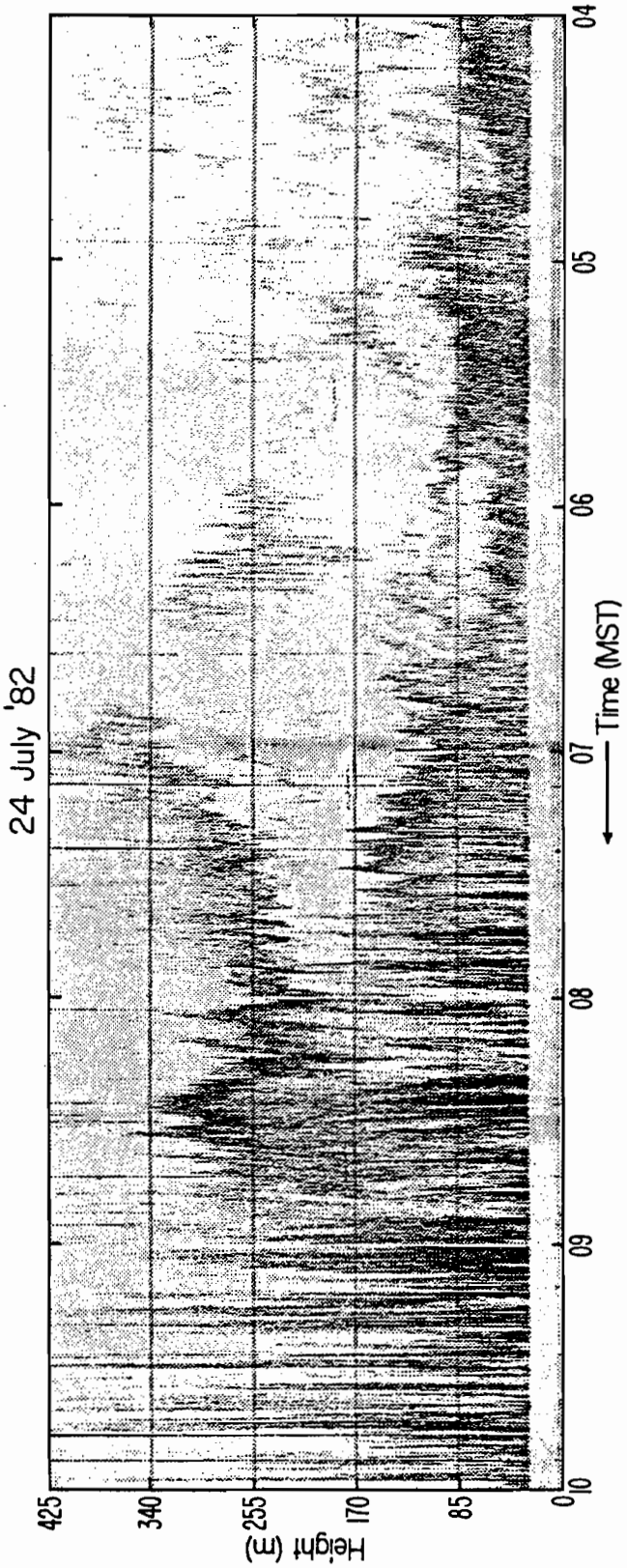
24 July '82
Height (m)
425
340
255
170
85
0
10
09
08
07
06
05
04
Time (MST)

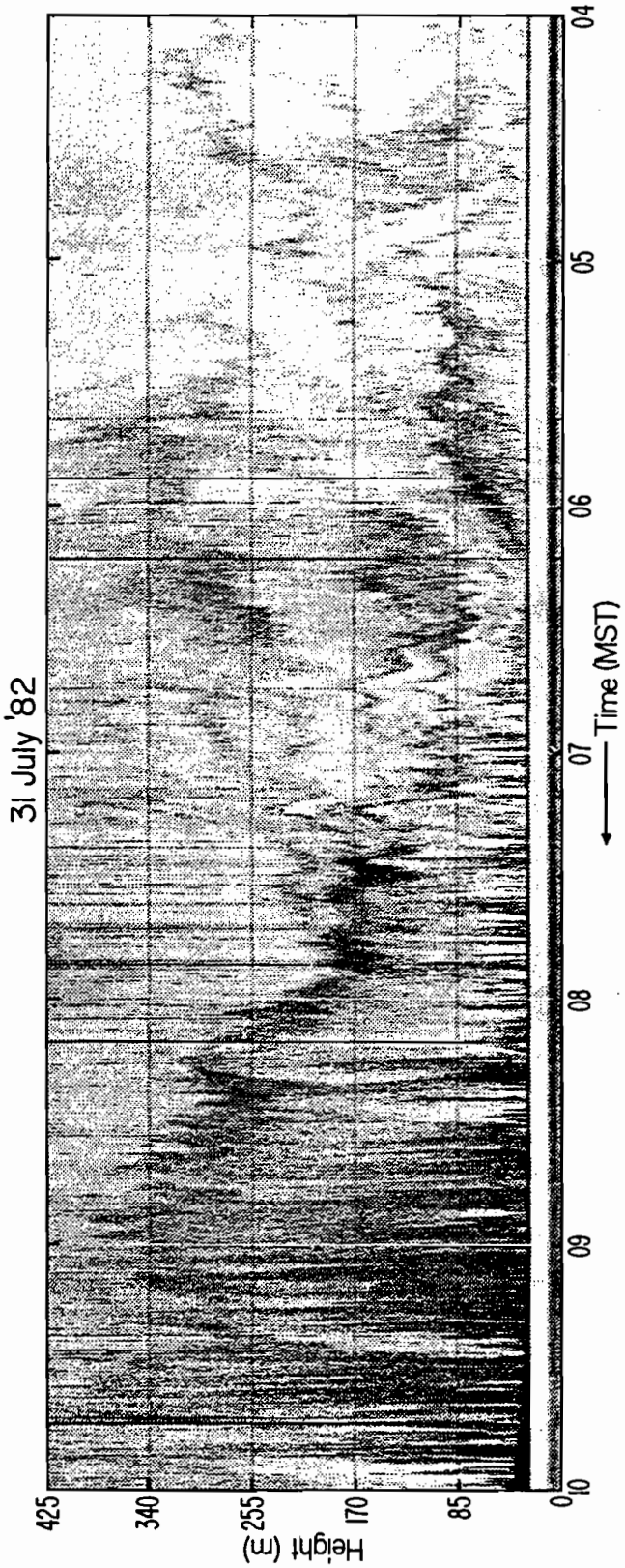
31 July '82
Height (m)
425
340
255
170
85
0
04
05
06
07
08
09
10
Time (MST)

APPENDIX C

SURFACE AND 500 mb WEATHER MAPS

Taken from NOAA's "Daily Weather Map" weekly series. Upper map is surface with isobars at 4 mb intervals and lower map is 500 mb. Box with cross hatch is Colorado. Wind flags are in knots and contours on 500 mb map are in feet. (19,100 feet = 5805 m).

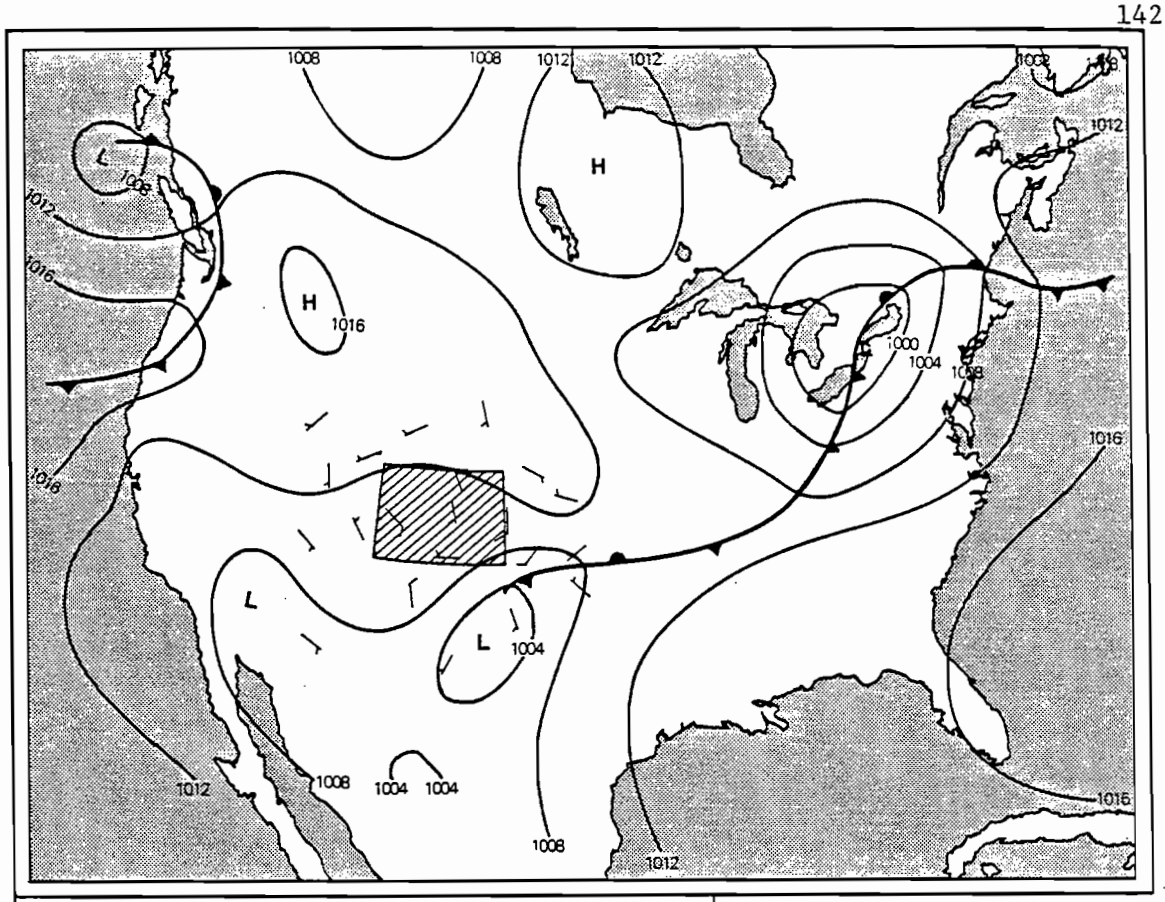

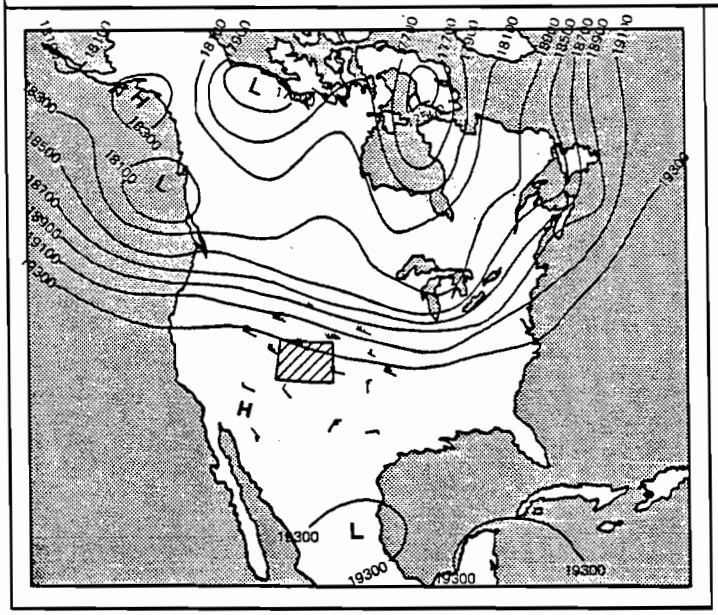

June 22, '81
0500 MST

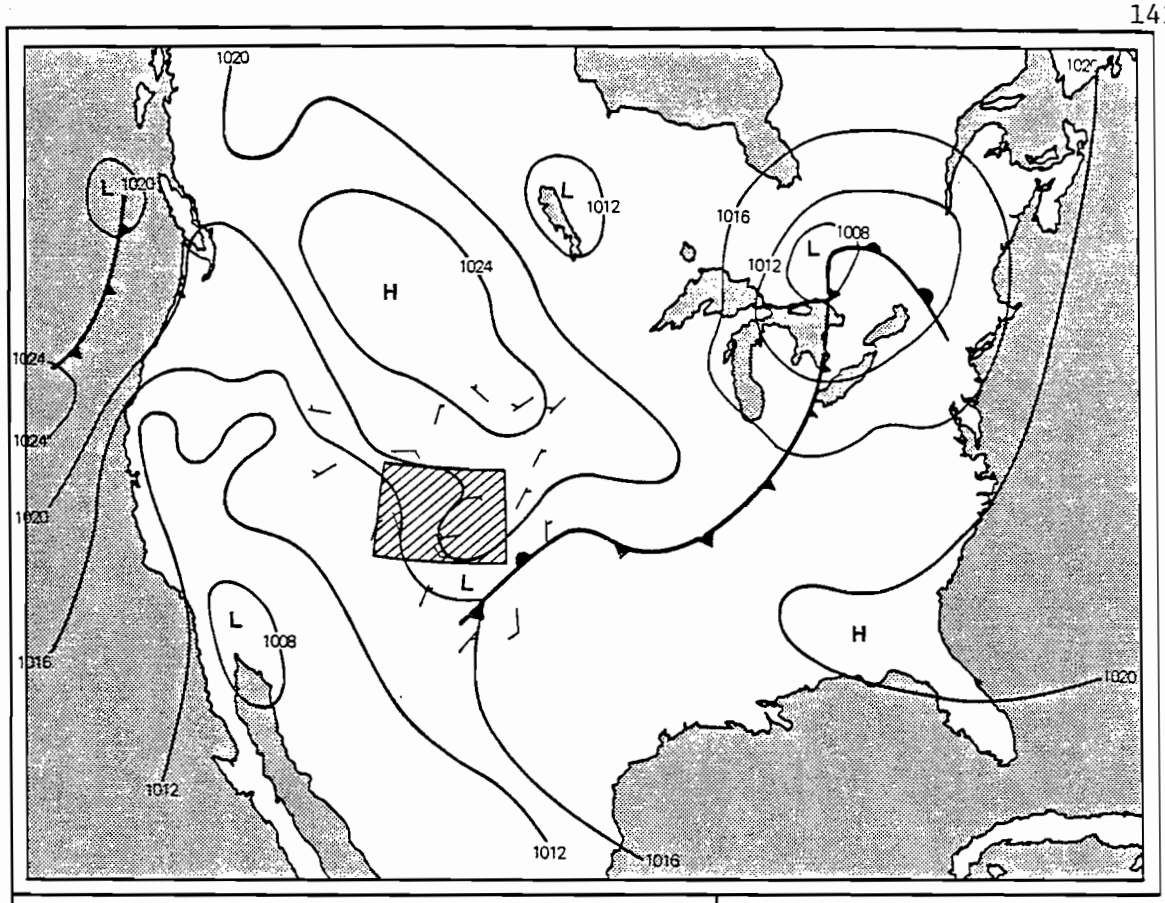

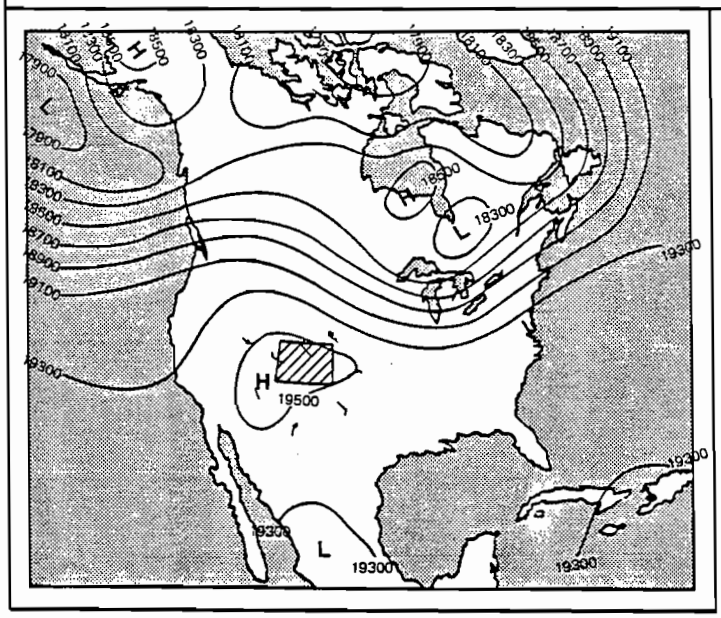

June 25, '81
0500 MST

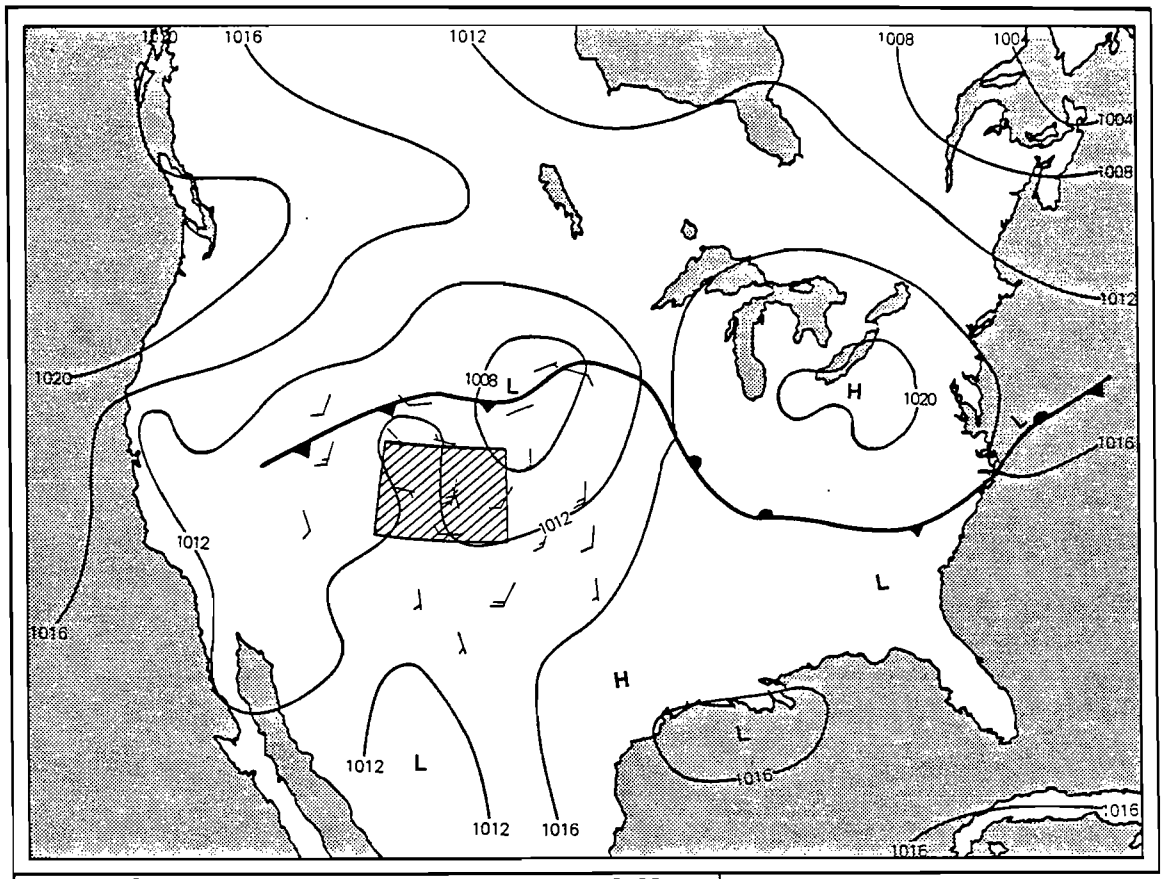

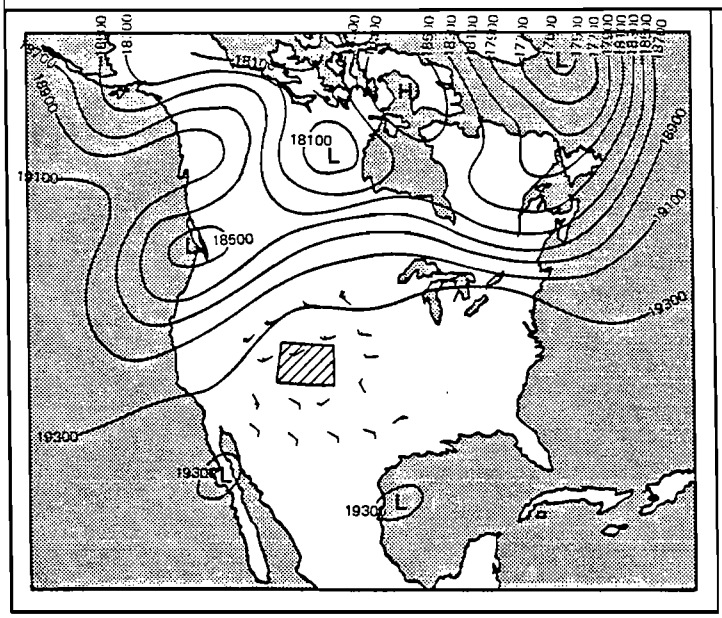

July 11, '81
0500 MST

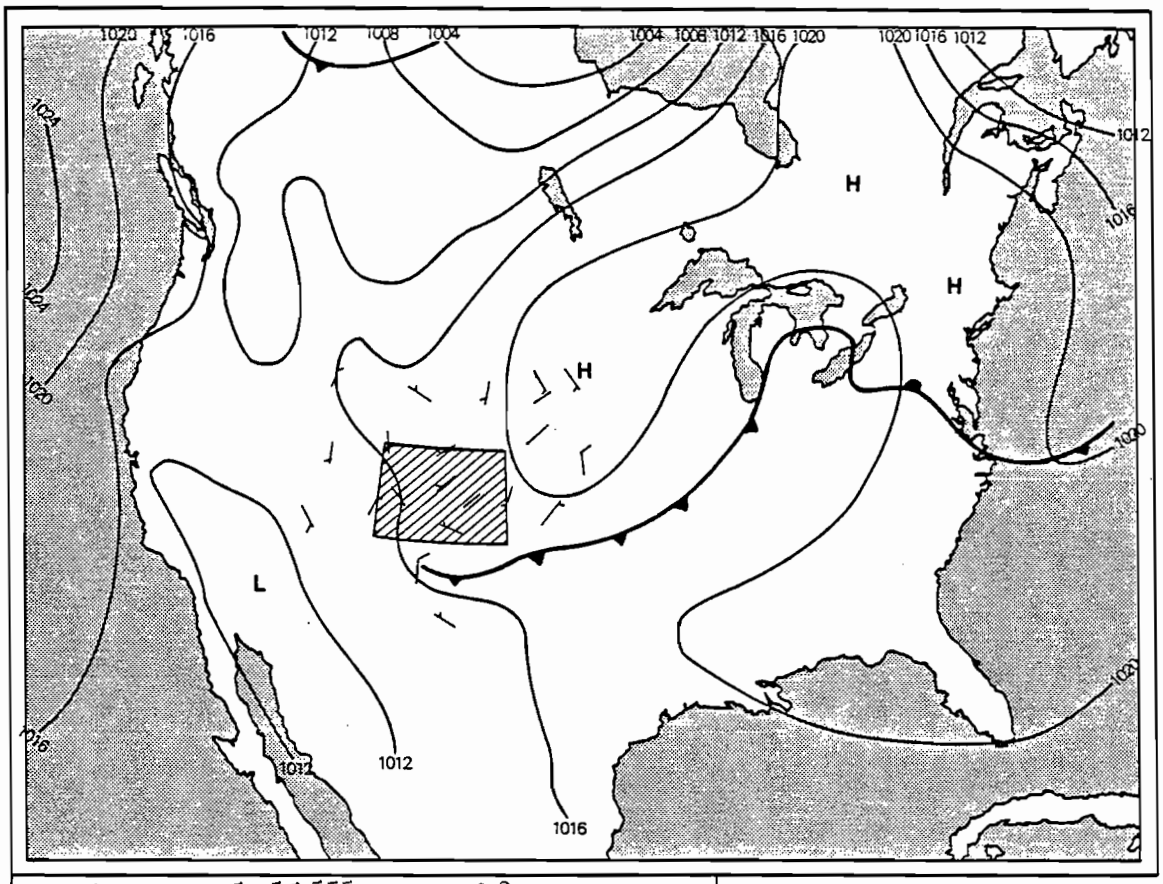

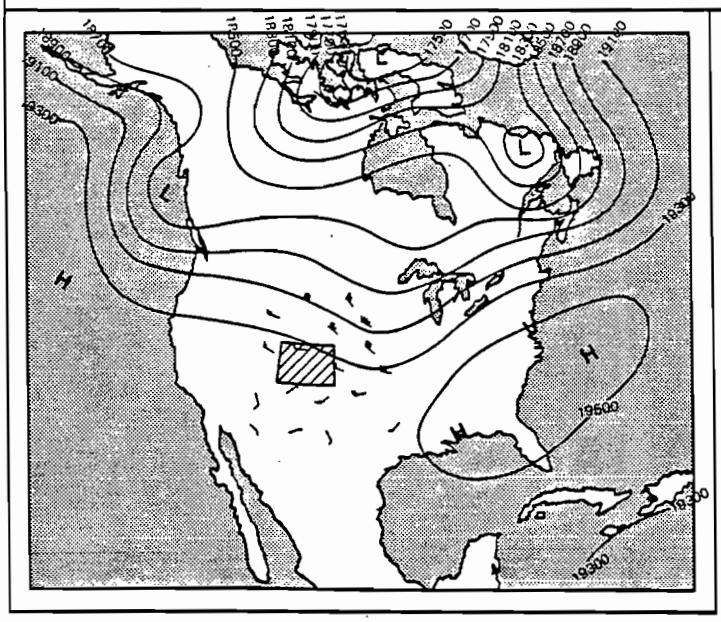

July 28, '81
0500 MST

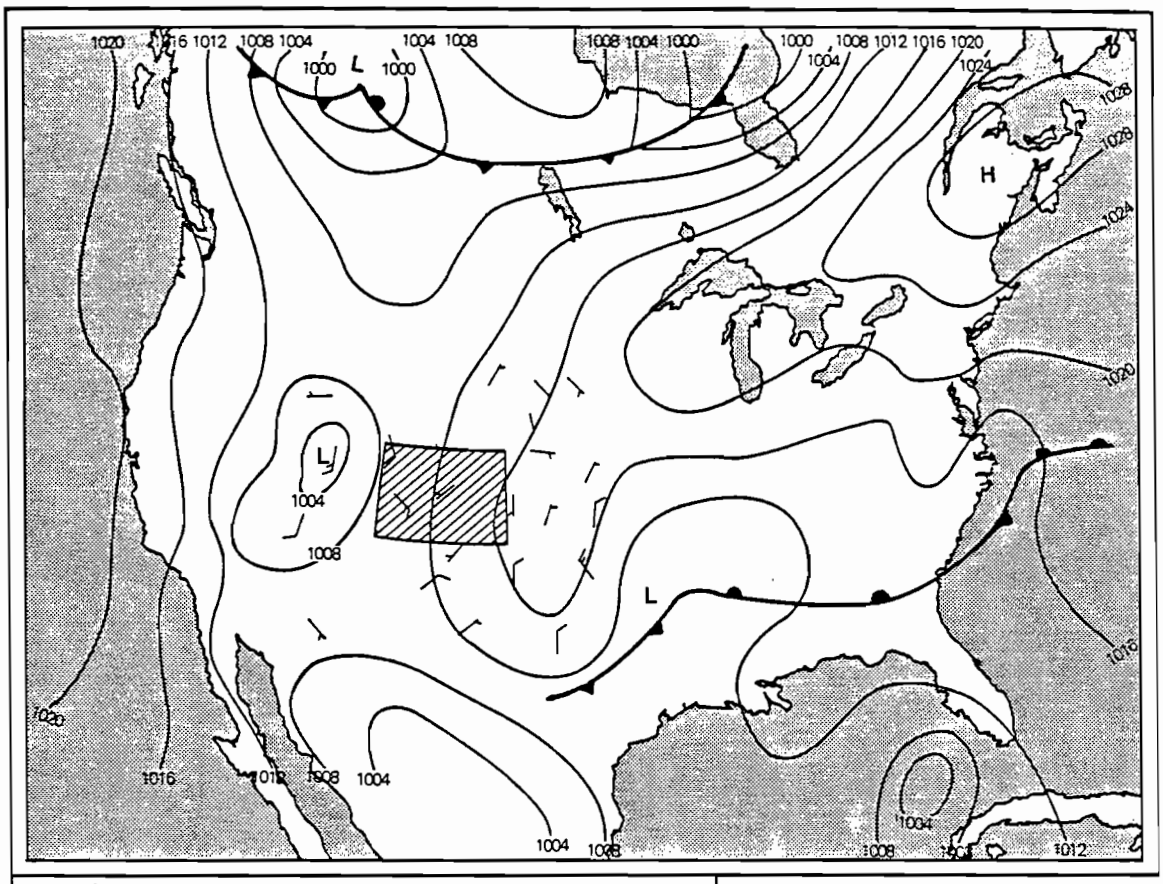

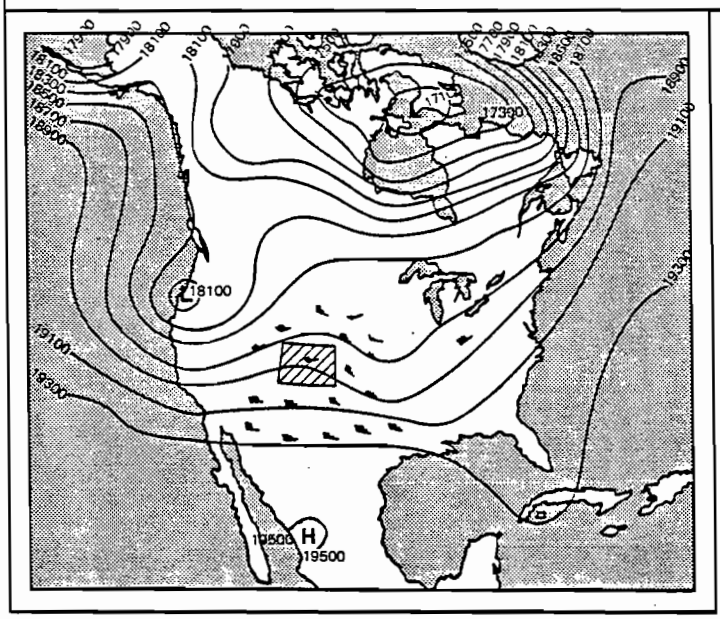

June 4, '82
0500 MST

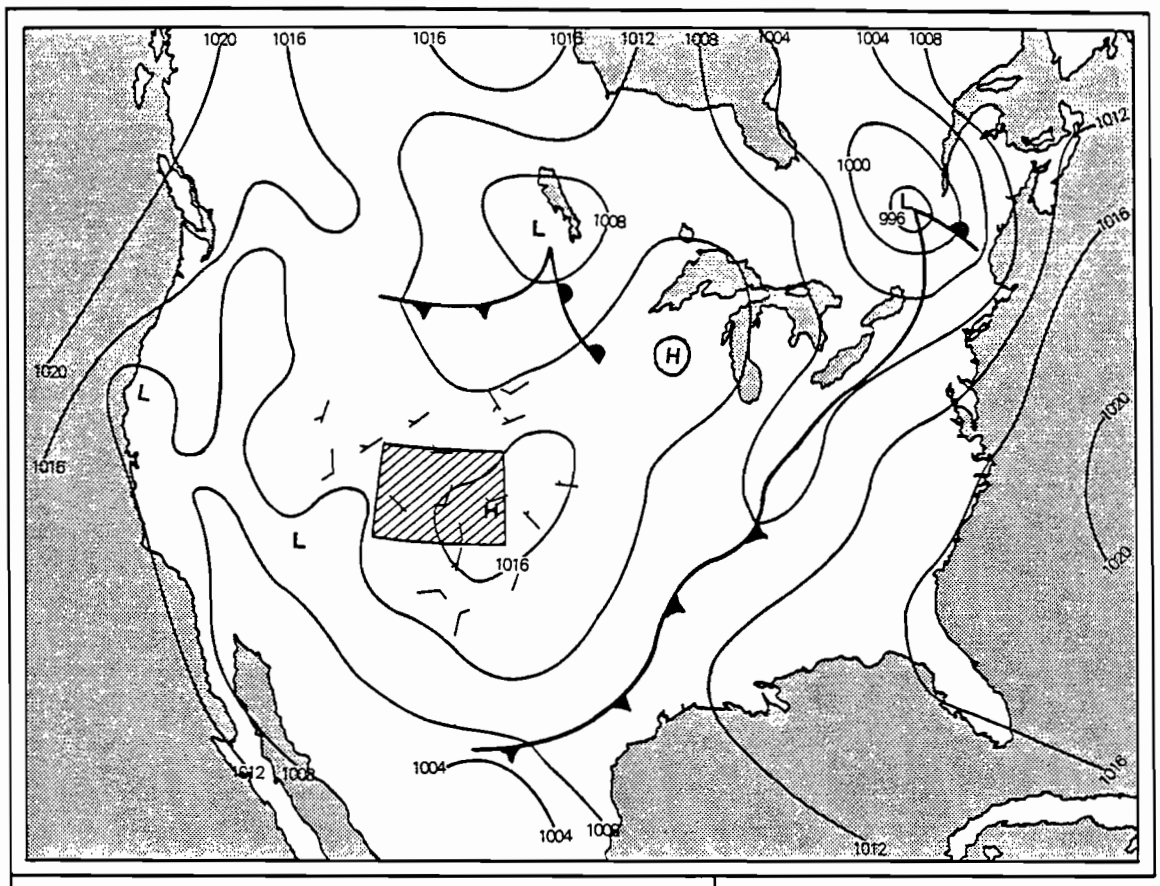

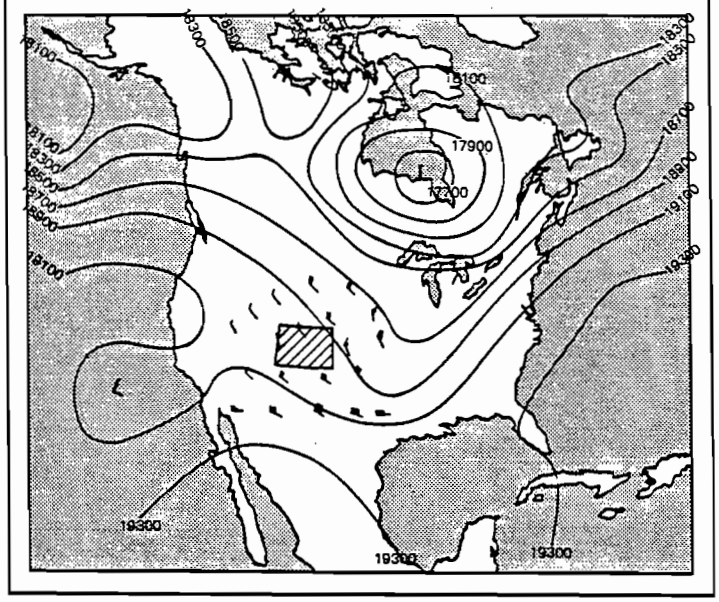

June 16, '82
0500 MST

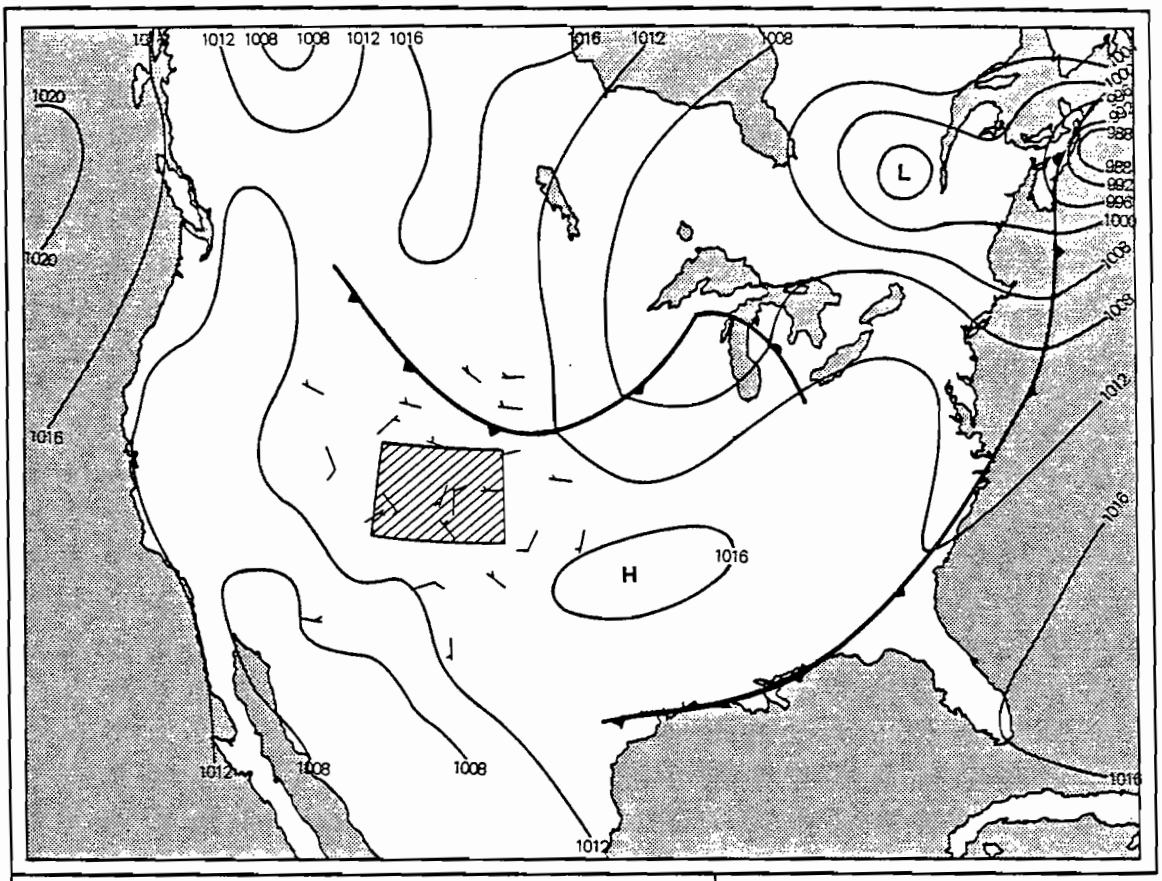

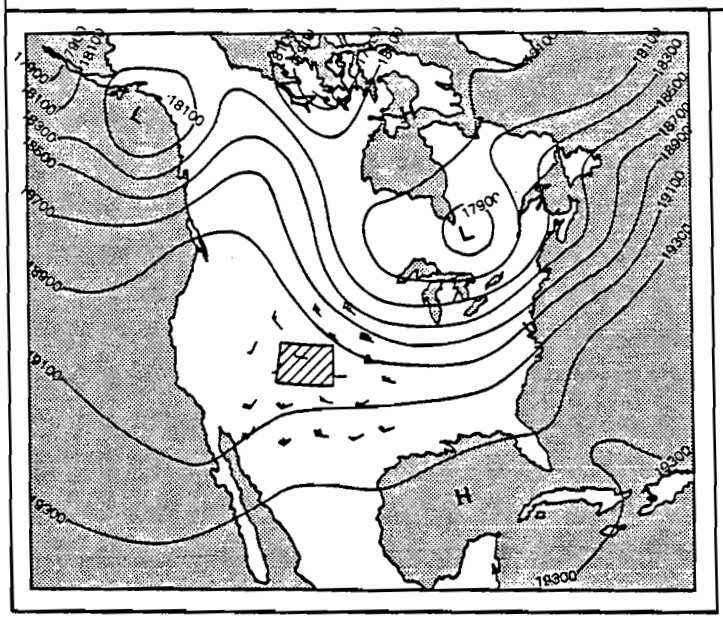

June 20, '82
0500 MST

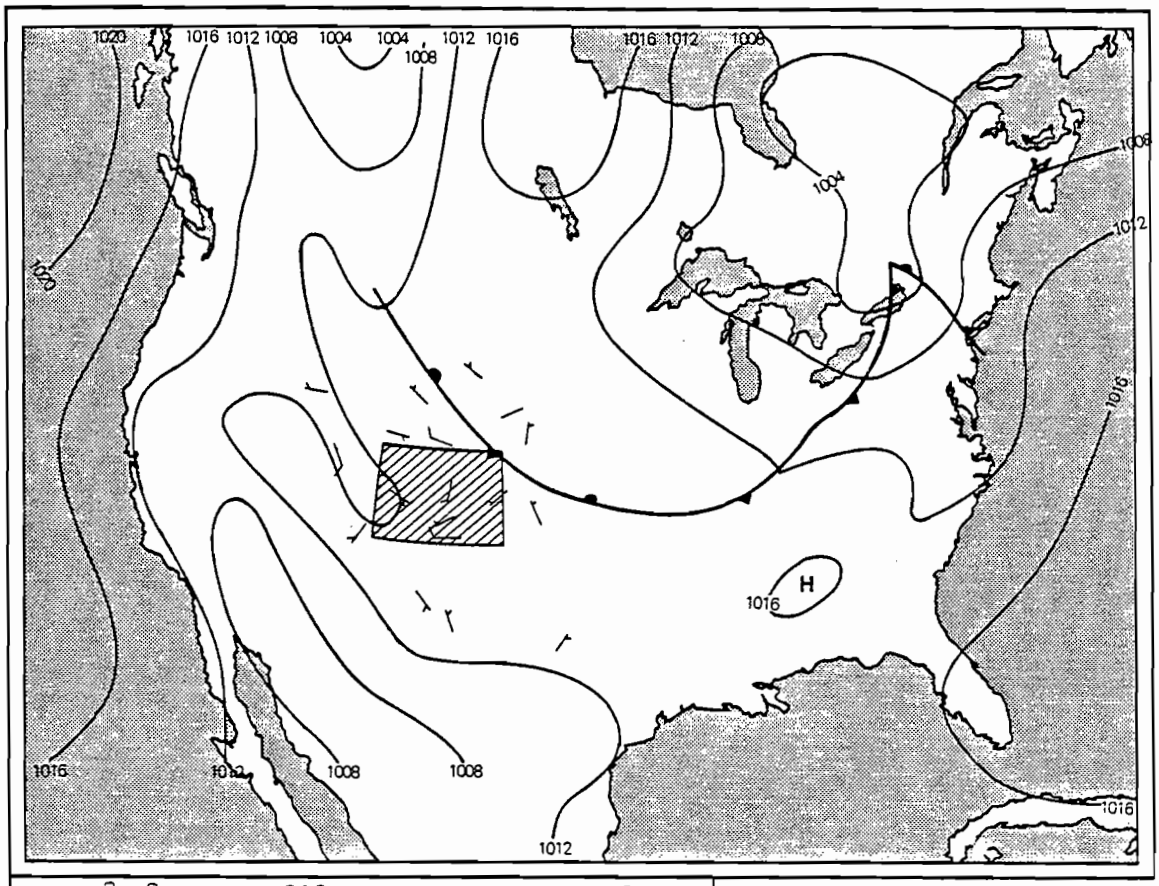
1020
1016
1012
1008
1004
H
1016
L
17900
June 21, '82
0500 MST

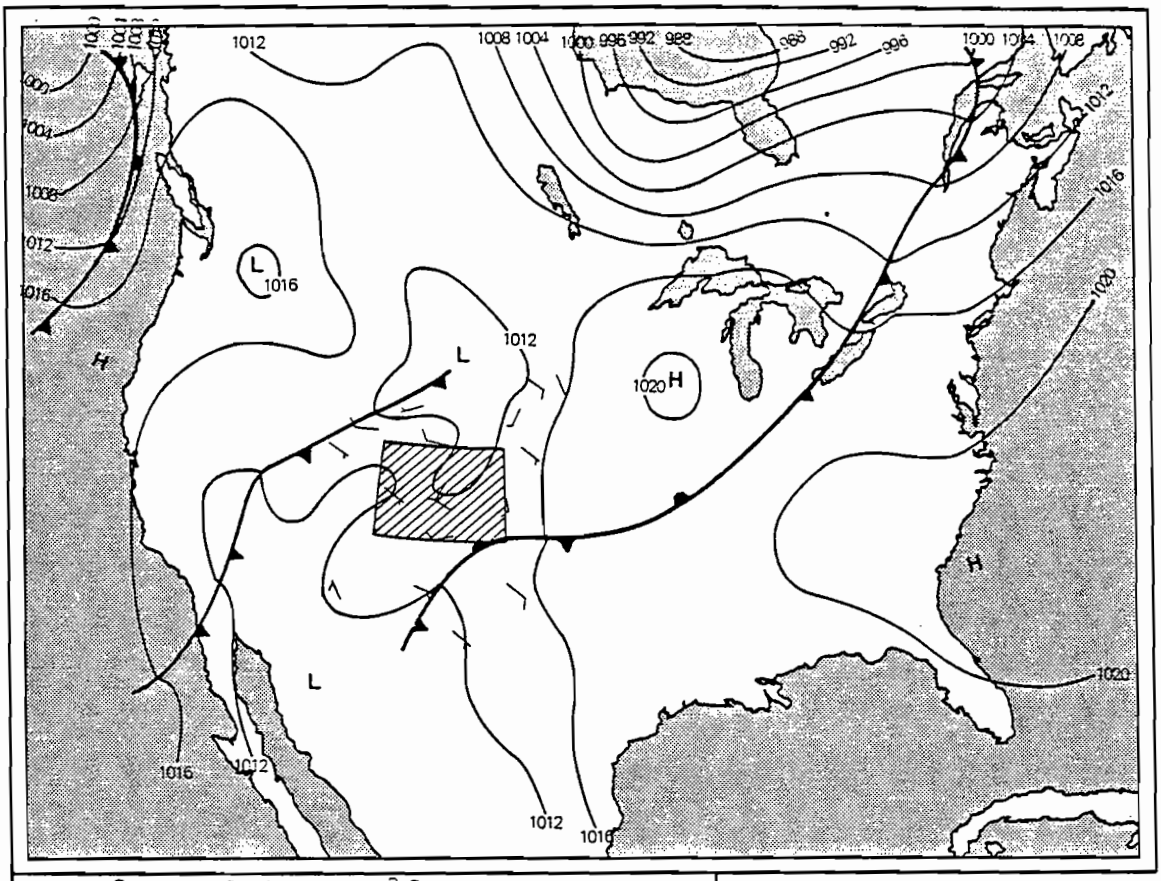

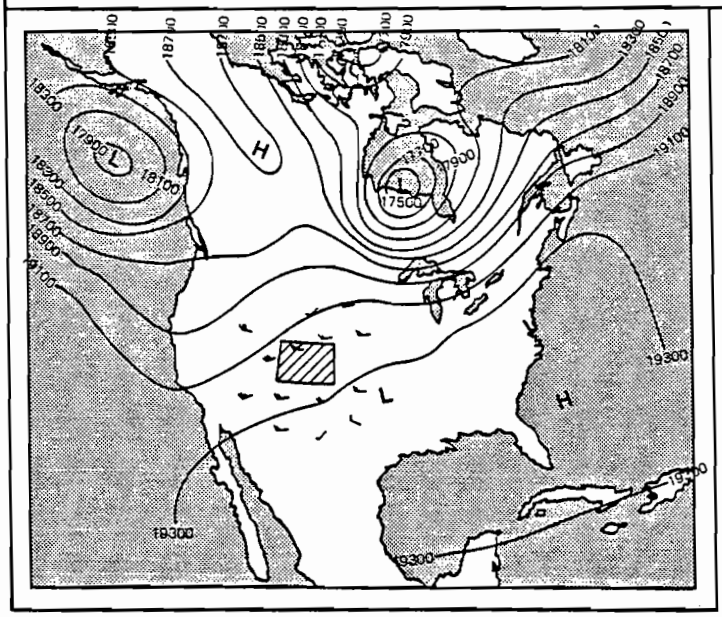

July 8, '82
0500 MST

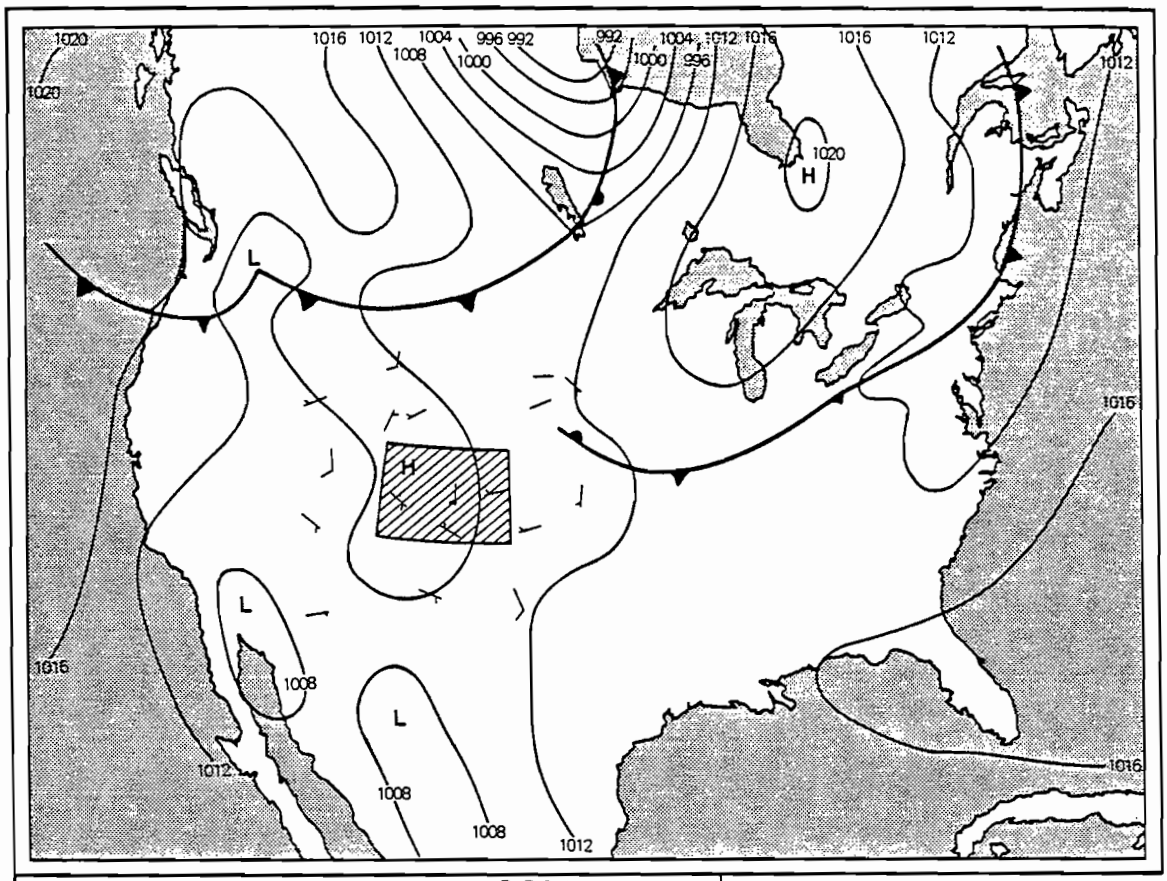

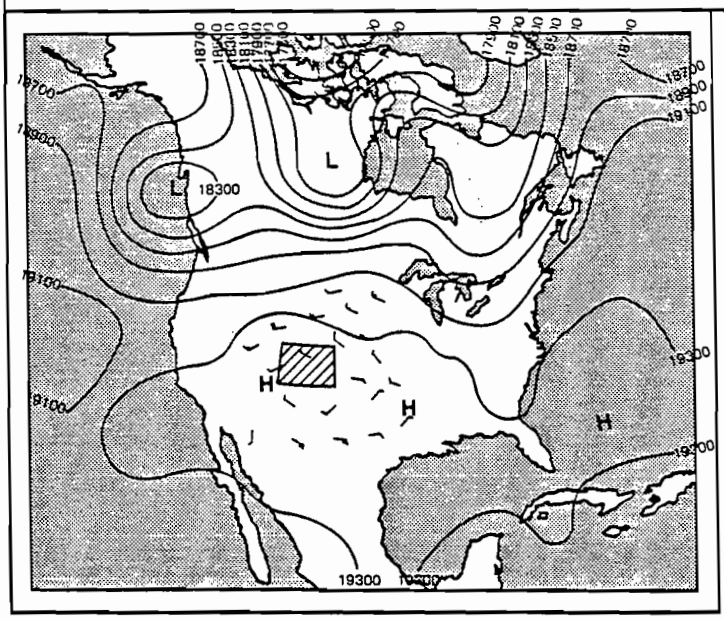

July 20, '82
0500 MST

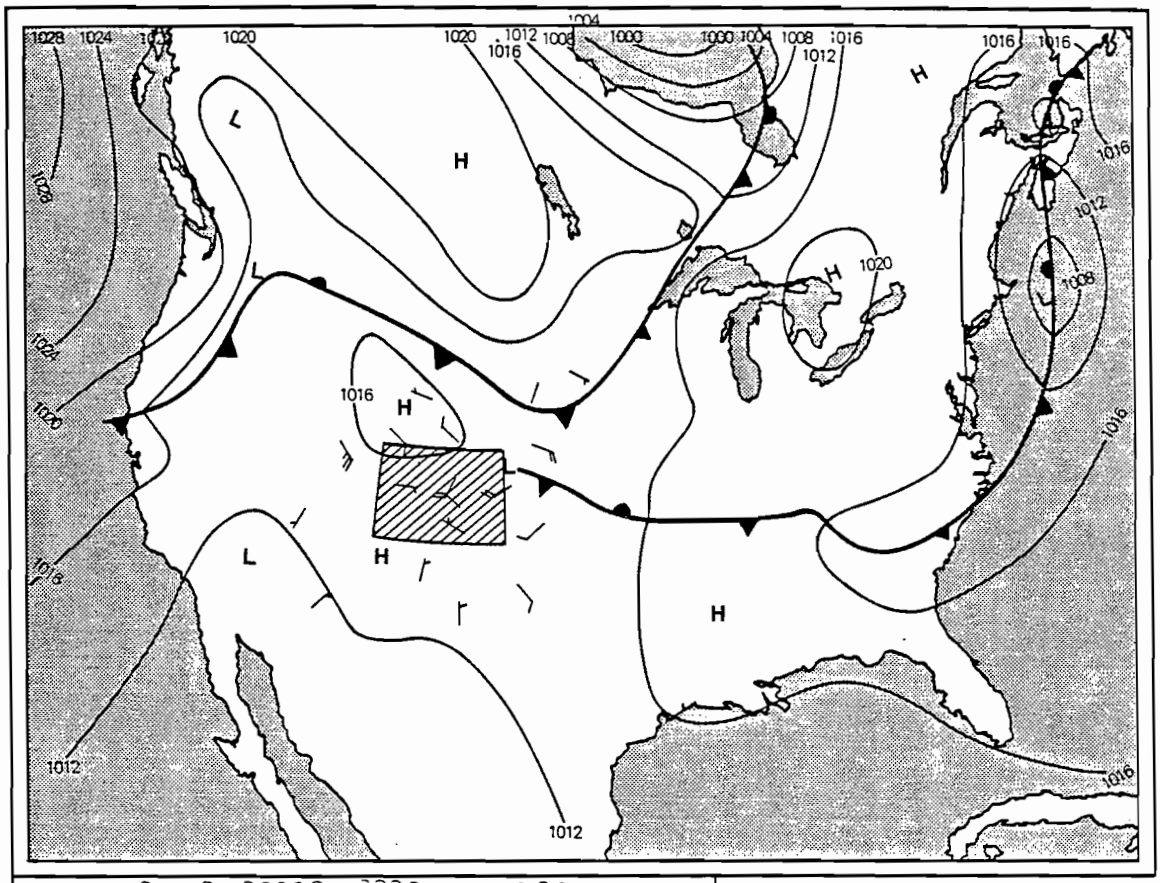

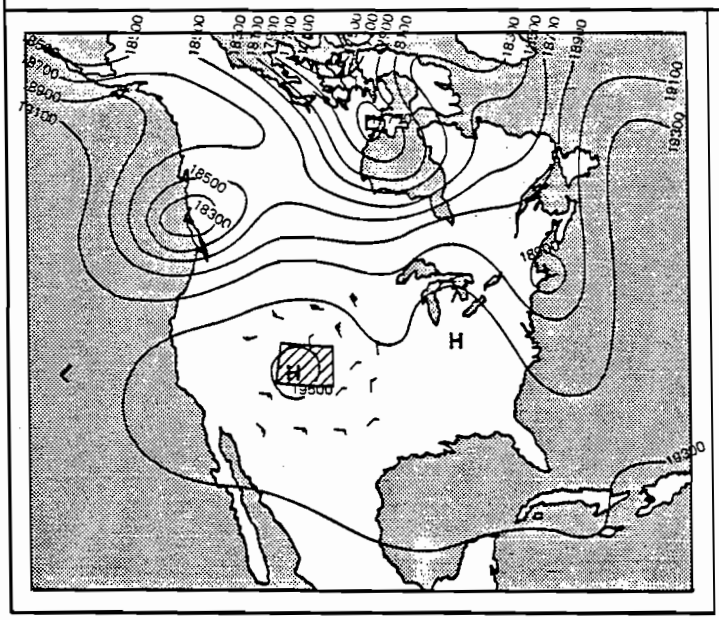

July 21, '82
0500 MST

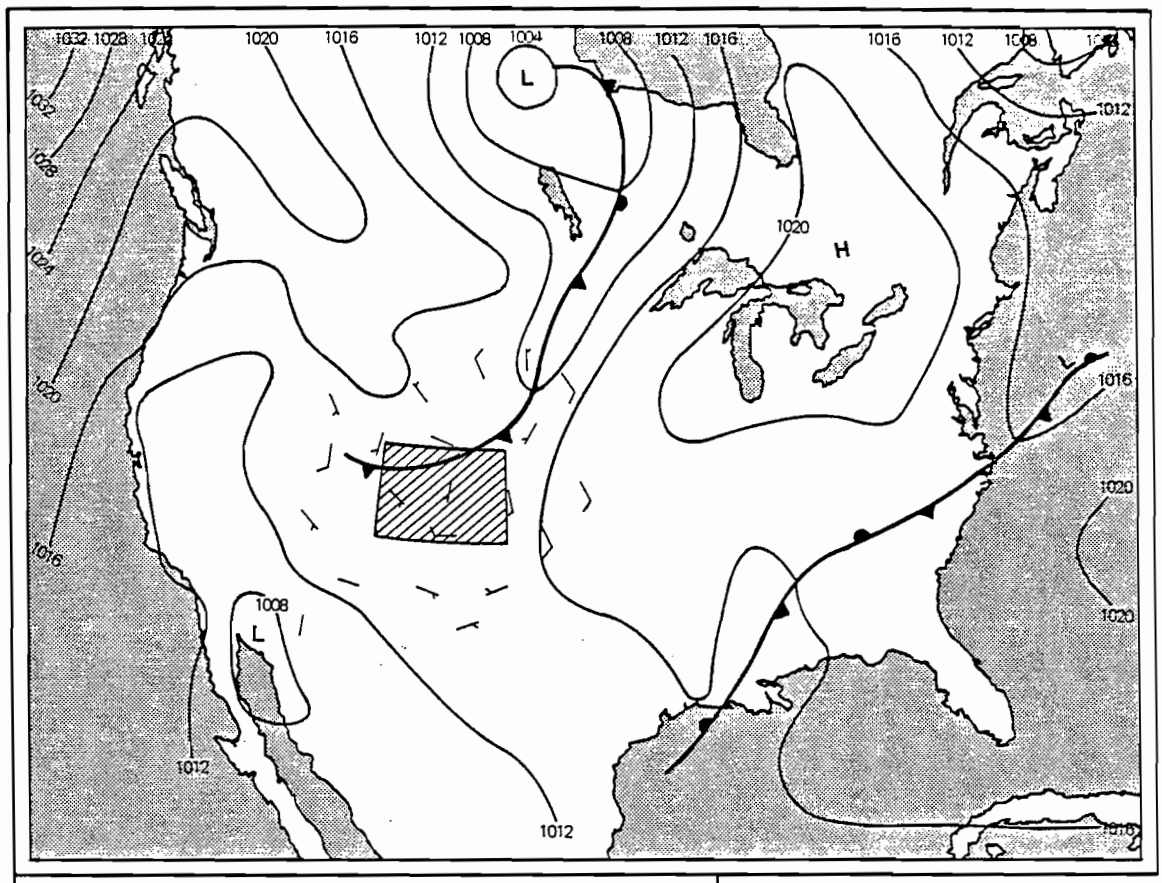

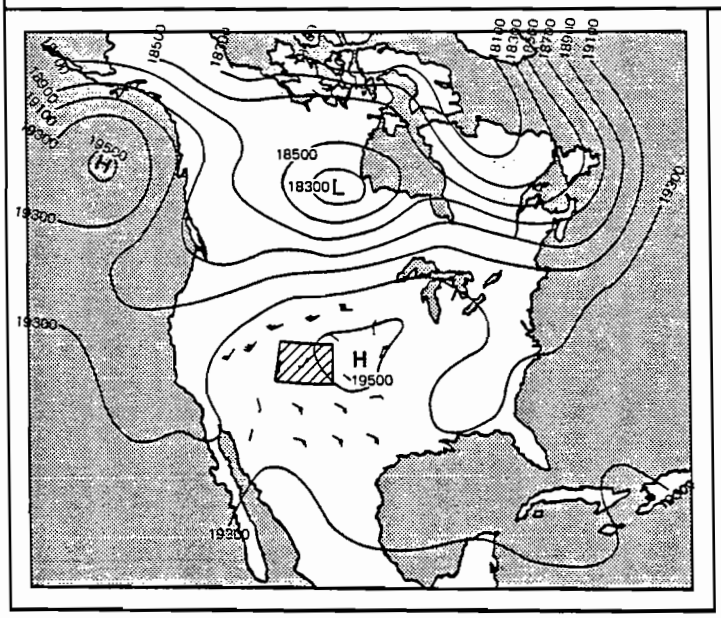

July 24, '82
0500 MST

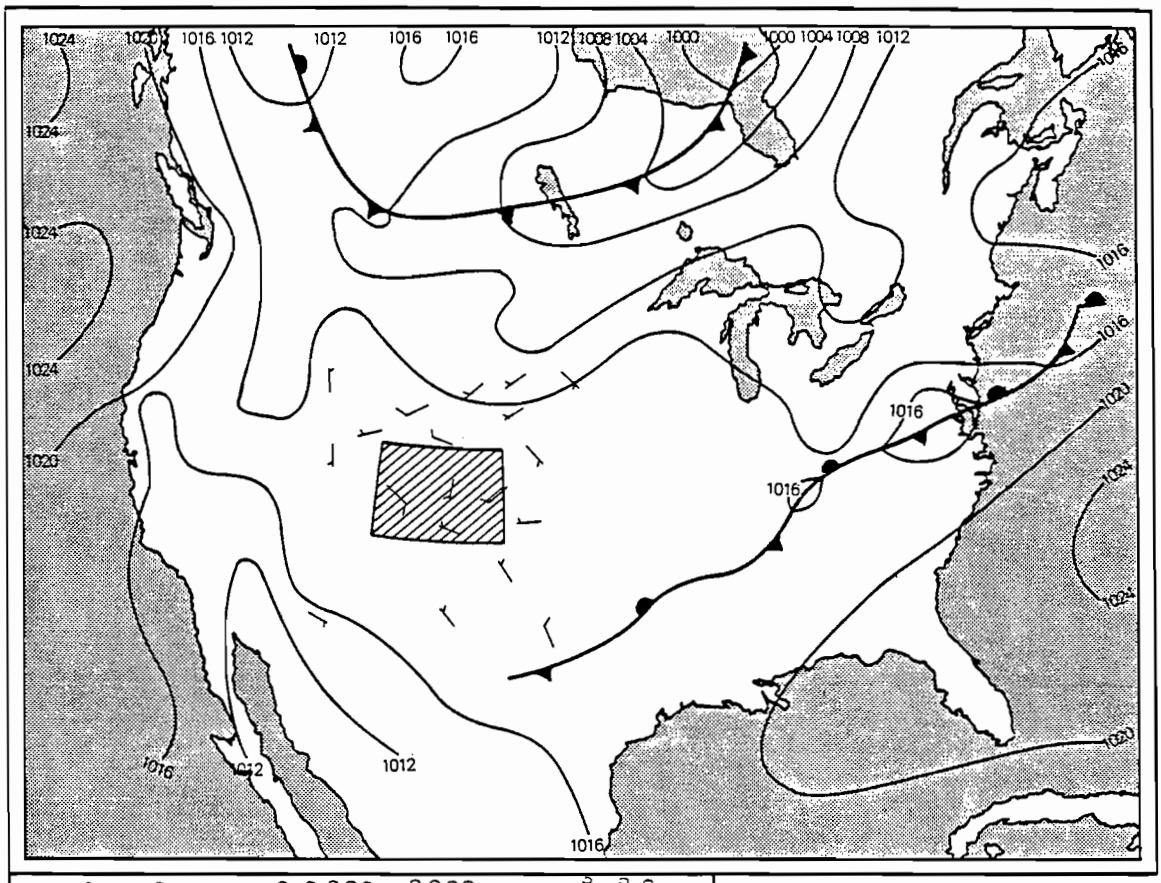

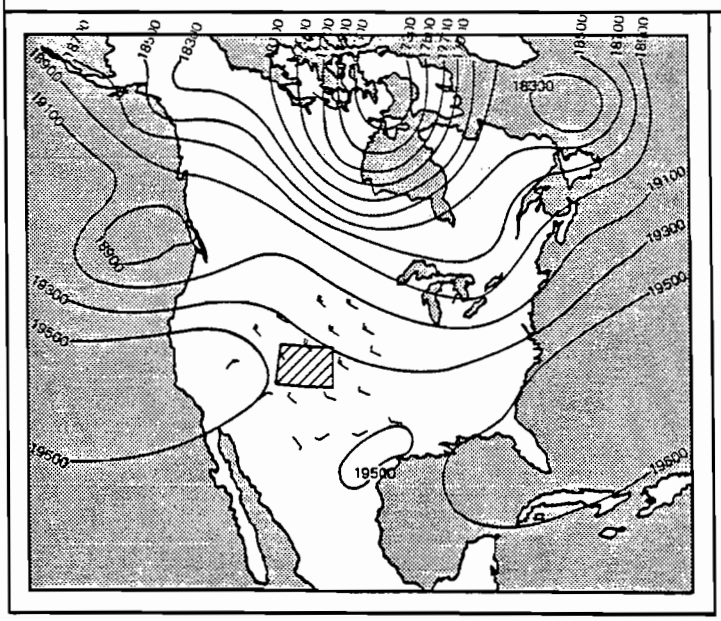

July 31, '82
0500 MST

APPENDIX D

DENVER (127/05 MST) SKEW T-log P PLOTS

Surface to 500 mb, includes mandatory and significant levels. Wind flags are in ms^{-1} and MB on dew point temperature plots signifies a motor boating humidity signal from the rawinsonde package. The skew T-log P base plate is taken from a standard Skew-T diagram.

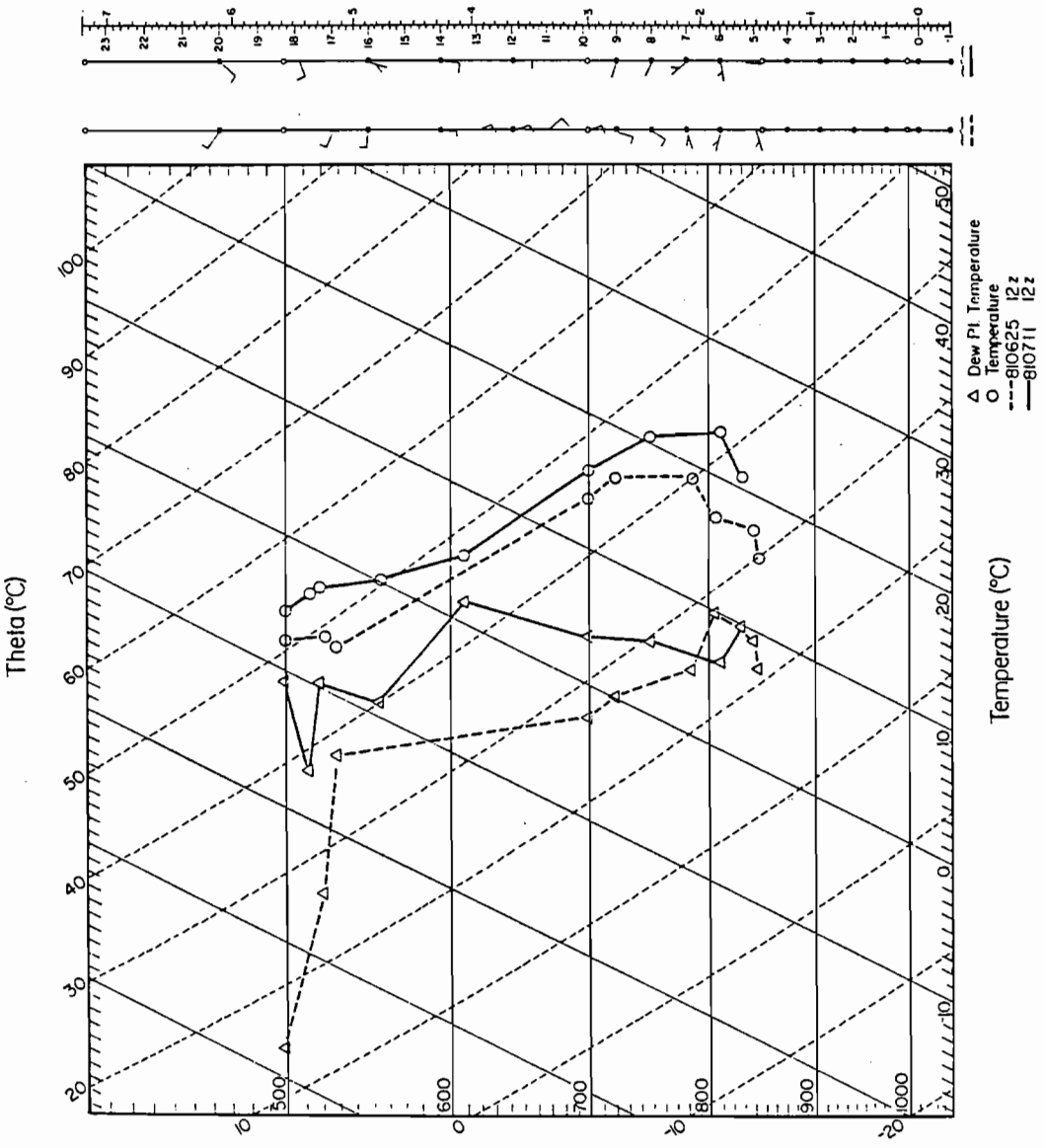
Theta (°C)
Temperature (°C)
Δ Dew Pt Temperature
O Temperature
---810625 12z
——810711 12z

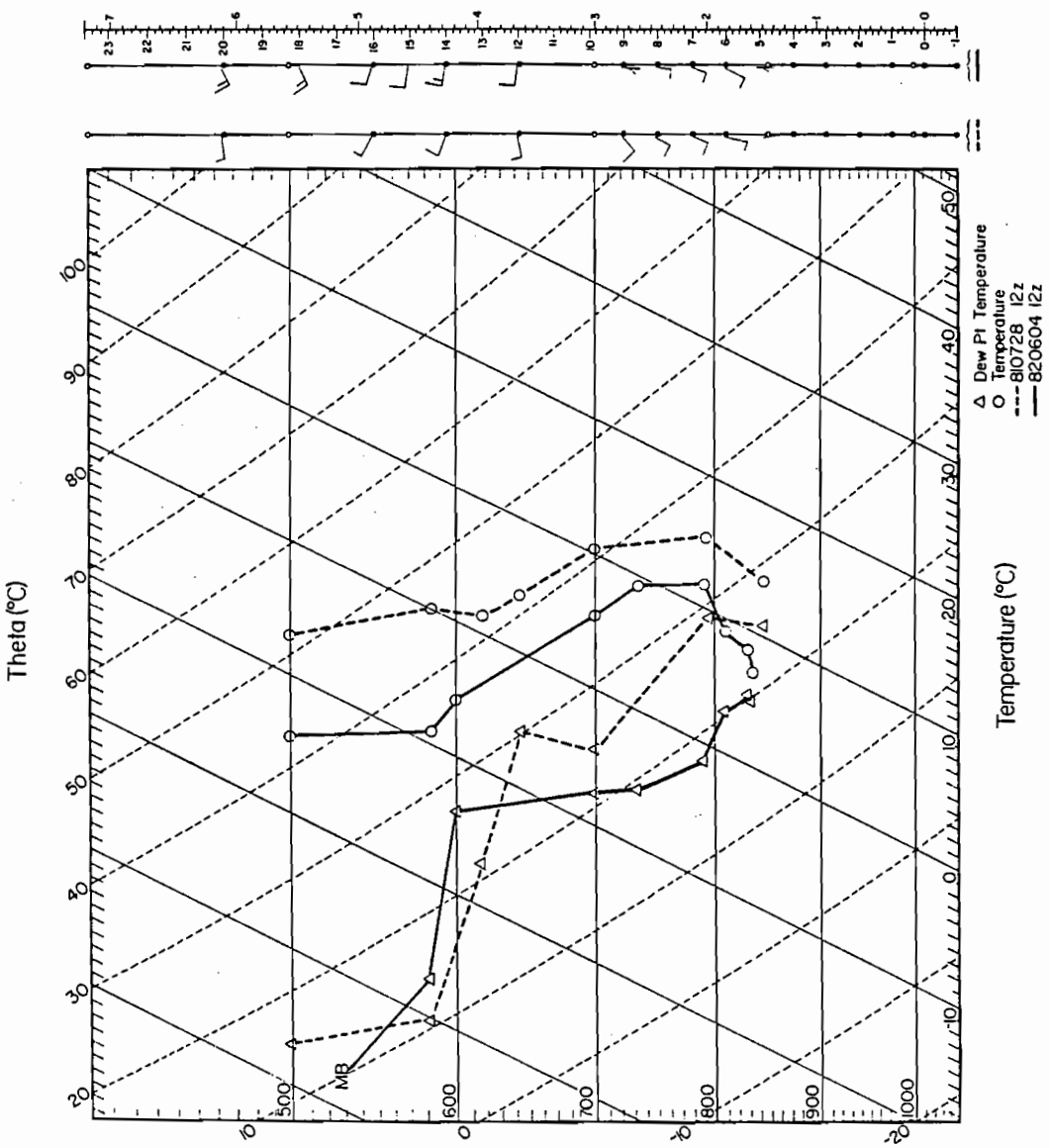
Theta (°C)
Temperature (°C)
Δ Dew Pt Temperature
○ Temperature
810728 12z
820604 12z
MB
500
600
700
800
900
1000

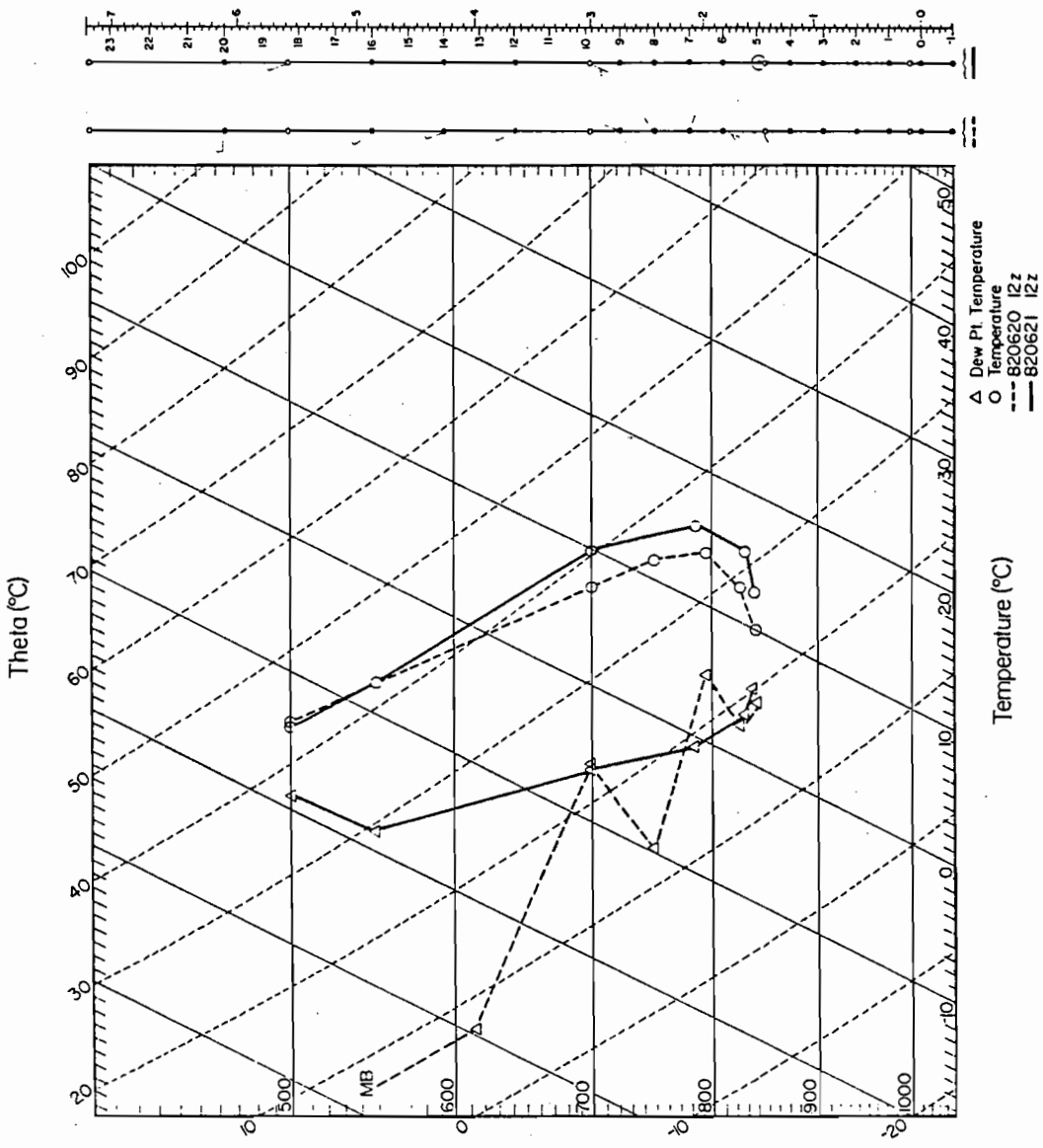
Theta (°C)
Temperature (°C)
MB
Dew Pt. Temperature
Temperature
820620 12z
820621 12z

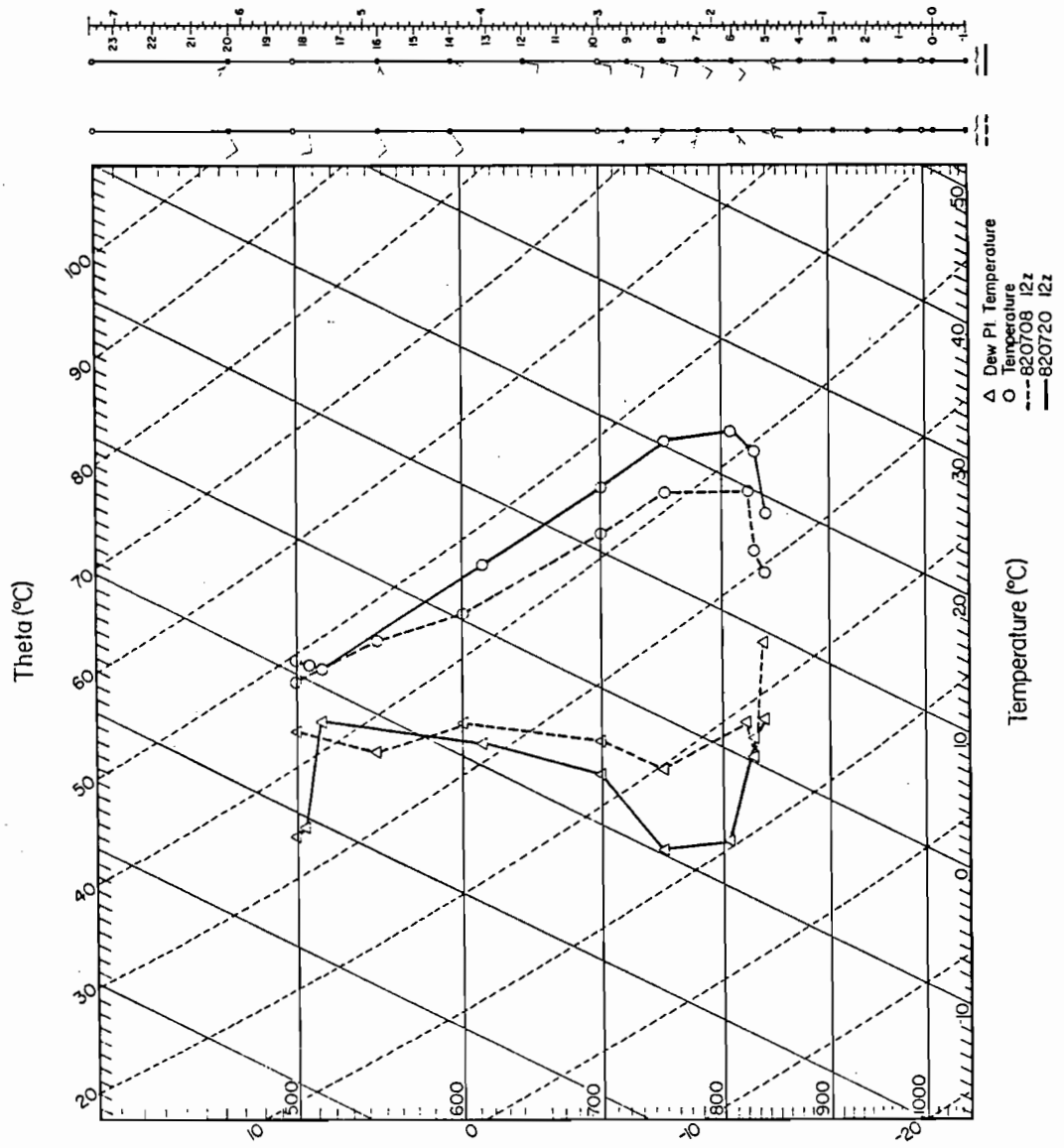
Theta (°C)
Temperature (°C)
Dew Pt Temperature
Temperature
820708 12z
820720 12z

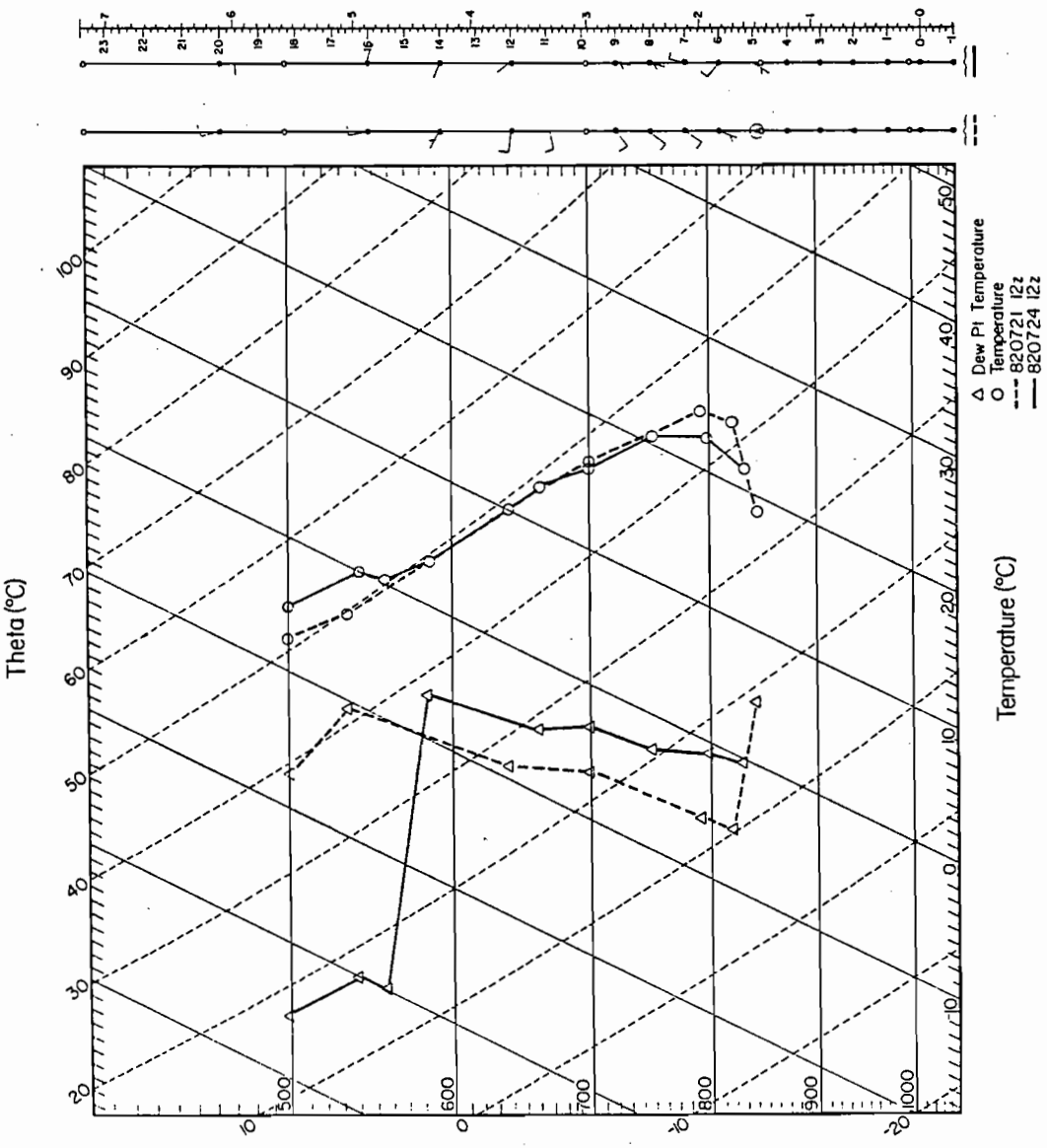
Theta (°C)
Temperature (°C)
Dew Pt Temperature
Temperature
820721 12z
820724 12z

APPENDIX E

Hypsometric Equation

$$P_1 = P_o \cdot e^{\left(-\frac{gz_1}{R_d T}\right)}$$

Possion's Equation

$$\theta = T \cdot \left(\frac{P_o}{P}\right)^{R_d/C_p}$$

Specific Humidity Equation (Murray, 1967)

$$q \cong \varepsilon \frac{e_p}{P_o} \cdot \frac{1000g}{1kg}$$

$$\varepsilon = \frac{M_w}{M_d} \qquad e_p = 6.1078 \cdot \left(e^{a(T_d-273)/(T_d-b)}\right)$$

Richardson number

$$Ri = \frac{g\beta}{(\partial\vec{u}/\partial z)^2}$$

β $= \frac{\partial\theta}{\theta\partial z}$ = vertical stability.

g = gravity.

$\partial\vec{u}/\partial z$ = vertical wind shear.